A Mathematical Model for the Cardiovascular System with a Measurable Pulsatile Pressure Output

Aurelio A. de los Reyes V

Prof. Dr. Franz Kappel, Dissertation Supervisor

A Thesis presented for the degree of
Doktor der Naturwissenschaften

Institute for Mathematics and Scientific Computing
University of Graz, Austria

March 2010

Dedicated to

Amy Grace Guillermo

Gloria Roldan

Aurelio brothers

A Mathematical Model for the Cardiovascular System with a Measurable Pulsatile Pressure Output

Aurelio A. de los Reyes V

Submitted for the degree of Doktor der Naturwissenschaften
March 2010

Abstract

Mathematical modeling of the cardiovascular system yields a range of applications in physiology and medicine to support the life scientists and clinical workers. In particular, cardiovascular modeling has been used to study the behavior of blood pressures in the peripheral and systemic compartments, cardiac output, ventricular elastance and contractility in the human circulatory system under various conditions such as constant workload and orthostatic stress. In this study, a global lumped compartment cardiovascular model was developed to predict the pulsatile pressures in the finger arteries. It is a modification and integration of an existing non-pulsatile model developed by Kappel and a simplified pulsatile left ventricle model by Olufsen. Linking the average flow model with the pulsatile flow was the main difficulty. The current model includes a finger artery compartment to reflect a typical site of measurement of pulsatile pressures. The left ventricle is the source of pulse waves in the system. The left ventricular elastance is modeled to reflect variations in the stiffness of heart muscles during the exercise condition. A sigmoidal function, which is dependent on the heart rate was used to characterize the maximum elastance of the left ventricle. The aorta compartment is incorporated to indicate pressure changes detected by the baroreceptors which act as sensors in the cardiovascular system. The goal of the study is to model and investigate the blood pressure regu-

latory mechanisms specifically during the exercise phase as in the bicycle ergometer test. It is aimed at designing a feedback control represented by the baroreceptor loop. The fundamental approach is to obtain a stabilizing control by minimizing a cost functional, thus steering the system to the equilibrium exercise state. The current model is reduced, modified and simplified to acquire a new system, which in some sense, is not so different from the original. Though the character of the system is changed, the modified model serves as the basis for the construction of feedback control. Numerical simulations showing the dynamics of the states during rest and exercise conditions are presented. Moreover, simulations on the behavior of the controlled system from initial equilibrium rest phase to equilibrium exercise phase are provided.

2010 AMS Mathematics Subject Classification: 92C30, 49J15

Key Words: pulsatile cardiovascular model, left ventricular elastance, baroreceptor loop, regulation of the cardiovascular system, feedback law, linear-quadratic regulator problem, stabilizing control

Declaration

The work in this thesis is based on research carried out at the Mathematics and Medical Physiology Modeling Group, Institute for Mathematics and Scientific Computing, University of Graz, Austria. No part of this thesis has been submitted elsewhere for any other degree or qualification and it is all my own work unless referenced to the contrary in the text.

Acknowledgements

I would like to express my deepest gratitude to Prof. Dr. Franz Kappel for his exceptional supervision. As an advisor, he provided me with his full professional support in dealing with this PhD research project. His constant encouragement helped and challenged me throughout my studies. He is not only a mentor but a colleague with great stories and sense of humor. He is well respected due to his wide range of knowledge, good interpersonal skills and humility which are worthy to emulate.

Many thanks to all the faculty and staff of the Institute for Mathematics and Scientific Computing for providing me with a very conducive working environment. To Dr. Jerry Batzel who indirectly supervised my work and invested time to give his valuable input to the thesis. He is very patient with my "unforgivable mistakes" in mathematics. Sharing stressful times with him in the same office made my PhD life more exciting. To Prof. Dr. Stephen Keeling who encouraged me to put my best effort into every academic endeavor. He imparted excellent class lectures and offered academic career advice to focus on things I enjoy doing. To Prof. Dr. Georg Propst and Prof. Dr. Gundolf Haase for sharing their time with other (international) students. To Frau Gerlinde Krois who assisted me throughout my academic program. To Fabian Tschiatschek who configured and installed all the software I needed in my laptop and office computer.

I gratefully acknowledge the financial support administered by the Austrian Academic Exchange Service (ÖAD) through a scholarship grant under the Technologistipendien Südostasien (Doktorat) scheme. This research is also funded in part by

the “AGRID” project under the generous support of Prof. Haase.

My Christian family in Graz made my stay meaningful and worthwhile. The church of Christ (eine Gemeinde des Herrn Jesus Christus) in Schillerplatz 5 warmly welcomed and accepted me. They provided not only for my spiritual but for my physical needs as well. Special thanks to Thomas and Petra Lang, whom I consider my Austrian Big Brother and Big Sister for their generosity and big hearts. To Agnes Goldgrüber, my Austrian Mother and Manfred Kellner, my Austrian uncle. To the International Baptist Church, especially to Curt and Melinda Brown, my American Big Brother and Big Sister.

I want to thank my best friends Dennis Bacani and Juancho Collera who are also completing their PhD in Mathematics, for sharing the ups and downs in doing research abroad. To Perlas Caranay for the encouragement in pursuing my studies. To the University of the Philippines Baguio and Diliman Math faculty for their continuous cheers and inspiration.

Thanks to Dr. Michelle Vallejos for providing an example of audacity and perseverance. She listens to my personal complaints and supports me financially in times of urgent need. To Dr. Irene Rodriguez, Dr. Ma. Pythias Espino and Dr. Marrick Neri for their wisdom and advice.

Deep gratitude to all my Thai, Austrian and other international friends. To my Filipino family in Graz for camaraderie.

Most especially, to Amy Grace Guillermo and my family to whom this thesis is dedicated. To my mother who can take credit for all my achievements.

Finally, I would like to express my praises to God for his guidance, protection and all the blessings He has bestowed upon me. To Him be the glory and thanksgiving.

Contents

List of Figures

List of Tables

Introduction

It is an amazing fact that the human body is composed of thousands of built-in control mechanisms embedded in it. Intricate and complicated, the control systems operate within the organs to control the function of its individual parts. Some convey information throughout the entire body to regulate the interactions between the organs. Examples of which are the following: the genetic control systems within the cells that control intracellular functions and life processes, the insulin control system which regulates the glucose concentration in the extracellular fluid, the control of body temperature, and the regulation of oxygen and carbon dioxide in the extracellular fluid.

In the cardiovascular system, the rate of blood flow through most tissues is controlled in relation to the tissue need. The microvessels of each tissue continuously monitor tissue needs, such as the oxygen supply and other nutrients and the accumulation of carbon dioxide and waste products. In turn, the local blood vessels respond by dilating or contracting to control local blood flow to that level required for the tissue activity. Also, the nervous control system provides additional help in controlling tissue blood flow. In addition, the heart is controlled to provide the necessary cardiac output so that it pumps the required amount of blood flow. It is regulated by the sum of all the local tissue flow. Furthermore, the arterial pressure is controlled by either local blood flow or cardiac output control. For prolonged periods, the kidneys also play a major role in pressure control by secreting pressure-controlling hormones and by regulating the blood volume. Further details can be found in Guyton and Hall (2006) [15].

The human body is designed to operate in an optimal way. It works in such a way that the consumption of energy is minimized. In the cardiovascular system, the work done for ejection of the stroke volume needs to be minimized. Numerous models have been developed to investigate various parts of the circulatory system under the basic assumption that an optimality criterion is satisfied. Such studies can be found in Doubek (1978) [21], Kenner and Pfeiffer (1980) [28], Noldus (1976) [36], Ono, et al. (1982) [40] and Pfeiffer and Kenner (1981) [45]. For survey of models of this type, refer to Noordergraaf (1969) [37] and Swan (1984) [53].

The goal of this PhD thesis is two-fold. First is to develop a global pulsatile cardiovascular system which incorporates the essential subsystems. We are interested in obtaining a pulsatile pressure in the finger arteries where real-time measurements can be obtained and the numerical simulations can be validated. We extended the basic model developed by Kappel and Peer (1993) [26] and related works (e.g. Lafer (1996), [31], Kappel et al. [25], Timischl (1998) [54], etc.) to model pulsatility of blood flow by using Olufsen's model of the left ventricle (see Olufsen et al. (2009) [46]). Most of the cardiovascular system models and their short-term responses are modifications and/or extensions of Grodins compartment model, see for instance, Grodins (1959) [12] and (1963) [13]. Second is to design a feedback law mechanism described by the baroreceptor loop that stabilizes the system from an initial equilibrium rest condition to an equilibrium exercise condition. We want to construct a model for basic cardiovascular control mechanisms assuming that the regulation is optimal with respect to the cost criterion. The idea is to describe the overall cardiovascular reaction to a constant ergometric workload imposed on a test person on a bicycle-ergometer test.

Our approach is to use the concept of optimal control theory. In medicine, one of its purposes is to gather information about the nature of the controller and analyze its predictions. It aides in understanding the aspects of control of the normal and diseased situation of an organism. An important example of an application of optimal control theory in medicine is the use of an optimal feedback control for the

automatic delivery of drugs such as insulin or hypotensive drugs via microprocessors. For further applications of optimal control theory in biomedicine, see for instance, Swan (1984) [53] and Noordergraaf and Melbin (1982) [38].

The thesis is organized as follows: Chapter 1 reviews the basic concepts in cardiovascular physiology. It talks briefly about the functions of the cardiovascular system and some of its parts, the heart and its valves which have roles in the modeling process, the phases of the cardiac cycle including the systole and diastole, and the cardiac output. In addition, some control mechanisms in the cardiovascular system are discussed. It includes the baroreceptor loop and the local metabolic controls which are necessary for our purpose.

Chapter 2 is mainly devoted to the mathematical modeling of the cardiovascular system. The electric analog of the model under study is presented and the different compartments are discussed. A linear relation is used to model the blood volume in the compartment. The mass balance equations play a role in describing the blood flow in the compartments. The filling and ejection processes in the right ventricle are presented. Since we want to model the action of the left ventricle as a pump, a section on opening and closing of the heart valves is included. Model adaptation and modification of the time-varying elastance function is necessary to attain the objective of the study, i.e. to model rest and exercise condition. Thus, a separate section deals with it. To study the cardiovascular response under an ergometric workload, metabolic and autoregulation processes are modeled. Lastly, a section on the contractility of the right ventricle is presented including the Bowditch effect mechanism.

Chapter 3 provides some of the basic concepts in control theory with emphasis on the linear-time invariant systems. Important definitions and relevant results are presented without proofs. The chapter begins by defining linear control systems. Stability deals with the overall behavior of the system. Controllability talks about steering the system from a given initial state to other given final state. A section on stabilizability answers the question of how to find a control function that could

steer the response of the system to zero state. Another important concept is reconstructibility which discusses how to determine the behavior of the state from the behavior of the output. Detectability in the context of linear-time invariant systems is defined. The section on linear state feedback control discusses how the control system adjusts to operate satisfactorily. It presents the feedback feature of the control system, the linear control law and how to stabilize a controllable system by the state feedback. The deterministic linear optimal regulator problem section leads to an optimization problem minimizing a cost functional. A section providing a result on nonlinear systems is included.

Chapter 4 presents the overall cardiovascular system model in consideration and the corresponding block diagram. Then a motivation for the control problem is discussed. Periodic solutions and the determination of equilibrium values are presented. The following three sections, namely, system modifications and reductions, the linear-quadratic regulator problem and the optimal linear feedback control lead to the construction of the linear feedback. The nonlinear control problem is then reiterated to conclude the chapter.

Chapter 5 is dedicated to the numerical computations and simulations. The section on the left ventricle provides the computation for the start and end of filling and ejection processes. Simulations of the pressure and volume curves including the pressure-volume diagram of the left ventricle is presented. A thorough discussion on the computation of the mean values (respectively, equilibrium values) is included. Graphical comparisons of the state variables during rest and exercise equilibrium conditions are provided. The remainder of the section presents simulations showing the dynamics of the controlled system.

Chapter 6 summarizes the results obtained in this study. Moreover, the limitations of the model and further investigations are presented.

Appendix A contains the tables for the variables and parameter values used in

the model.

Finally, Appendix B provides the derivations of some relevant equations in the model and the formula for the entries in the Jacobian $\mathcal{F}(\hat{x}, \hat{p}, W, 0)$ with respect to $\hat{x}$ and $\mathcal{B}(\check{x}, \check{p}, W, 0)$ with respect to $\check{x}$.

Chapter 1

Basic Cardiovascular Physiology and Control Mechanisms

In modeling the cardiovascular system, relevant concepts underlying its physiology should be understood. In this chapter, we present some physiological facts needed in the modeling process. The first four sections are dedicated to the physiology of the cardiovascular system and the biological processes and activities in the heart. The last two sections provide a brief overview of the physiological controls of blood flow, the baroreceptor and local metabolic controls. Most of the materials covered in this chapter can be found in the textbook of Medical Physiology by Guyton and Hall (2006) [15] and Batzel et al. (2007) [2]. Some other relevant references are Hoppensteadt and Peskin (2002) [19], Klabunde (2005) [29], Levick (2003) [32], Ottesen (2004) [41], and Westerhof et al. (2005) [55].

1.1 The Cardiovascular System

The human cardiovascular system is a transport system in which its primary task is to provide the various cells with the needed oxygen and other substrates for metabolism. Carbon dioxide and other waste products of metabolism must be removed. Moreover, it transports hormones and enzymes which regulate cell functions. In general, its function is to maintain an appropriate environment in all the tissue fluids of the body for optimal survival and function of the cells. The cardiovascular

system consists of two vascular circuits: the pulmonary circuit and the systemic circuit. The pulmonary circuit carries blood through the lung region while the systemic circuit transports blood through the tissue region.

Let us try to understand the role of each part in the cardiovascular system. The *arteries* transport blood under high pressure to the tissues. They have strong vascular walls, and blood flows at a high velocity in the arteries. The *arterioles* are the last small branches of the arterial system serving as control ducts through which the blood is released into the capillaries. They have strong muscular walls that can constrict or dilate, the arterioles thus having the capability of vastly altering blood flow in each tissue bed in response to the need of the tissue. The *capillaries* provide venue where fluid, nutrients, electrolytes, hormones, and other substances exchange with the blood and the interstitial fluid. For this purpose, they have very thin walls and have numerous minute capillary pores permeable to water and other small molecular substances. The *venules* collect blood from the capillaries. They gradually merge into progressively larger veins. The *veins* act as conduits for transport of blood from the venules back to the heart. Venous walls are thin since the pressure in the venous system is very low. However, they are muscular enough to contract or expand serving as a controllable reservoir for extra blood.

Figure 1.1 depicts the blood flow in the cardiovascular system through the systemic and pulmonary circuits. The oxygenated (red) blood, rich in oxygen (O_2), is pumped by the left ventricle into aorta, the first vessel of the arterial tree distributing the blood to all regions of the body. The vasculature branches into progressively smaller vessels, from larger to smaller systemic arteries, further on to systemic arterioles and down to the systemic capillaries. In the capillary region, O_2 and nutrients needed for metabolism are delivered and waste products such as carbon dioxide (CO_2) are removed. Leaving the systemic capillaries, the deoxygenated (blue) blood enriched with CO_2 and depleted of O_2, enters the systemic venous system. The venous blood then reaches the right atrium through veins of progressively larger diameter (venules, small veins, superior and inferior vena cava). The venous

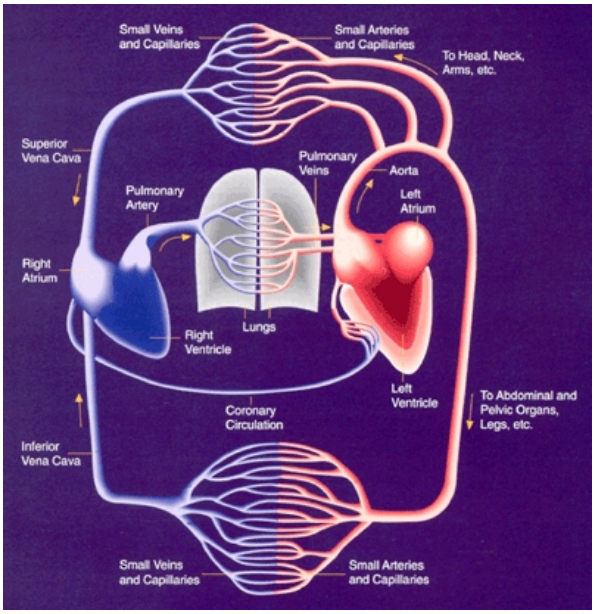

Figure 1.1: The blood flow in the cardiovascular system. (source: http://www.niaaa.nih.gov /NR/rdonlyres/ BF321698-FDCA-443F-9D66-6E00F445CDAF/0/270f1.gif)

blood is then collected by the right ventricle, which pumps it into the pulmonary artery and the pulmonary arterial tree distributing the blood to the alveolar region of the lungs. In the pulmonary capillaries, the CO_2 in the blood is removed and replaced with O_2 making the blood turn red. Then the blood flows through the pulmonary veins to the left atrium and further collected by the left ventricle and the cycle starts over again.

1.2 The Heart

The heart plays the central role in the cardiovascular system. It functions as two separate pumps: a *right heart* that pumps blood through the pulmonary circuit, and a *left heart* that pumps blood through the systemic circuit. Each of these hearts is composed of an atrium and a ventricle. Thus, the heart consists of four chambers in total: left atrium, left ventricle, right atrium, and right ventricle. The atria act as weak primer pump helping to efficiently load the ventricle with sufficient blood. The ventricles serve as the primary pumps propelling the blood to the system either through the pulmonary circulation by the right ventricle or the systemic

circulation by the left ventricle. The left ventricle has a much thicker and muscular wall than the right ventricle since it has to generate greater pressures. There are four valves within the heart that ensure the blood flows correctly, from atria to ventricle (atrioventricular valves), and then to the arterial circulations through the outflow valves. The atrioventricular valves are the *tricuspid valve* for the right ventricle and the *mitral valve* for the left ventricle. While the outflow valves are the pulmonary valve for the right ventricle and the aortic valve for the left ventricle. These valves work like gates that only open one way and when pushed on. Each valve opens and closes once per heart beat or about once every second. Figure 1.2 shows the four chambers of the heart and the heart valves.

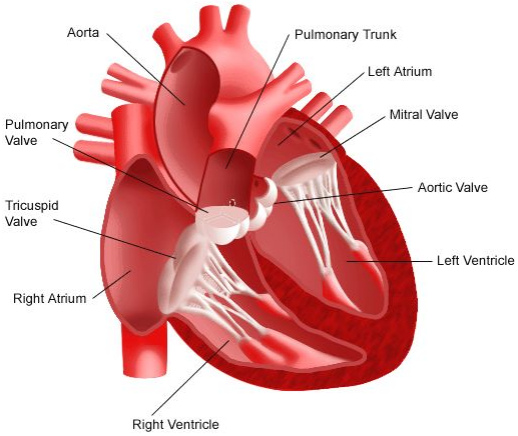

Figure 1.2: The heart. (source: http://bwh-www.bhexhale.com/womenshealth/hearthealth/ assets/ images/ lowlevel_imgs/ heart-valves/img.gif)

1.3 The Cardiac Cycle

Cardiac cycle refers to the the cardiac events that occur from the beginning of one heartbeat to the beginning of the next. It consists of two phases namely, ***systole*** and ***diastole***. Systole is a period of contraction. It starts with the contraction of the heart muscles causing the ventricular pressure to increase. During this period, the atrioventricular valves are closed. As long as the ventricular pressure is lower than the pressure in the artery (aorta or pulmonary artery), the outflow valves are

closed. In this phase of contraction, the volume in the ventricle does not change and thus called *isovolumetric contraction*. Once the ventricular pressure reaches the pressure in the artery, the outflow valve opens. It is about 80 [mmHg] for the left ventricle and about 10 [mmHg] for the right ventricle. Then the ejection phase of the systole starts. Each ventricle ejects approximately 65% of the volume which was in the ventricle at the beginning of the systole during resting condition. The quotient $\frac{\text{“ejected volume”}}{\text{“ventricular volume”}}$ at the beginning of the systole is known as the *ejection fraction* of the ventricle. The ventricular pressure continues to increase during the ejection phase. For the left ventricle it goes up to approximately 120 [mmHg] and about 25 [mmHg] for the right ventricle. At the end of the systole the heart muscle starts to relax causing a rapid decrease in the ventricular pressure. When the ventricular pressure falls below the arterial pressure (now is higher than the pressure at the beginning of the systole), the outflow valve closes and the diastole starts. Diastole is a period of relaxation. The first phase of the diastole is an *isovolumetric relaxation* of the heart muscle in which ventricular volume is not changed though its pressure is tremendously decreased. The ventricular pressure drops until it reaches the pressure in the atria which is about 5 [mmHg] for the left ventricle and 8 [mmHg] for the right ventricle. Then the inflow valves open. The heart muscle relaxation continues causing a further drop in the ventricular pressure below the arterial pressure. As a consequence of the pressure difference, blood flows into the ventricle known as the filling phase. The diastole ends when the heart muscle starts to contract increasing ventricular pressure above the pressure in the atria and the inflow valve closes.

Figure 1.3 illustrates the cardiac cycle. This figure is adapted from Klabunde (2005) [29]. Refer to this material for detailed information concerning the phases in the cardiac cycle.

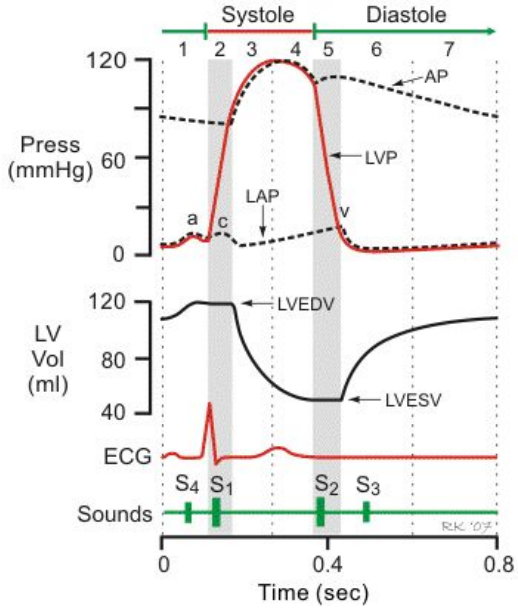

Figure 1.3: The cardiac cycle. (source: http://www.cvphysiology.com/Heart%20Disease/HD002%20cardiac%20cycle%202007r1.gif)

1.4 Cardiac Output

Cardiac output is the amount of blood pumped into the aorta each minute by the heart which flows through the circulation, in particular, the cardiovascular system. It varies widely with the level of activities of the body. Some of the factors that directly affect the cardiac output are the basic level of body metabolism, person's age, person's body size and person's activity such as exercise. The normal resting cardiac output for young, healthy men is about 5.6 [L/min] ($\approx$ 93.33 [mL/sec]). For women, it is about 4.9 [L/min] ($\approx$ 81.67 [mL/sec]).

The cardiac output is given as the product of the heart rate and the ventricular stroke volume (V_{str}), the blood volume ejected each time the heart beats. V_{str} is the difference between the *end-diastolic volume* V_{dias} and the *end-systolic volume* V_{syst}. V_{dias} is the volume of the ventricle prior to contraction, that is, the volume in the ventricle at the end of the filling process when the inflow valve closes. V_{syst} is the residual blood volume left in the ventricle after ejection, that is, the volume remaining in the ventricle after the outflow valve closes at the end of the systole. Three primary mechanisms regulate the end-diastolic and end-systolic volume, and there-

fore, stroke volume. These are the preload, afterload and inotropy (cf. Klabunde (2005) [29]).

The left ventricular pressure-volume loop is depicted in Figure (1.4). It also points out the phases when the mitral and aortic valves are open and closed, filling and ejection processes, isovolumetric relaxation and contraction, and the left ventricular stroke volume.

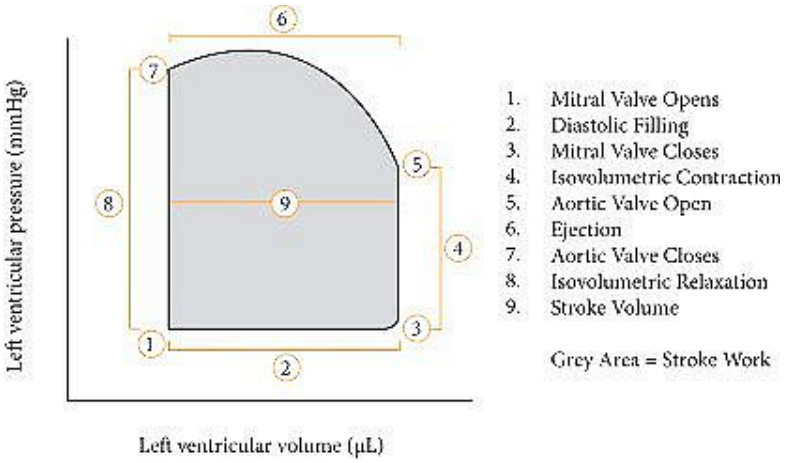

Figure 1.4: The pressure-volume loop of the left ventricle. (source: http:// www.adinstruments.com/ solutions/images_new/ pv01.jpg)

There are numerous control mechanisms acting in the cardiovascular system. These act to adjust the blood flow in different body regions depending on various needs. There are global and local control loops. The global control loops including the central nervous system provide overall conditions which are necessary to sustain flows controlled by autoregulatory mechanisms of the various tissue regions and organs. For our purpose, we will consider only the baroreceptor loop control. It is one of the most important global control loops, as far as short-term regulation of the cardiovascular system is concerned. We will also consider local regulatory mechanisms which regulate local blood flow to meet local metabolic demands. The following sections presents the baroreceptor and local metabolic controls.

1.5 Central Nervous Regulation: Baroreceptors

The nervous control of the cardiovascular system has global functions, such as redistributing blood flow to different areas of the body, increasing or decreasing pumping activity by the heart, and, providing rapid control of systemic arterial pressure. The autonomic nervous system controls the circulation. It consists of the sympathetic and parasympathetic nervous system.

The sympathetic innervation of the small arteries and arterioles allows an increase or decrease of resistance to blood flow and thereby a decrease or increase in the rate of blood flow through the tissues. On the other hand, sympathetic innervation of the large veins decreases or increases the volume of these vessels. Moreover, sympathetic stimulation increases the activity of the heart, both increasing the heart rate and enhancing its strength of contraction. The parasympathetic nervous system controls the heart rate through its parasympathetic nerve fibers to the heart in the vagus nerves. Parasympathetic stimulation decreases the heart rate.

The capability of the nervous control of the circulation to cause rapid increases in arterial pressure is one of its most important functions. An example is the increase in pressure during muscle exercise. The best known nervous mechanisms for arterial pressure control is the *baroreceptor reflex* or *baroreceptor loop*. Basically, it is initiated by stretch receptors called the *baroreceptors* or *pressoreceptors*. They are spray-type nerve endings located at the carotid sinus and the aortic arch (see Figure 1.5). An increase in the arterial pressure stretches the baroreceptors and causes them to transmit nerve impulses to the central nervous system (i.e., medulla of the brain). "Feedback" impulses are then sent back through the autonomic nervous system causing the arterial pressure to reach the required level.

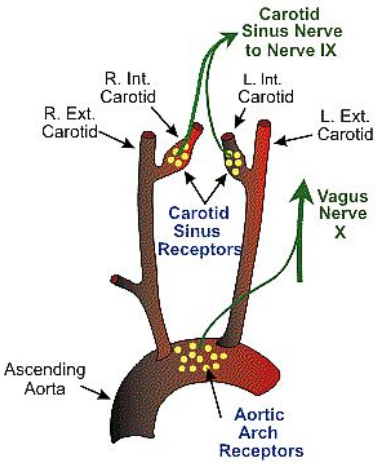

Figure 1.5: The arterial baroreceptors. (source: http://mor.phe.us/jtw/Gateway/Projects/ Vertebrates/images/ EvolutionOfTheHeart/ArterialBaroreceptors.gif)

1.6 Local Metabolic Control

The ability of a tissue to control the local blood flow in proportion to the metabolic needs is one of the fundamental principles of circulatory function. Some of the specific needs for blood flow include the delivery of oxygen and other nutrients, such as glucose, amino acids and fatty acids to the tissues, removal of carbon dioxide and hydrogen ions from the tissues and the transport of various hormones and other substances to the different tissues. In addition, some organs have specific needs. For example, blood flow to the skin determines the heat loss from the body and helps control body temperature. Also, kidneys need adequate quantities of blood plasma to excrete the waste products of the body.

One should note the fact, that it is impossible to allow a very large blood flow all the time through every tissue of the body to satisfy its needs. Because, this would require many times more blood flow than the heart can pump. It has been shown through experiments that the blood flow to each tissue is usually regulated at the minimal level that will supply the tissue's requirements. In tissues for which the delivery of oxygen is the most important, blood flow is always controlled at a level only slightly more than required to maintain full tissue oxygenation. Controlling

the blood flow in an exact way provides sufficient oxygen to the tissues while at the same time keeping the workload on the heart at a minimum.

There are two phases for the local blood flow control, namely: acute control and long-term control. In our case, we will just briefly talk about the acute control. This is achieved by rapid changes in local vasodilation or vasoconstriction of the arterioles, metarterioles, and precapillary sphincters. This occurs within seconds to minutes providing rapid maintenance of appropriate local tissue blood flow. It has been shown that increasing the rate of metabolism in a local tissue up to eight times than the normal, increases the blood flow acutely about fourfold. Also, when the availability of oxygen to tissues decreases, the blood flow through the tissues increases too. Two basic theories were proposed for the regulation of local blood flow when either the rate of tissue metabolism changes or the availability of oxygen changes. First is the *vasodilator theory* proposing that the greater the rate of metabolism or the less the availability of oxygen or some other nutrients to a tissue, the greater the rate of formation of vasodilator substances in the tissue cells. These vasodilator substances are believed to diffuse through the tissues causing dilation. The second theory is known as the *oxygen lack* (more generally, *nutrient lack) theory*. Oxygen and other substances are metabolic nutrients required to cause vascular muscle contraction. Thus, in the absence of adequate oxygen, the blood vessels would relax and therefore naturally dilate. Moreover, an increased consumption of oxygen in the tissues due to increased metabolism could decrease the availability of oxygen to the smooth muscle fibers in the local blood vessels that would cause local vasodilation. The aforementioned theories could explain acute flow regulation in response to the metabolic needs of the tissues. Thus far, we considered the mechanism of local blood flow control in response to the tissue's metabolic needs. This mechanism is called ***metabolic mechanism***.

Chapter 2

Mathematical Modeling of the Cardiovascular System

In this chapter, cardiovascular modeling procedures will be discussed. The mathematical modeling is focused on the reaction of the cardiovascular system to a constant ergometric workload. Modeling discussions are mainly followed from Kappel and Peer (1993) [26] and related works, Batzel et. al (2007) [2] and Olufsen et.al (2009) [46].

The cardiovascular model presented here is depicted in Figure 2.1. It includes arterial and venous pulmonary, left and right ventricles, systemic aorta, finger arteries, and arterial and venous systemic compartments. In the compartments, pressures and compliances are denoted by P and c, respectively. The resistances are denoted by R. In the right ventricle, Q stands for the cardiac output and S for the contractility. The subscripts of P, c, Q and S stand mainly for the name of the compartments. That is, $ap, vp, \ell v, sa, fa, as, vs$, and rv correspond respectively to the arterial pulmonary, venous pulmonary, left ventricle, systemic aorta, finger arteries, arterial systemic, venous systemic and right ventricle compartments. For the resistances, $R_{mv}(t)$ and $R_{av}(t)$ denote the time-varying mitral valve and aortic valve resistances, respectively, R_{pp} is the pulmonary peripheral resistance, R_{sc_1} is the systemic circuit resistance connecting the aorta and the finger compartments, R_{sc_2} is the systemic circuit resistance joining the aorta and the rest of the arterial

systemic compartments, R_{sp_f} is the systemic peripheral resistance between finger and the venous systemic compartments and R_{sp} is the systemic peripheral resistance from the arterial systemic to the venous systemic compartments. Moreover, $E_{\ell v}(t)$ is the time-varying elastance of the left ventricle.

This model is a combination of two existing cardiovascular models: a non-pulsatile global model adapted from the earlier work of Kappel and Peer (1993) [26] and a simplified pulsatile left heart model by Olufsen et al. (2009) [46]. The non-pulsatile global model incorporates all the essential subsystems such as systemic and pulmonary circulation, left and right ventricles, baroreceptor loop, etc. It is based on a four compartment model by Grodins describing the mechanical part of the cardiovascular system. Included in the model are the basic mechanisms such as Starling's law of the heart, the Bowditch effect and autoregulation in the peripheral regions. This model considered the mean values over one heart cycle instead of the instantaneous values. It has been developed to investigate the response of the system to a short term submaximal workload. The basic control autoregulatory mechanisms were constructed assuming that the regulation is optimal with respect to a cost criterion. The model provided a satisfactory description of the overall reaction of the cardiovascular system under a constant ergometric workload imposed on a test person on a bicycle-ergometer. Further studies have been done to include the respiratory system, see Timischl (1998) [54]. The model was also extended and used to describe the response of the cardiovascular-respiratory system under orthostatic stress condition, see for example Fink et al. (2004) [34] and Kappel et al. (2007) [24].

On the other hand, in the study done by Olufsen et. al (2009) [46], a simple lumped parameter cardiovascular model was developed to analyze cerebral blood flow velocity and finger blood pressure measurements during orthostatic stress (sit-to-stand). This pulsatile left heart model utilizes a minimal cardiovascular structure to close the circulatory loop. The model consists of two arterial compartments and two venous compartments combining vessels in the body and the brain, and a heart compartment representing the left ventricle. It was simplified to account for the

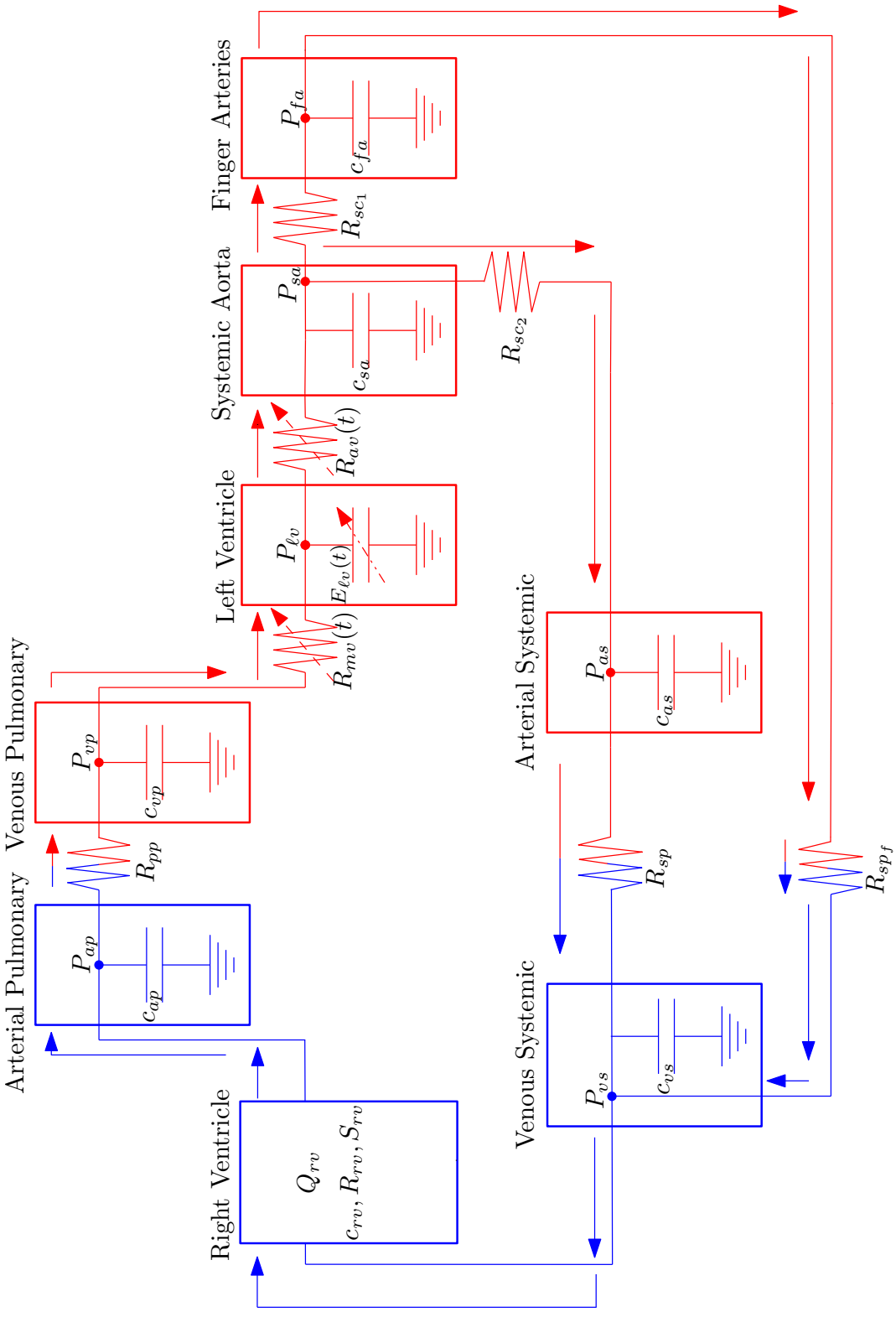

Figure 2.1: The electric circuit analog of the global pulsatile model depicting the blood flow in the pulmonary and systemic circuit including the systemic aorta and finger arteries compartment.

cardiovascular dynamics during (sitting) rest condition.

The first goal of the modeling effort is to integrate the (Olufsen) left heart model with the (Kappel) global cardiovascular model. The main objective of the study is to develop a global pulsatile lumped compartment model that predicts pressures in the systemic and pulmonary circulation, as well as the pulsatile pressures in the finger arteries.

Figure 2.2 shows the combined cardiovascular model depicting the non-pulsatile (Kappel) part, pulsatile left heart (Olufsen) model and the modifications made. The systemic aorta compartment is added for it is the site of the baroreceptor loop. Finger arteries compartment is included to reflect measurements of pulsatile pressures.

The current model is mathematically formulated in terms of an electric circuit analog. The blood pressure difference plays the role of voltage, the blood flow plays the role of current, the stressed volume plays the role of an electric charge, the compliances of the blood vessels play the role of capacitors, and the resistances are the resistors. The stressed volume in a compartment is the difference between total and unstressed volume (i.e., the volume in a compartment at zero transmural pressure). Thus, stressed volume is the additional volume added to the unstressed volume when positive transmural pressure causes a stretching of the vascular walls.

The following are the basic assumptions of the modeling process:

- The vessels in the arterial and venous parts of the systemic or pulmonary circuits are lumped together as a single compartment for each of these parts. Each compartment is considered as a vessel with compliant walls in which its volume is characterized by the pressure in the vessel. Thus, these vessels are called *compliance vessels*.
- The systemic peripheral or pulmonary peripheral region is composed of capillaries, arterioles, and venules which are lumped together into a single vessel. These vessels are considered to be pure resistance to blood flow and characterized only

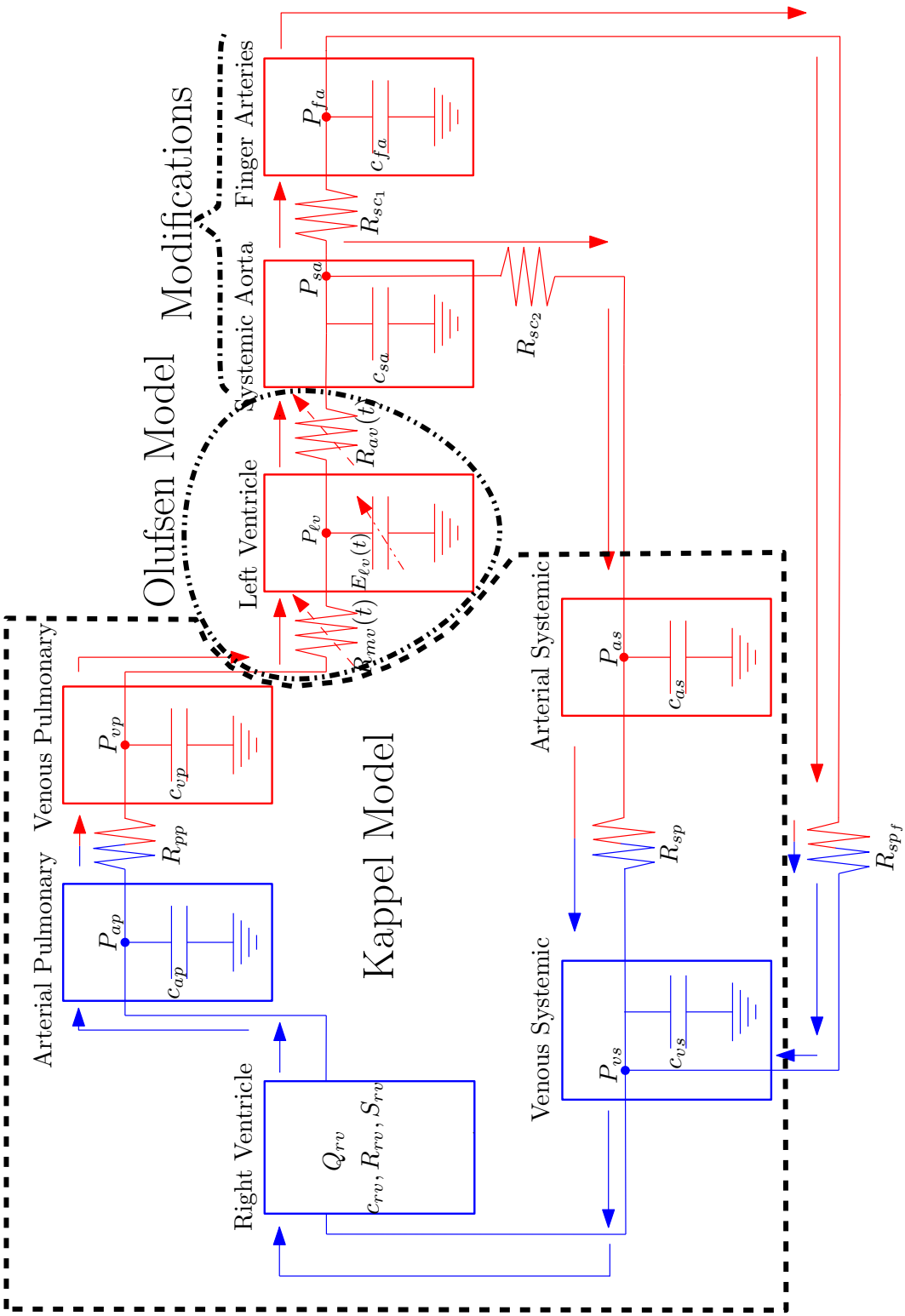

Figure 2.2: The cardiovascular model showing the (Kappel) non-pulsatile global model, (Olufsen) pulsatile left heart model and the model modifications.

by flow through the vessel. Therefore these vessels are called *resistance vessels*.

- The atria are not represented in the model. It is assumed that the right atrium is part of the venous systemic compartment and the left atrium is part of the venous pulmonary compartment.

2.1 Blood Volume in the Compartment

For each compartment, we associate the pressure $P(t)$ and the volume $V(t)$ of the blood. Assuming linear relationship between the transmural pressure and the total volume, we have

$$V(t) = cP(t), \tag{2.1}$$

where c represents the compliance of the compartment which is assumed to be constant. In this case, the unstressed volume is zero and the stressed volume equals the total volume in the compartment. Generally, the total volume in the compartment can be expressed as

$$V(t) = cP(t) + V_u, \tag{2.2}$$

where V_u denotes the unstressed volume. A more physiologically realistic approach is to consider that the relation between pressure and total volume is $V = f(P)$ which is nonlinear. In this case the unstressed volume is given by $V_u = f(0)$ and the compliance, $c(P)$ at pressure P is $f'(P)$ assuming smoothness on f.

For simplicity, we used (2.2) assuming $V_u = 0$ in most of the compartments except in the left ventricle. This is mainly to avoid introduction of additional parameters which cannot be observed directly. This however introduces a modeling error that needs to be considered for further investigations.

2.2 Blood Flow and Mass Balance Equations

The blood flow is described in terms of the mass balance equations, that is, the rate of change for the blood volume $V(t)$ in a compartment is the difference between the

flow into and out of the compartment (see Figure 2.3).

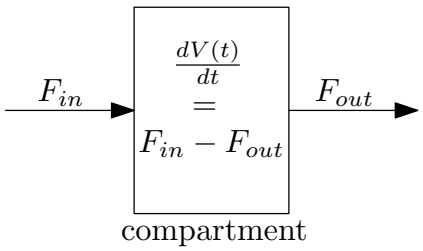

Figure 2.3: The rate of change for the volume in a compartment assuming mass balance equation.

For a generic compartment, we have

$$\frac{dV(t)}{dt} \;=\; \frac{d}{dt}\left(cP(t)\right) \;=\; F_{in} - F_{out}\;, \tag{2.3}$$

where c denotes the compliance, $P(t)$ the blood pressure in the compartment and F_{in} and F_{out} are the blood flows into and out of the compartment, respectively. The loss term in the current compartment is the gain term in the adjacent compartment. Also, the flow F between two compartments can be described by Ohm's law. That is, it depends on the pressure difference between adjacent compartments and on the resistances R against blood flow. Thus we have the relation

$$F \;=\; \frac{1}{R}\left(P_1 - P_2\right), \tag{2.4}$$

where P_1 and P_2 are pressures from adjacent generic compartments 1 and 2, respectively. Hence, for systemic peripheral flow F_{sp} and pulmonary peripheral flow F_{pp}, we have

$$\begin{aligned} F_{sp} \;&=\; \frac{1}{R_{sp}}\left(P_{as} - P_{vs}\right) + \frac{1}{R_{sp_f}}\left(P_{fa} - P_{vs}\right)\;, \\ F_{pp} \;&=\; \frac{1}{R_{pp}}\left(P_{ap} - P_{vp}\right)\;. \end{aligned} \tag{2.5}$$

The blood flow out of the venous systemic compartment is the cardiac output $Q_{rv}(t)$ which is the blood flow into the arterial pulmonary. The cardiac output generated by the right ventricle is given by

$$Q_{rv}(t) \;=\; HV_{\mathrm{str}}(t), \tag{2.6}$$

where H is the heart rate and $V_{\text{str}}(t)$ is the stroke volume, that is the blood volume ejected by one beat of the ventricle.

Moreover, the change in the volume in the left ventricle $\frac{dV_{\ell v}(t)}{dt}$ as modeled in [46] is

$$\frac{dV_{\ell v}(t)}{dt} = \frac{P_{vp}(t) - P_{\ell v}(t)}{R_{mv}(t)} - \frac{P_{\ell v}(t) - P_{sa}(t)}{R_{av}(t)} , \tag{2.7}$$

where $P_{vp}(t), P_{\ell v}(t)$ and $P_{sa}(t)$ are the blood pressures in the venous pulmonary, left ventricle and systemic aorta compartments and the time-varying elastances $R_{mv}(t)$ and $R_{av}(t)$ in the mitral valve and aortic valve, respectively.

2.3 Filling and Ejection Processes in the Right Ventricle

In this section, we will consider the filling process in some detail and the ejection process in a global manner. We will follow the discussions in Batzel et. al (2007) [2] to model these processes in the right ventricle. Let us consider the inflow into the ventricle which depends on the pressure difference between the filling pressure and the pressure in the right ventricle when the inflow valve (tricuspid valve) is open. As in equation (2.4) (taking note that $F = \frac{dV(t)}{dt}$),

$$\frac{dV_{rv}(t)}{dt} = \frac{1}{R_{rv}} \left(P_{vs}(t) - P_{rv}(t)\right) , \tag{2.8}$$

where $V_{rv}(t)$ is the volume in the right ventricle at time t after the filling process has begun, $P_{rv}(t)$ is the pressure in the right ventricle, $P_{vs}(t)$ is the venous systemic filling pressure representing the pre-load to the right ventricle, and R_{rv} is the total resistance to the inflow into the right ventricle.

Also, let us assume the following as in Batzel et al. (2007) [2]:

- During the diastolic period, $P_{vs}(t) \equiv P_{vs}$ is a constant. In fact, $P_{vs}(t)$ does not vary much. Also, we assume that the arterial pressure P_{ap}, denoting the after-load to the right ventricle, remains constant during systolic period. It is

also important to note that the systolic period duration is shorter than that of the diastolic period.

- The end-systolic volume at the end of a heart beat is the same as the end-systolic volume of the previous beat.
- The compliance c_{rv} of the relaxed ventricle remains constant during the diastolic period.

Now, let us talk about the filling process in the right ventricle. During this phase, the right ventricle is in a relaxed state and has the end-systolic volume. That is, $V_{rv}(0) = V_{\text{rv,syst}}$, which is the initial condition for the differential equation (2.8). Assuming that the relaxed right ventricle has unstressed volume $V_u = 0$, its volume-pressure relation would be given by

$$V_{rv}(t) \;=\; c_{rv} P_{rv}(t) \;. \tag{2.9}$$

Solving $P(t)$ in terms of $V_{rv}(t)$ and c_{rv} in equation (2.9) and plugging it in equation (2.8) will yield the following differential equation

$$\frac{dV_{rv}(t)}{dt} + \frac{1}{c_{rv}R_{rv}} V_{rv}(t) - \frac{1}{R_{rv}} P_{vs} \;=\; 0 \;, \quad V_{rv}(0) = V_{\text{rv,syst}} \;. \tag{2.10}$$

Integrating the above equation using the constant of variation formula will obtain

$$V_{rv}(t) \;=\; V_{\text{rv,syst}} e^{-t(c_{rv}R_{rv})^{-1}} + c_{rv}P_{vs}\left(1 - e^{-t(c_{rv}R_{rv})^{-1}}\right) \;. \tag{2.11}$$

Let the duration of the filling process be denoted by $t_d = t_d(H)$. After t_d the volume in the right ventricle is the end-diastolic volume, $V_{rv}(t_d) = V_{\text{rv,diast}}$ which is given by

$$V_{\text{rv,diast}} \;=\; V_{\text{rv,syst}} e^{-t_d(H)(c_{rv}R_{rv})^{-1}} + c_{rv}P_{vs}\left(1 - e^{-t_d(H)(c_{rv}R_{rv})^{-1}}\right) \;. \tag{2.12}$$

Setting

$$k_r(H) \;=\; e^{-t_d(H)(c_{rv}R_{rv})^{-1}} \quad \text{and} \quad a_r(H) \;=\; 1 - k_r(H) \;, \tag{2.13}$$

we have

$$V_{\text{rv,diast}} \;=\; V_{\text{rv,syst}} k_r(H) + c_{rv}P_{vs}a_r(H) \;. \tag{2.14}$$

For the duration of the diastole we assume

$$t_d \;=\; t_d(H) \;=\; \frac{1}{H} - \frac{\kappa}{H^{1/2}} \;, \tag{2.15}$$

where κ is in the range of $0.3 - 0.4$ when time is measured in seconds and in the range of $0.0387 - 0.0516$ when time is measured in minutes. The time duration of the systole $t_s = \frac{\kappa}{H^{1/2}}$ is known as the *Bazett's formula* (cf. Bazett (1920) [3]). Then clearly equation (2.15) follows from $t_d + t_s = \frac{1}{H}$.

Let us now consider the ejection process. At the start of the ejection, the right ventricle contains the end-diastolic volume $V_{\text{rv,diast}}$. Then it ejects the stroke volume $V_{\text{rv,str}}$ against the arterial pulmonary blood pressure P_{ap} and thus leaving the end-systolic volume $V_{\text{rv,syst}}$. Hence, the stroke volume in the right ventricle is given by

$$V_{\text{rv,str}} \;=\; V_{\text{rv,diast}} - V_{\text{rv,syst}} \;. \tag{2.16}$$

According to the Frank-Starling mechanism (cf. Patterson, et al. (1914) [43]), a larger distention of the heart caused by increased filling of the ventricle during diastole causes an increased force of contraction during the following systole. Using this concept, we have the relation

$$V_{\text{rv,str}} \;=\; S_{rv}\frac{V_{\text{rv,diast}}}{P_{ap}} \;, \tag{2.17}$$

where P_{ap} is the arterial pulmonary pressure and S_{rv} is the contractility of the right ventricle characterizing its force of contraction. Obviously, we must have

$$V_{\text{rv,str}} \leq V_{\text{rv,diast}} \;, \tag{2.18}$$

otherwise more blood volume will be ejected than has been contained in the right ventricle. Thus, the above relation (2.17) suggests that

$$\frac{S_{rv}}{P_{ap}} \;\leq\; 1 \;. \tag{2.19}$$

A smooth function that approximates $\min(S_r, P_{ap})$ is given by

$$f_\epsilon(S_r, P_{ap}) \;=\; \begin{cases} S_r & \text{if } 0 \leq S_r \leq (1-\epsilon)P_{ap} \;, \\ -\dfrac{1}{4\epsilon P_{ap}}S_r^2 + \dfrac{1+\epsilon}{2\epsilon}S_r - \dfrac{(1-\epsilon)^2}{4\epsilon}P_{ap} & \text{if } (1-\epsilon)P_{ap} < S_r \leq (1+\epsilon)P_{ap} \;, \\ P_{ap} & \text{if } S_r > (1+\epsilon)P \;, \end{cases} \tag{2.20}$$

where $\epsilon < 0$ is arbitrarily small. In Kappel et al. (1997) [25] and Timischl (1998) [54], this function is defined as

$$f(S_{rv}, P_{ap}) \;=\; 0.5\,(S_{rv} + P_{ap}) - 0.5\left((P_{ap} - S_{rv})^2 + 0.001\right)^{1/2} \;. \tag{2.21}$$

This function also chooses the minimum between S_{rv} and P_{ap}. The term 0.001 is used to smoothen $f(S_{rv}, P_{ap})$ around $S_{rv} = P_{ap}$. The latter is used in the numerical simulations due to its sufficient smoothness property. Hence, S_{rv} in (2.17) can be replaced by $f(S_{rv}, P_{ap})$ obtaining

$$V_{\mathrm{rv,str}} \;=\; f(S_{rv}, P_{ap})\frac{V_{\mathrm{rv,diast}}}{P_{ap}} \;. \tag{2.22}$$

Using equations (2.14), (2.16) and (2.22), the stroke volume of the right ventricle $V_{\mathrm{rv,str}}$ can be expressed as

$$V_{\mathrm{rv,str}} \;=\; \frac{c_{rv}P_{vs}a_r(H)f(S_{rv}, P_{ap})}{a_r(H)P_{ap} + k_r(H)f(S_{rv}, P_{ap})} \;. \tag{2.23}$$

We can now write the right ventricular cardiac output as

$$Q_{rv} \;=\; H\frac{c_{rv}P_{vs}a_r(H)f(S_{rv}, P_{ap})}{a_r(H)P_{ap} + k_r(H)f(S_{rv}, P_{ap})} \;. \tag{2.24}$$

2.4 Opening and Closing of the Heart Valves

In this section, we will model the opening and closing of the heart valves in the left heart, namely, the mitral and the aortic valves. In order to model the left ventricle as a pump, the opening and closing of the mitral and aortic valves must be included. During the diastole, the mitral valve opens allowing the blood to flow to the left ventricle while the aortic valve is closed. Then the heart muscles start to contract, increasing the pressure in the left ventricle. When the left ventricular pressure exceeds the aortic pressure, the aortic valve opens, propelling the pulse wave through the vascular system (cf. Olufsen et. al (2005) [39]).

Rideout (1991) [47] originally proposed a model of the succession of opening and closing of these heart valves. A piecewise continuous function was later developed by Olufsen et al., see for example [39] and [46]. This function represents the vessel

resistance which characterized the "open" valve state using a small baseline resistance and the "closed" state using a value of larger magnitudes. The time-varying resistances are given as

$$\begin{aligned} R_{mv}(t) &= \min\left(R_{mv,open} + e^{(-2(P_{vp}(t)-P_{\ell v}(t)))}, 10\right) , \\ R_{av}(t) &= \min\left(R_{av,open} + e^{(-2(P_{\ell v}(t)-P_{sa}(t)))}, 10\right) , \end{aligned} \tag{2.25}$$

where $R_{mv}(t)$ and $R_{av}(t)$ are the time varying mitral valve and aortic valve resistances, respectively. The first equation suggests that when $P_{\ell v}(t) < P_{vp}(t)$, the mitral valve opens and the blood enters the left ventricle. As $P_{\ell v}(t)$ increases and becomes greater than $P_{vp}(t)$, the resistance exponentially grows to a large value. A similar remark can be deduced from the second equation. The value 10 is chosen to ensure that there is no flow when the valve is closed and remains there for the duration of the closed valve phase. The open and closed transition is not discrete. An exponential function is used for the partially opened valve, with the amount of "openness" (cf. Olufsen et. al (2009) [46]).

For simplicity purposes, one can assume that the time dependent resistances $R_{mv}(t)$ and $R_{av}(t)$ are given by

$$\begin{aligned} R_{mv}(t) &= \begin{cases} \infty & \text{for } P_{\ell v}(t) > P_{vp}(t) , \\ R_{mv,open} & \text{for } P_{\ell v}(t) \leq P_{vp}(t) , \end{cases} \\ R_{av}(t) &= \begin{cases} \infty & \text{for } P_{\ell v}(t) < P_{sa}(t) , \\ R_{av,open} & \text{for } P_{\ell v}(t) \geq P_{sa}(t) . \end{cases} \end{aligned} \tag{2.26}$$

This means that when the left ventricular pressure is greater than the venous pulmonary pressure (i.e., $P_{\ell v}(t) > P_{vp}(t)$), the mitral valve resistance is so large that flow to the left ventricle is impossible. This is the state when the mitral valve is closed. As soon as the left ventricular pressure reaches the venous pulmonary pressure, the mitral valve opens and the blood flows to the left ventricle. In this case, the mitral valve resistance is assumed to be a constant value. The mitral valve remains open as long as left ventricular pressure is less than the venous pulmonary pressure. Similarly, when the left ventricular pressure is less than the pressure in the aorta, the aortic valve is closed and its resistance is too large making the blood flow to

the systemic aorta compartment impossible. When left ventricular pressure reaches the systemic aortic pressure, the aortic valve opens and remains open as long as it exceeds the systemic aortic pressure. Here, the blood flows from the left ventricle to the systemic aorta compartment with the aortic resistance assumed to be constant during this duration. This time-varying resistance formulation expressed in (2.26) is used in our numerical simulations.

2.5 Time-Varying Elastance Function

The slope of a pressure-volume curve which has pressure on the y-axis and volume on the x-axis is called the *ventricular elastance* or simply the *elastance*. It is a measure of "stiffness" of the ventricles. Elastance and compliance are inverse of each other.

According to Ottesen et al. (2004) [41], the relationship between the left ventricular pressure $P_{\ell v}$ and the stressed left ventricular volume $V_{\ell v}(t)$ is described by

$$P_{\ell v}(t) = E_{\ell v}(t)\left(V_{\ell v}(t) - V_d\right) \ , \tag{2.27}$$

where $E_{\ell v}(t)$ is the time-varying ventricular elastance and V_d (constant) is the ventricular volume at zero diastolic pressure (or simply the unstressed left ventricular volume).

In [46], the time-varying elastance function $E_{\ell v}(t)$ is given by

$$E_{\ell v}(t) = \begin{cases} E_m + \dfrac{E_M - E_m}{2}\left[1 - \cos\left(\dfrac{\pi t}{T_M}\right)\right], & 0 \le t \le T_M \\ E_m + \dfrac{E_M - E_m}{2}\left[\cos\left(\dfrac{\pi}{T_r}\left(t - T_M\right)\right) + 1\right], & T_M \le t \le T_M + T_r \\ E_m, & T_M + T_r \le t < T \ . \end{cases} \tag{2.28}$$

This is a modification of a model developed by Heldt et al. (2002) [17]. Here, T_M denotes the time of peak elastance, and T_r is the time for the start of diastolic relaxation. These are both functions of the length of the cardiac cycle T. These

parameters are set up as fractions where $T_{M,frac} = T_M/T$ and $T_{r,frac} = T_r/T$. Moreover, E_m and E_M are the minimum and maximum elastance values, respectively. The above elastance function (2.28) is sufficiently smooth. Its derivative can be easily computed as follows

$$\frac{dE_{\ell v}(t)}{dt} = \begin{cases} \dfrac{E_M - E_m}{2}\left[\dfrac{\pi}{T_M}\sin\left(\dfrac{\pi t}{T_M}\right)\right], & 0 \le t \le T_M \\ \dfrac{E_M - E_m}{2}\left[-\dfrac{\pi}{T_r}\sin\left(\dfrac{\pi}{T_r}(t - T_M)\right)\right], & T_M \le t \le T_M + T_r \\ 0, & T_M + T_r \le t < T\ . \end{cases} \tag{2.29}$$

Below is a figure showing the left ventricular time-varying elastance as given in (2.28).

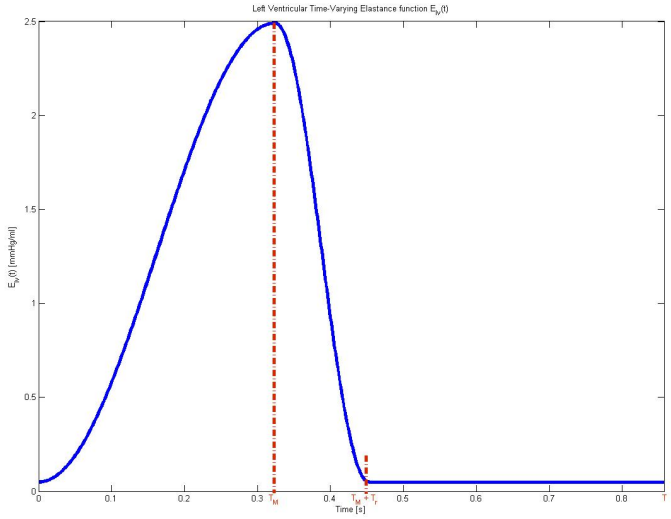

Figure 2.4: The left ventricular time-varying elastance function $E_{\ell v}(t)$ during one cardiac cycle (60/70 sec).

In our model, further modifications of the elastance function in (2.28) have been done. The maximum elastance E_M can be interpreted as a measure of the contractile state of the ventricle, see Palladino (2002) [42] and Sunagawa and Sagawa (1982) [52]. For the normal resting heart, E_M can be a constant parameter . However, during exercise phase, the contractility of the heart muscles may vary and could depend on the heart rate. That is, an increase in heart rate may result in an increased ventricular elastance. Thus we considered E_M as a function dependent on the heart

rate H. Such function must be positive-valued, bounded and continuous. We chose the Gompertz function for $E_M(H)$, a sigmoidal function given by

$$E_M(H) = a \exp(-b \exp(-cH)) \ , \tag{2.30}$$

where a, b, c are positive constants. Figure 2.5 shows the maximum elastance using Gompertz function with varying constants a, b and c. The constant a determines the upper bound of the function, b shifts the graph horizontally and c is the measure of the steepness of the curve.

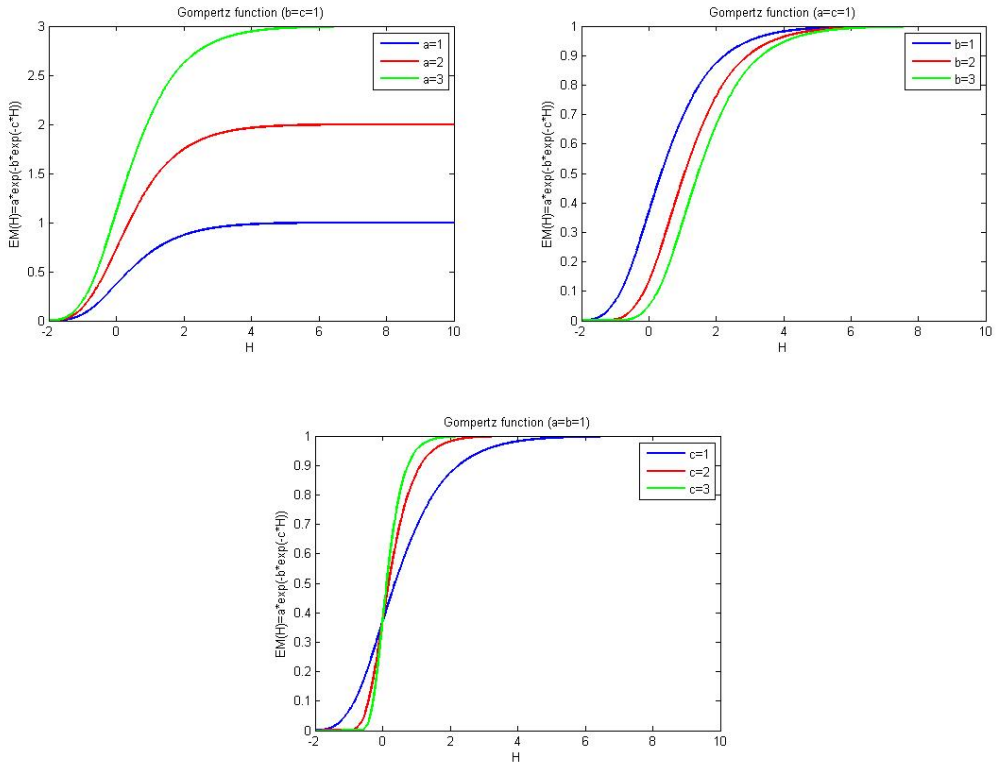

Figure 2.5: The maximum elastance E_M expressed in terms of Gompertz function with varying values for constants a, b and c.

In Ottesen (2004) [41] and Olufsen et al. (2009) [46], $E_M = 2.49$ [mmHg/mL]. Figure 2.6 depicts the maximum elastance curve where constants a, b and c were estimated obtaining $E_M = 2.4906$ [mmHg/mL] at $H = 70/60$ beats per second.

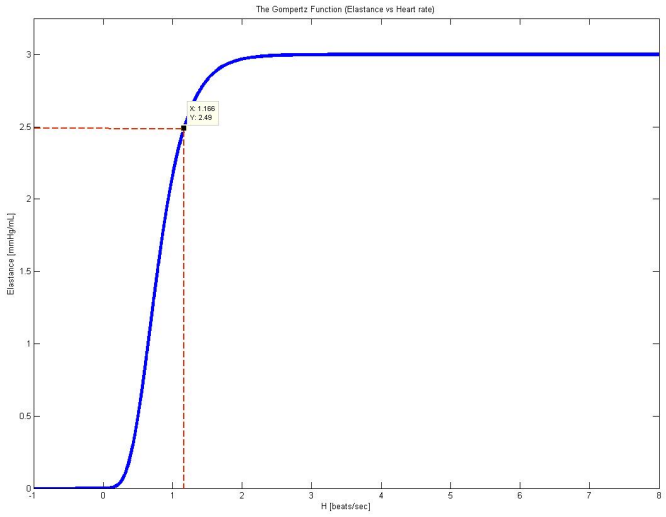

Figure 2.6: The maximum elastance E_M expressed as a sigmoidal function dependent on the heart rate H.

Since, E_M is now H-dependent, T_M which is the time of peak elastance should be H-dependent as well. We considered T_M as the time for systolic duration which is defined by the Bazett's formula given by

$$T_M = \frac{\kappa}{H^{1/2}} \ , \tag{2.31}$$

where κ is the same constant introduced in equation (2.15). Figure 2.7 depicts the elastance function with varying heart rates. As the heart rate increases, the maximum elastance value increases as well. Notice also the decrease in the time for peak elastance and the smaller support of the elastance curve.

2.6 Local Regulation Process and Autoregulation

In this section, we will model the local metabolic control and autoregulation processes. In particular, we will consider only the case of exercise below the anaerobic threshold. Thus, the amount of energy consumed by the muscles is equal to the aerobic energy supply. For an elaborate discussion of exercise physiology refer to Falls (1968) [9] and Rowell (1993) [48].

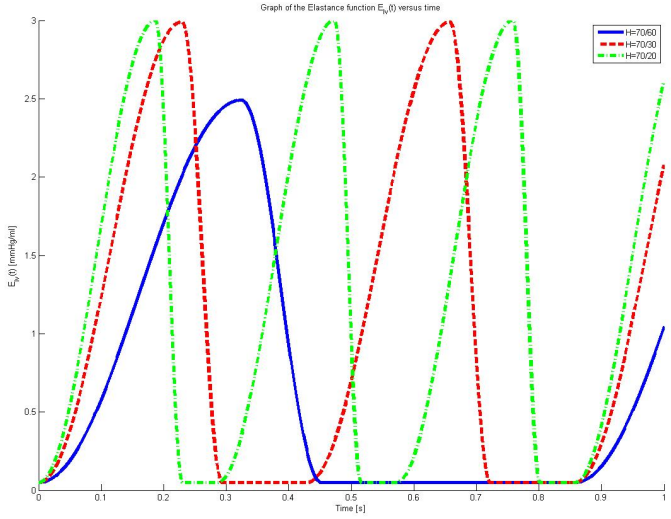

Figure 2.7: The elastance function with varying heart rates.

Let us start modeling the metabolic control. Let the metabolic rate for the tissue region M_{T} be partially satisfied by the O_2 supply provided by the blood flow in the tissue region and partially by anaerobic biochemical reactions providing an anaerobic energy flow M_b. As in Kappel and Peer (1993) [26] and related works, we have the relation

$$M_{\mathrm{T}} \;=\; F^*_{sp}\,(C_{\mathrm{a,O_2}} - C_{\mathrm{v,O_2}}) + M_b \;, \tag{2.32}$$

where F^*_{sp} denotes the blood flow in the arterial systemic region, $C_{\mathrm{a,O_2}}$ denotes the concentration of O_2 in the arterial blood which is assumed to be constant and $C_{\mathrm{v,O_2}}$ is the concentration of O_2 in the venous blood in the capillary region. This is a modification of Fick's law for basic energy (oxygen) balance equation. Incorporated here is the energy source provided by ATP (adenosine triphosphate) and creatine phosphate which is tapped during periods of exercising (aerobic oxidation). Moreover, for the biochemical energy flow, we assume that it is directly proportional to the rate of change of $C_{\mathrm{v,O_2}}$,

$$M_b \;=\; -K\frac{d}{dt}C_{\mathrm{v,O_2}} \;, \tag{2.33}$$

where K is a positive constant. Equation (2.33) suggests that a positive amount of M_b is supplied whenever $C_{\mathrm{v,O_2}}$ is lowered.

In order to model the cardiovascular system response to a constant ergometric workload W imposed on a test person on a bicycle ergometer, the following empirical formula for the metabolic rate is used

$$M_{\mathrm{T}} \;=\; M_0 + \rho W \;, \tag{2.34}$$

where M_0 is the metabolic rate in the systemic tissue region corresponding to zero workload and ρ is a positive constant.

In any tissue of the body, an increase in the arterial pressure causes an increase in the blood flow as well. However, in most tissue, the blood flow returns to the normal level in less than a minute, though the arterial pressure remains elevated. The return of blood flow toward normal is called ***autoregulation*** of blood flow.

Autoregulation will be considered as one of the fundamental regulation mechanisms in our model. This plays an important role during phases of exercising. The role of autoregulation is to guarantee a sufficient blood flow in the relevant tissues. The most efficient way to increase the blood flow in a tissue region locally is to increase the diameter of the arterioles in that region. These would in turn, decrease the resistance to blood flow. Thus, autoregulation can be accomplished essentially by decreasing the resistance in the relevant tissue. Also, in general, local dilation of the arterioles is influenced by substances which are set free locally due to increased functional activity of the organ or tissue region (functional activation). This mechanism is supported by a local metabolic regulation, where by-products of the local metabolism cause dilation of the arterioles. Following Peskin (1981) [44] we have

$$R_{sp} \;=\; A_{\mathrm{pesk}} C_{\mathrm{v,O_2}} \;, \tag{2.35}$$

where A_{pesk} is a positive constant.

In our model, we do not consider an autoregulation mechanism in finger arteries. This is due to the idea that in an ergometer bicycle test, the arms are held in a fixed position. And therefore, not directly involved in an exercise activity. Hence,

instead of using equation (2.5) for the systemic peripheral flow, we use

$$F_{sp}^{*} \;=\; \frac{1}{R_{sp}}\left(P_{as}-P_{vs}\right)\;. \tag{2.36}$$

Differentiating (2.35) and combining it with equations (2.36), (2.32) and (2.33), we obtain the following differential equation for R_s:

$$\frac{dR_{sp}}{dt} \;=\; \frac{1}{K}\left(A_{\mathrm{pesk}}\left(\left(\frac{P_{as}-P_{vs}}{R_{sp}}\right)C_{\mathrm{a,O_2}}-M_{\mathrm{T}}\right)-\left(P_{as}-P_{vs}\right)\right)\;. \tag{2.37}$$

2.7 The Contractility of the Right Ventricle

Since our modeling effort is directed towards describing the reaction of the cardiovascular system to an ergometric workload, we need to include the regulation of the heart rate and the contractilities of the ventricle in response to the activity. We will not model the baroreceptor in detail. The idea is to construct a feedback control regulating the heart rate in dependence of the the arterial systemic pressure. We assume that the contractilities vary according to variations in the heart rate.

There is a heart mechanism called the *Bowditch effect*. It roughly states that changing the heart rate causes a concordant change in the ventricular contractilities (cf. Levick (2003) [32]). For further details concerning Bowditch effect refer to Franz, et al. (1983) [11], Seed and Walker (1988) [51] and Wohlfart (1979) [56]. In this study, we adapted the model presented in Batzel et al. (2007) [2] (see also [26]) where sympathetic and parasympathetic activities were not considered directly. Thus, the variations of the contractilities can be described by the following second order differential equation

$$\frac{d^2S_{rv}}{dt^2}+\gamma_{rv}\frac{dS_{rv}}{dt}+\alpha_{rv}S_{rv}=\beta_{rv}H\;, \tag{2.38}$$

where α_{rv},β_{rv} and γ_{rv} are constants, and $\alpha_{rv},\beta_{rv}>0$. This set-up guarantees that the contractility S_{rv} varies in the same direction as the heart rate H. Introducing the state variable $\sigma_{rv}=\frac{dS_{rv}}{dt}$ and transforming (2.38) into systems of first order differential equations, we have

$$\begin{aligned}\frac{dS_{rv}}{dt}&=\sigma_{rv}\;,\\ \frac{d\sigma_{rv}}{dt}&=-\alpha_{rv}S_{rv}-\gamma_{rv}\sigma_{rv}+\beta_{rv}H\;.\end{aligned} \tag{2.39}$$

Chapter 3

Basic Concepts in Control Theory

This chapter will provide the basic concepts in control theory specifically the linear control systems in finite dimensional state spaces. In particular, time-invariant control systems will be presented. The proofs and further details of the theorems are not presented but instead referred to in some literatures. Main references for this material are from unpublished notes on control theory by Kappel (2005) [23], PhD thesis by Timischl (1998) [54] and the book on Linear Optimal Control Systems by Kwakernaak and Sivan (1972) [30]. Other relevant references are mentioned during the discussion.

3.1 Linear Control Systems

Let us start by giving a mathematical definition of a linear control system.

Definition 3.1.1 *Let* $A(t) \in \mathbb{R}^n \times \mathbb{R}^n$, $B(t) \in \mathbb{R}^n \times \mathbb{R}^p$ *and* $C(t) \in \mathbb{R}^k \times \mathbb{R}^n$ *be defined on an interval* I. *A* **linear control system** *is given by the following equations:*

$$\frac{dx(t)}{dt} = A(t)x(t) + B(t)u(t) \ , \tag{3.1}$$

$$y(t) = C(t)x(t) \ , \tag{3.2}$$

where $x(t) \in \mathbb{R}^n$, $u(t) \in \mathbb{R}^p$ *and* $y(t) \in \mathbb{R}^k$ *for* $t \in I$. *The interval* I *can be a closed interval,* $I = [t_0, t_e]$, $t_0 < t_e < \infty$ *or* $I = [t_0, \infty)$. *The elements of the matrices*

$A(\cdot)$, $B(\cdot)$ and $C(\cdot)$ are assumed to be in $\mathscr{L}^2(I;\mathbb{R})$.

In the above definition, t denotes the time variable where $t \in I$ and $x(t)$ is called the ***state*** or the ***response*** of the system at time t. The function $u(t)$ is called the ***input*** respectively the ***control*** of the system and $u(\cdot)$ is assumed to be in $\mathscr{L}^2(I;\mathbb{R}^p)$. Equation (3.1) is called the ***state equation*** for the system. If an initial value $x_0 \in \mathbb{R}^n$ and input $u(\cdot) \in \mathscr{L}^2(I;\mathbb{R}^p)$ are given, then (3.1) has a unique solution $x(\cdot)$ in the **sense of Caratheodory**, that is, $x(\cdot)$ is absolutely continuous on I with $x(t_0) = x_0$ and the derivative of $x(\cdot)$ exists almost everywhere on I and is a function in $\mathscr{L}^2(I;\mathbb{R}^n)$. Moreover, equation (3.1) is satisfied a.e. on I. In general, if we know $u(\cdot)$ which characterizes the external influence on the system, then we can think of the state of a system as a quantity which provides the necessary information needed in order to predict the future behavior of the system. Once the solution $x(\cdot)$ of (3.1) with initial value x_0 is obtained, equation (3.2) determines $y(\cdot) \in \mathscr{L}^2(I;\mathbb{R}^k)$, which is called the ***output*** of the system. Generally speaking, we do not have access to the state $x(\cdot)$ itself but only to some function of the state. The coordinates of $y(\cdot)$ can be thought of as those quantities of the system that we can measure.

Figure 3.1 represents a diagram for an idealized situation of a control system. However, in practice, we have to distinguish between the system (or plant) and the model for the system, which is given by equations (3.1) and (3.2). A real situation is depicted in Figure 3.2. Of course, it is expected that the model describes the dynamics of the system sufficiently well, so that the input-output behavior of the model is sufficiently close to that of the system.

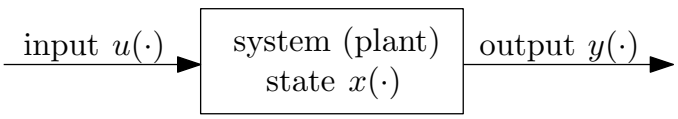

Figure 3.1: An idealized diagram of a control system.

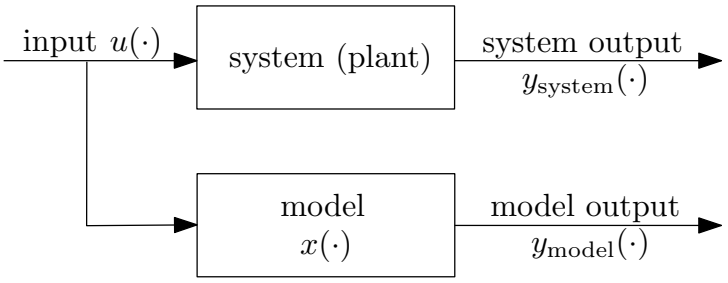

Figure 3.2: The control system.

There are some generalizations of equations 3.1 and 3.2 which we will provide but will not be given much emphasis. For example, in Dai (1989) [8], instead of (3.1) the following equation has been adapted:

$$E(t)\frac{dx(t)}{dt} \;=\; A(t)x(t) + B(t)u(t), \quad t \in I \;, \tag{3.3}$$

where $E(t)$ is an $n \times n$ matrix which is non-invertible everywhere on I. Such systems are called linear *descriptor systems* or linear *singular control systems*. Basically, descriptor systems arise when there is an added (linear) constraint for the state variables. Also, a more general form of the output equation (3.2) is

$$y(t) \;=\; C(t)x(t) + D(t)u(t), \quad t \in I \;. \tag{3.4}$$

This is a scenario which reflects the input influencing the output directly (see for instance Brockett (1969) [5]).

In systems theory, system (3.1) and (3.2) is called a linear *continuous-time system* (or control system). The time-set for such a system is a bounded or an unbounded closed interval in $\mathbb{R}$. Another important class of systems are *discrete-time systems*, where the time-set is a finite sequence, $t_0 < t_1 < \cdots < t_e$, or infinite sequence, $t_0 < t_1 < \cdots$ and equations (3.1) and (3.2) are replaced by

$$\begin{aligned} x(t_{k+1}) &= \; A(t_k)x(t_k) + B(t_k)u(t_k), \quad k = 1, 2, \ldots, \\ y(t_k) &= \; C(t_k)x(t_k), \quad k = 0, 1, \ldots \;. \end{aligned} \tag{3.5}$$

For discrete-time systems theory, we refer to the literature for instance Kwakernaak and Sivan (1972) [30], Chapter 6.

For our discussion purposes, we will focus primarily on the ***linear time-invariant, continuous systems***. This is a special case of the system characterized by equations (3.1) and (3.2) where the matrices A, B, and C are constant in time. Thus we have

$$\begin{aligned} \frac{dx(t)}{dt} &= Ax(t) + Bu(t), \quad t \in \mathbb{R} \ , && (3.6) \\ y(t) &= Cx(t), \quad t \in \mathbb{R} \ . && (3.7) \end{aligned}$$

This time, we will present the basic theorems on the solution of the state equation (3.1) including the transition matrix and diagonlization. For detailed discussions and proofs, we refer to Kwakernaak and Sivan (1972) [30] and Luenberger (1979) [33].

Theorem 3.1.2 *Consider the linear homogeneous system of the form*

$$\frac{dx(t)}{dt} = A(t)x(t) \ . \tag{3.8}$$

If the elements of the matrix $A(t)$ are continuous functions of t, then the system (3.8) *always has a solution corresponding to a given initial state vector, $x(t_0)$. The solution can be expressed as*

$$x(t) = \Phi(t, t_0)x(t_0), \quad \textit{for all } t \ . \tag{3.9}$$

The ***transition matrix*** $\Phi(t, t_0)$ *is the solution of the matrix differential equation*

$$\begin{aligned} \frac{d\Phi(t, t_0)}{dt} &= A(t)\Phi(t, t_0), \quad \textit{for all } t \ , \\ \Phi(t_0, t_0) &= I \ , \end{aligned} \tag{3.10}$$

where I is the n-dimensional identity matrix.

Below is a theorem listing the properties of a transition matrix.

Theorem 3.1.3 *The transition matrix $\Phi(t, t_0)$ of the state equation* (3.1) *has the following properties:*

1. $\Phi(t_2, t_1)\Phi(t_1, t_0) = \Phi(t_2, t_0)$ *for all* t_0, t_1, t_2;
2. $\Phi(t, t_0)$ *is nonsingular for all* t, t_0;

3. $\Phi^{-1}(t, t_0) = \Phi(t_0, t)$ *for all* t, t_0*;*

4. $\dfrac{d\Phi^T(t_0, t)}{dt} = -A^T(t)\Phi^T(t_0, t)$ *for all* t, t_0*,*

where the superscript T *denotes the transpose.*

Once the transition matrix is obtained, solutions to the state equation (3.1) can easily be found. This is provided in the next theorem.

Theorem 3.1.4 *The solution of the state equation* (3.1) *is*

$$x(t) \;=\; \Phi(t, t_0)x(t_0) + \int_{t_0}^{t} \Phi(t, \tau)B(\tau)u(\tau)\, d\tau \;, \tag{3.11}$$

for all t *provided that* $A(t)$ *is continuous and* $B(t)$ *and* $u(t)$ *are piecewise continuous for all* t*.*

The transition matrix for the linear time-invariant system has an explicit form.

Theorem 3.1.5 *The linear time-invariant system*

$$\frac{dx(t)}{dt} \;=\; Ax(t) \tag{3.12}$$

has the transition matrix

$$\Phi(t, t_0) \;=\; e^{A(t-t_0)} \;, \tag{3.13}$$

where the exponential of a square matrix M *is defined via the series*

$$e^M \;=\; I + M + \frac{1}{2!}M^2 + \frac{1}{3!}M^3 + \cdots \tag{3.14}$$

which converges for all M*.*

An explicit form of the transition matrix for the linear time-invariant system can be obtained by diagonalization of A.

Theorem 3.1.6 *Suppose that the constant* $n \times n$ *matrix* A *has* n *distinct eigenvalues* $\lambda_1, \lambda_2, \ldots, \lambda_n$ *and corresponding eigenvectors* $e_1, e_2, \ldots, e_n$*. Let us define* $n \times n$ *matrices:*

$$T \;=\; (e_1, e_2, \cdots, e_n) \;, \tag{3.15}$$

$$\Lambda \;=\; diag\,(\lambda_1, \lambda_2, \cdots, \lambda_n) \;. \tag{3.16}$$

That is, the matrix T consists of the eigenvectors of A as columns and the matrix Λ is a diagonal matrix whose diagonal elements are the eigenvalues of A. Then the following holds:

1. *T is nonsingular and A can be represented as*

$$A \;=\; T\Lambda T^{-1}\;. \tag{3.17}$$

   Equivalently, T diagonalizes A, that is, $T^{-1}AT = \Lambda$.

2. *The transition matrix has the form*

$$\Phi(t) \;=\; e^{At} \;=\; Te^{\Lambda t}T^{-1} \quad \textit{and} \quad e^{\Lambda t} \;=\; \textit{diag}\left(e^{\lambda_1 t}, e^{\lambda_2 t}, \cdots, e^{\lambda_n t}\right) \tag{3.18}$$

3. *The solution of* (3.12) *can be written as*

$$x(t) \;=\; \sum_{i=1}^{n} \mu_i e^{\lambda_i t} e_i\;, \tag{3.19}$$

   where the scalars μ_i depend on the initial condition $x(0)$ via $(\mu_1, \mu_2, \ldots, \mu_n)^T = T^{-1}x(0)$.

Item 3 of the above theorem shows that the response $x(t)$ of the linear time-invariant system (3.12) is a composition of motions along the eigenvectors of A. Such motions are called **modes** of the system. If an initial state $x(0)$ is chosen to lie in the direction of one eigenvector, the whole motion will stay along that direction. In general, a particular mode is excited by choosing the initial state to have a component along the corresponding eigenvector.

It can also be noted from the above theorem that the transition matrix can be facilitated by diagonalizing the matrix A. If A does not have n linearly independent eigenvectors it cannot be diagonalized but it can be brought into the so-called Jordan normal form from which the transition matrix can be found. The response $x(t)$ of the linear time-invariant system (3.12) may contain aside from purely exponential terms of the form $e^{\lambda_i t}$ also terms of the form $te^{\lambda_i t}, t^2e^{\lambda_i t}, \ldots$ and so on (refer to Kwakernaak and Sivan (1972) [30] for details).

3.2 Stability

In this section we will discuss the overall time behavior of a system. We are interested in whether or not the solutions of the state equation tend to grow indefinitely as $t \to \infty$. For simplicity, let us assume that we are dealing with an ***autonomous system***. Such a system has no input $u(t)$ or more precisely, a system where u is a fixed function of time. Thus we will consider differential equations of the form

$$\frac{dx(t)}{dt} \;=\; f(x(t)) \;. \tag{3.20}$$

Let us introduce a ***nominal solution*** $x_0(t)$ satisfying the differential equation (3.20). If $x_0(t) = x_e$, a constant, then it is said to be an ***equilibrium state*** of the system.

Definition 3.2.1 *Let $x(t)$ be an arbitrary solution to the differential equation* (3.20)*. The nominal solution $x_0(t)$ of* (3.20) *is* **asymptotically stable** *if the following holds:*

1. *It is* **stable in sense of Lyapunov**, *that is, for any t_0 and any $\epsilon > 0$ there exists a $\delta(\epsilon)$ (could depend on t_0) such that*

$$\|x(t_0) - x_0(t_0)\| \leq \delta \quad \textit{implies} \quad \|x(t) - x_0(t)\| < \epsilon \quad \textit{for all } t \geq t_0 \;. \tag{3.21}$$

2. *For all t_0 there exists a $\rho > 0$ (could depend on t_0) such that*

$$\|x(t_0) - x_0(t_0)\| < \rho \quad \textit{implies} \quad \|x(t) - x_0(t)\| \longrightarrow 0 \;\; \textit{as} \;\; t \longrightarrow \infty \;. \tag{3.22}$$

Moreover, if the nominal solution satisfies item 1 and for any $x(t_0)$ and any t_0

$$\|x(t) - x_0(t)\| \longrightarrow 0 \;\; \textit{as} \;\; t \longrightarrow \infty \;, \tag{3.23}$$

then it is said to be **asymptotically stable in the large**.

From the above definition, $\|x\|$ denotes the norm of a vector x. Any norm is possible because all norms are equivalent in $\mathbb{R}^n$. In particular, one can use the Euclidean norm

$$\|x\| \;=\; \sqrt{\sum_{i=1}^{n} x_i^2} \;. \tag{3.24}$$

Stability in the sense of Lyapunov guarantees that if the initial state is chosen close enough to the nominal solution, the state does not depart too far from the nominal solution. Asymptotic stability, in addition to stability in the sense of Lyapunov, implies that the solution always approaches the nominal solution provided that the initial deviation is within a certain region. Finally, asymptotic stability in the large implies that all other solutions eventually approach the nominal solution regardless of the choice of the initial condition.

Definition 3.2.2 *The linear homogeneous system* (3.8) *is stable in a certain sense (of Lyapunov, asymmptotically or asymptotically in the large), if the zero solution* $x_0 \equiv 0$ *is stable in that sense.*

For any linear system, asymptotic stability and asymptotic stability in the large is the same since solutions may be scaled up or down without changing their behavior.

Theorem 3.2.3 *The linear homogeneous system* (3.8) *is asymptotically stable if and only if it is asymptotically stable in the large.*

Definition 3.2.4 *The linear homogeneous system* (3.8) *is* **exponentially stable** *if there exist positive constants* α *and* β *such that for any initial state* $x(t_0)$*,*

$$\|x(t)\| \;\leq\; \alpha e^{-\beta(t-t_0)} \|x(t_0)\|\,, \qquad t \geq t_0\ . \tag{3.25}$$

It can be inferred from the definition above that a system which is exponentially stable has the property that the state converges exponentially to the zero state no matter what the initial state is.

For the following material we will provide basic theorems and definitions that establish under what conditions linear time-invariant system possess any forms of stability we have presented.

It is clear from item 3 of Theorem 3.1.6 that the stability of the system is determined by the eigenvalues λ_i of A.

Theorem 3.2.5 *The linear time-invariant system* (3.12) *is stable in sense of Lyapunov if and only if*

1. *all the eigenvalues of A have nonpositive real parts, and*

2. *to any eigenvalue on the imaginary axis with multiplicity m there correspond exactly m eigenvectors of the matrix A.*

The second condition of the theorem prevents the terms that grow as t^k. If A has no multiple characteristic values on the imaginary axis then this condition is always satisfied. The next theorem is for asymptotic stability.

Theorem 3.2.6 *The linear time-invariant system* (3.12) *is asymptotically stable if and only if all the eigenvalues of A have strictly negative real parts.*

Notice that it is the matrix A that determines whether a linear time-invariant system is asymptotically stable. Thus we can have the following definition:

Definition 3.2.7 *The $n \times n$ matrix A is asymptotically stable if all its characteristic values have strictly negative real parts.*

It can be shown that the state space of a linear time invariant system can be decomposed into two subspaces in which the response of the system from an initial state in the first subspace always converges to zero state while the response from a nonzero initial state in the other subspace diverges.

Definition 3.2.8 *Consider the linear time-invariant system* (3.12)*. Suppose that A has distinct eigenvalues. We define the* **stable subspace** *for this system as the real linear subspace spanned by the eigenvectors of A corresponding to eigenvalues with strictly negative real parts. Similarly, the* **unstable subspace** *for this system is the real subspace spanned by the eigenvectors of A corresponding to eigenvalues with nonnegative real parts.*

A similar decomposition can be extended to a more general linear time-invariant systems, particularly for nondiagonalizable matrix A. As a consequence of this definition, the whole $\mathbb{R}^n$ can be expressed as the direct sum of the stable and the unstable subspace.

3.3 Controllability (Reachability)

One basic question concerning a control system is, in what way can it be influenced by choosing appropriate controls u? Specifically, we want to know whether or not a given system can be steered from any given initial state to any other given final state. This leads to the following definition of controllability.

Definition 3.3.1 *Suppose the control system is given by equations* (3.1) *and* (3.2).

1. *Given $x_0, x_1 \in \mathbb{R}^n$ and $t_0 \in I$, an interval defined in 3.1.1. The state x_0 at time t_0 is* **controllable** *to x_1, if and only if there exists a time $t_1 > t_0$ and a control function $u \in \mathscr{L}^2([t_0, t_1]; \mathbb{R}^p)$ such that $x(t_1) = x_1$.*

2. *Control system* (3.1), (3.2) *is* **completely controllable** *at t_0, if and only if every state $x_0 \in \mathbb{R}^n$ is at time $t_0 \in I$ controllable to any state x_1.*

Another concept related to controllability is reachability. A state x_1 at time $t_1 \in I$ is said to be ***reachable*** from x_0 if and only if there exists a $t_0 < t_1, t_0 \in I$ and a control function $u \in \mathscr{L}^2([t_0, t_1]; \mathbb{R}^p)$ such that $x(t_1) = x_1$. Moreover, the control system (3.1), (3.2) is ***completely reachable*** at time t_1 if and only if every $x_1 \in \mathbb{R}^n$ is at $t_1 \in I$ reachable from every other state x_0.

The following is a characterization of controllability:

Theorem 3.3.2 *Consider the control system* (3.1), (3.2). *Let us introduce the* **controllability Grammian** *of system as*

$$W(t_0, t_1) = \int_{t_0}^{t_1} \Phi(t_0, \tau) B(\tau) B(\tau)^T \Phi(t_0, \tau)^T \, d\tau \ . \tag{3.26}$$

1. *A state $x_0 \in \mathbb{R}^n$ at time $t_0 \in I$ is controllable to the other state x_1 if and only if there exists a $t_1 > t_0$ such that*

$$x_0 - \Phi(t_0, t_1) x_1 \ \in \ range W(t_0, t_1) \ . \tag{3.27}$$

2. *The control system* (3.1), (3.2) *is completely controllable at t_0 if and only if there exists a $t_1 > t_0$ such that*

$$rank W(t_0, t_1) = n \quad (or\ equivalently\ range W(t_0, t_1) = \mathbb{R}^n) \ . \tag{3.28}$$

The corollary below is an offspring of the above theorem:

Corollary 3.3.3 *1. The control system* (3.1), (3.2) *is completely controllable if and only if there exists a* $t_1 > t_0$ *such that for any* $x_0, x_1 \in \mathbb{R}^n$, *a control* $u \in \mathscr{L}^2([t_0, t_1]; \mathbb{R}^p)$ *can be found such that the trajectory of the system corresponding to* u *and originating from* x_0 *at time* t_0 *reaches* x_1 *at time* t_1.

2. Suppose that x_0 *can be controlled to* 0 *at time* t_0 *and let* $y \in \mathbb{R}^n$ *be an element with* $W(t_0, t_1)y = x_0$. *Then a control*

$$u(t) \;=\; -B(t)^T \Phi(t_0, t)^T y, \quad t_0 \le t \le t_1 \;, \tag{3.29}$$

steers x_0 *to* 0 *in the interval* $[t_0, t_1]$.

Now, we will consider controllability issues for linear time-invariant continuous system given by equations (3.6), (3.7).

Theorem 3.3.4 *Consider the control system* (3.6).

1. A state x_0 *at time* 0 *(or at any time* $t_0 \in \mathbb{R}$*) is controllable to zero if and only if*

$$x_0 \;\in\; \textit{range}\left(B, AB, \ldots, A^{n-1}B\right) \;. \tag{3.30}$$

2. The linear time-invariant system (3.6) *is completely controllable at any time* $t_0 \in \mathbb{R}$ *if and only if*

$$\textit{rank}\left(B, AB, \ldots, A^{n-1}B\right) \;=\; n \;. \tag{3.31}$$

The pair (A, B) is said to be ***controllable*** if the rank condition of item 2 of the above theorem is satisfied. Also, note from the theorem that controllability for the time-invariant linear system is independent of t_0 and t_1. Thus, it can also be expected that in the above theorem, '(completely) controllable' can be replaced by '(completely) reachable'.

The subspace

$$\text{range}\left(B, AB, \ldots, A^{n-1}B\right) \;=\; \sum_{i=0}^{n-1} \text{range}\, A^i B \tag{3.32}$$

is called the ***controllable subspace*** for system (3.6).

Below is an interesting criterion for the controllability of a pair (A, B) established by Hautus (1969) in [16].

Theorem 3.3.5 *Suppose $A \in \mathbb{R}^{n\times n}$ and $B \in \mathbb{R}^{n\times p}$ are given. The pair (A, B) is controllable if and only if $p^T B \neq 0$ for any eigenvector (real or complex) p of A^T.*

A state transformation can be found representing the system in a canonical form which exhibits the controllability of the system.

Theorem 3.3.6 *Consider the linear time-invariant system* (3.6)*. Form a nonsingular transformation matrix $T = (T_1, T_2)$ where the columns of T_1 form a basis for the m-dimensional $(m \leq n)$ controllable subspace of* (3.6)*, i.e., $T_1 = (e_1, e_2, \cdots, e_m)$, and the column vectors of T_2 together with those of T_1 form a basis for the whole n-dimensional space, i.e., $T_2 = (e_{m+1}, e_{m+2}, \cdots, e_n)$. Define a transformed state variable $\tilde{x}(t)$ by*

$$\tilde{x}(t) \;=\; T^{-1}x(t)\ . \tag{3.33}$$

Then the state equation (3.6) *is transformed into the* **controllability canonical form** *expressed as*

$$\frac{d\tilde{x}(t)}{dt} \;=\; \begin{pmatrix} \tilde{A}_{11} & \tilde{A}_{12} \\ 0 & \tilde{A}_{22} \end{pmatrix} \tilde{x}(t) + \begin{pmatrix} \tilde{B}_1 \\ 0 \end{pmatrix} u(t)\ , \tag{3.34}$$

where $\tilde{A}_{11} \in \mathbb{R}^{m\times m}$, $\tilde{A}_{12} \in \mathbb{R}^{m\times(n-m)}$, $\tilde{A}_{22} \in \mathbb{R}^{(n-m)\times(n-m)}$, $\tilde{B}_1 \in \mathbb{R}^{m\times p}$, and the pair $(\tilde{A}_{11}, \tilde{B}_1)$ is completely controllable.

Remarks: Since T_1 and T_2 can freely be chosen to some extent, the controllability canonical form is not unique. But no matter how the transformation is chosen, the eigenvalues of $\tilde{A}_{11}$ are the same, respectively $\tilde{A}_{22}$. The eigenvalues of $\tilde{A}_{11}$ are referred to as the *controllable poles* of the system, while the eigenvalues of $\tilde{A}_{22}$ are the *uncontrollable poles*. Suppose that the eigenvalues of system (3.47) are distinct. Then the its controllable subspace is spanned by the eigenvectors corresponding to the controllable poles of the system. Consequently, the uncontrollable

subspace of the system is the subspace spanned by the eigenvectors corresponding to the uncontrollable poles of the system.

3.4 Stabilizability

Suppose that some of the eigenvalues of the matrix A of the linear time-invariant system (3.6) have nonnegative real parts. The question now is, can we find a control function $u(t)$ capable of steering the response of the linear time-invariant system (3.6) to the zero state? In order to control the system, it must be required that the unstable component can be completely controlled. Obviously, if the system is completely controllable, then it can be steered to the zero state. Thus we have the following definition:

Definition 3.4.1 *Consider the linear time-invariant system* (3.6).

1. *It is* **stabilizable** *if its unstable subspace is contained in its controllable subspace.*

2. *The pair* (A, B) *is stabilizable if the system* (3.6) *is stabilizable.*

Theorem 3.4.2 *Any asymptotically stable linear time-invariant system is stabilizable. Also, any completely controllable system is stabilizable.*

The stabilizability of a system can be verified when the state differential equation is in controllability canonical form.

Theorem 3.4.3 *Consider the linear time-invariant system* (3.6). *Suppose that it is transformed into the controllability canonical form as in equation* (3.47) *given in Theorem 3.3.6 where the pair* $(\tilde{A}_{11}, \tilde{B}_1)$ *is completely controllable. Then the system* (3.6) *is stabilizable if and only if the matrix* $\tilde{A}_{22}$ *is asymptotically stable.*

3.5 Reconstructibility (Observability)

In this section we are interested in which information on the state we can obtain by observing the output $y(\cdot)$ of the system on some time interval. That is, we will

discuss the problem whether it is possible to determine from the behavior of the output what the behavior of the state is.

Definition 3.5.1 *Consider the linear control system given by equations* (3.1), (3.2).

1. *A state* $x_0 \in \mathbb{R}^n$ *is* **non-reconstructible** *at time* $t_0 \in I$ *if and only if there exists a* $t_1 \in I$ *where* $t_1 < t_0$ *such that for all* $t \in [t_1, t_0]$ *and* $u \in \mathscr{L}^2([t_1, t_0]; \mathbb{R}^p)$

$$C(t)x(t; t_0, x_0, u(\cdot)) \;=\; C(t)x(t; t_0, 0, u(\cdot)) \;. \tag{3.35}$$

2. *The control system* (3.1),(3.2) *is said to be* **completely reconstructible** *at time* $t_0 \in I$ *if and only if* 0 *is the only state which is non-reconstructible at time* t_0.

Analogously, the notions of non-observable and completely observable are defined as follows: A state $x_0 \in \mathbb{R}^n$ is ***non-observable*** at time $t_0 \in I$ if and only if there exists a $t_1 \in I$ where $t_1 > t_0$ such that for all $t \in [t_0, t_1]$ and $u \in \mathscr{L}^2([t_0, t_1]; \mathbb{R}^p)$ $C(t)x(t; t_0, x_0, u(\cdot)) = C(t)x(t; t_0, 0, u(\cdot))$. The control system (3.1),(3.2) is ***completely observable*** at time $t_0 \in I$ if and only if 0 is the only state which is non-observable at time t_0.

Using the transition matrix representation, equation (3.35) can be written as

$$C(t)\Phi(t, t_0)x_0 \;=\; 0, \quad t \in [t_1, t_0] \;. \tag{3.36}$$

For $t_0, t_1 \in I,\ t_1 < t_0$, we define the mapping $\mathcal{C}_{t_0,t_1} : \mathbb{R}^n \to \mathscr{L}^2\left([t_1, t_0]; \mathbb{R}^k\right)$ by

$$\mathcal{C}_{t_0,t_1}x \;=\; C(\cdot)\Phi(\cdot, t_0)x, \quad x \in \mathbb{R}^n \;. \tag{3.37}$$

With this, condition (3.35) is equivalent to

$$x_0 \in \ker \mathcal{C}_{t_0,t_1} \;. \tag{3.38}$$

If a complementary subspace X of $\ker \mathcal{C}_{t_0,t_1}$ is chosen, i.e., $\mathbb{R}^n = X \oplus \ker \mathcal{C}_{t_0,t_1}$, then any state $x_0 \in \mathbb{R}^n$ has a unique representation as $x_0 = x_{01} + x_{02}$ where $x_{01} \in X$ and $x_{02} \in \ker \mathcal{C}_{t_0,t_1}$. Thus, we can say that the component x_{01} is reconstructible in the following sense: If for some $t^* < t_0$, $y(t) = Cx(t; t_0, x_{01}, 0) = 0$ on $[t^*, t_0]$, then

$x_{01} = 0$. Linearity of the system could be stated as follows: Suppose x_0, x_1 are two states of the system. If for some $t^* < t_0$, $t \in [t^*, t_0]$ and for all $u \in \mathscr{L}^2([t^*, t_0]; \mathbb{R}^p)$, we have $Cx(t; t_0, x_0, u(\cdot)) = Cx(t; t_0, x_1, u(\cdot))$, then $x_1 - x_0 \in \ker \mathcal{C}_{t_0,t_1}$. Since a special complementary subspace for $\ker \mathcal{C}_{t_0,t_1}$ is $(\ker \mathcal{C}_{t_0,t_1})^\perp$, we have the following definition: A state $x_0 \in \mathbb{R}^n$ is ***reconstructible*** at time $t_0 \in I$ if and only if there exists a $t_1 \in I$ where $t_1 < t_0$ such that $x_0 \in (\ker \mathcal{C}_{t_0,t_1})^\perp$.

Remark: In view of the above arguments, 'reconstructible' is not the negation of 'non-reconstructible'.

Theorem 3.5.2 *Consider the control system* (3.1), (3.2). *Let us introduce the* **reconstructibility Grammian** *of the system as*

$$H(t_0, t_1) = \int_{t_1}^{t_0} \Phi(\tau, t_0)^T C(\tau)^T C(\tau) \Phi(\tau, t_0)\, d\tau \ . \tag{3.39}$$

1. *A state x_0 at time t_0 is non-reconstructible if and only if there exists a $t_1 \in I$ where $t_1 < t_0$ such that*

$$x \in ker\, H(t_0, t_1) \ . \tag{3.40}$$

2. *The control system* (3.1), (3.2) *is completely reconstructible at $t_1 \in I$ if and only if there exists a $t_0 \in I$ where $t_0 < t_1$ such that*

$$rank\, H(t_0, t_1) = n \quad (or\ equivalently\ range\, H(t_0, t_1) = \mathbb{R}^n) \ . \tag{3.41}$$

Let us now turn to the reconstructibility of linear time-invariant control systems.

Theorem 3.5.3 *Consider the control system given by* (3.6), (3.7).

1. *A state $x_0 \in \mathbb{R}^n$ is non-reconstructible at time t_0 (or at any time) if and only if*

$$x_0 \in ker \mathcal{C} \ . \tag{3.42}$$

2. *The control system* (3.6), (3.7) *is completely reconstructible at some time t_0 (or at any time) if and only if*

$$rank \mathcal{C} \ = \ n \ . \tag{3.43}$$

Remarks: For time-invariant systems the notion 'non-reconstructible' is equivalent to 'non-observable' and similarly, 'completely reconstructible' is equivalent to 'completely observable'. The pair (C, A) is said to be ***observable*** if and only if condition (3.42) is satisfied. The subspace $\ker \mathcal{C}$ is called the ***unobservable subspace*** for the linear time-invariant system (3.6), (3.7).

Now, let us consider the structure of a linear time-invariant system which is not completely observable. For such systems, it is impossible to establish uniquely from the output what the state of the system is. We are interested to know what uncertainty remains. The following is a characterization of an unobservable subspace.

Theorem 3.5.4 *The unobservable subspace of the linear time invariant system system* (3.6),(3.7) *is the kernel (null space) of the* **observability matrix**

$$Q = \begin{pmatrix} C \\ CA \\ CA^2 \\ \vdots \\ CA^{n-1} \end{pmatrix} . \tag{3.44}$$

Unobservable subspace can be clarified by the following result:

Theorem 3.5.5 *Suppose that the output $y(t)$ and the input $u(t)$ of the linear time-invariant system* (3.6), (3.7) *are known over an interval $t_0 \leq t \leq t_1$. Then the initial state of the system at time t_0 is determined by the addition of an arbitrary vector from the unobservable subspace.*

Analogous to Theorem 3.3.6, we can obtain an observability canonical form for the linear time-invariant system.

Theorem 3.5.6 *Consider the linear time-invariant system* (3.6), (3.7). *Form a nonsingular transformation matrix $U = (U_1, U_2)^T$ where the m rows of U_1 form a basis for the m-dimensional $(m \leq n)$ subspace spanned by the rows of the observability matrix of the system. The $n - m$ rows of U_2 form together with the m rows*

of U_1 a basis for the whole n-dimensional space. Define a transformed state variable $\tilde{x}(t)$ by

$$\tilde{x}(t) \;=\; Ux(t)\ . \tag{3.45}$$

Then in terms of the transformed state variable the system is represented in the **observability canonical form**

$$\frac{d\tilde{x}(t)}{dt} \;=\; \begin{pmatrix} \tilde{A}_{11} & 0 \\ \tilde{A}_{21} & \tilde{A}_{22} \end{pmatrix} \tilde{x}(t) + \begin{pmatrix} \tilde{B}_1 \\ \tilde{B}_2 \end{pmatrix} u(t)\ , \tag{3.46}$$

$$y(t) \;=\; (\tilde{C}_1, 0)\tilde{x}(t)\ , \tag{3.47}$$

where $\tilde{A}_{11} \in \mathbb{R}^{m\times m}$, $\tilde{A}_{21} \in \mathbb{R}^{(n-m)\times m}$, $\tilde{A}_{22} \in \mathbb{R}^{(n-m)\times(n-m)}$, $\tilde{C}_1 \in \mathbb{R}^{k\times m}$, and the pair $(\tilde{C}_1, \tilde{A}_{11})$ is completely observable.

3.6 Detectability

In the preceding section, we noted that if the linear time-invariant system is not observable, there is always an uncertainty about the actual state of the system. Also, to any possible state, we can always add an arbitrary vector from the unobservable subspace (see Theorem 3.5.5). For such situations, the best one can hope for is that for any state in the unobservable subspace, the zero input response of the system converges to zero. Thus in this case, any state in the unobservable subspace is also in the stable space. Hence, whatever the unobservable component of the state is guessed, the error will not grow infinitely. This leads to the definition of detectability.

Definition 3.6.1 *The linear time-invariant system* (3.6), (3.7) *is* **detectable** *if and only if its unobservable subspace is contained in its stable subspace.*

The following theorem is a consequence of the definition:

Theorem 3.6.2 *Any asymptotically stable system of the form given by equations* (3.6), (3.7) *is detectable. Any completely observable system of the form given by equations* (3.6), (3.7) *is detectable.*

In the following sections we will discuss the importance of choosing appropriate controls. As given in Corollary 3.3.3, for system (3.1), (3.2) a state x_0 at time t_0 can be steered to the state 0 at a later time t_1 by choosing a control $u(t) = -B(t)^T\Phi(t_0,t)^T y,\ t_0 \le t \le t_1$ where y satisfies $W(t_0,t_1)y = x_0$. This is an ***open loop control*** and thus system (3.1), (3.2) is referred to as an ***open loop control system***.

What we are interested in is to have a control which is automatically determined at each time t on the basis of the state of the system at that time. For instance, one can take the control given by

$$u(t) \;=\; -F(t)x(t), \quad t \in I\ , \tag{3.48}$$

where $I = [t_0, \infty]$ and $F(\cdot) \in \mathscr{L}^2\left(I; \mathbb{R}^{p\times n}\right)$. Substituting this in system (3.1), (3.2) will yield

$$\begin{aligned} \dot{x}(t) =&\ \left(A(t) - B(t)F(t)\right)x(t), \quad t \in I\ , \\ y(t) =&\ C(t)x(t), \quad t \in I\ . \end{aligned} \tag{3.49}$$

System (3.49) is said to be a ***closed loop control system*** and equation (3.48) is called a ***(linear) feedback law***. Figure 3.3 represents a diagram of a closed loop system.

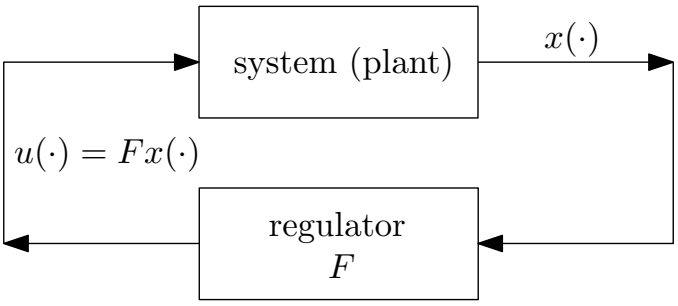

Figure 3.3: Closed loop system.

3.7 Linear State Feedback Control

The actual operation of the control system is compared to the desired operation and the input to the system is adjusted on the basis of this comparison. This is called

the *feedback* feature of most of the control systems. Thus feedback control systems are able to operate satisfactorily despite adverse conditions such as disturbances acting on the system itself or variations in plant properties.

An important aspect of the feedback system design is the stability of the control system. Sometimes its main objective is to actually stabilize the system if it is initially unstable, or to improve its stability if transient phenomena do not die out sufficiently fast.

Consider the linear time-invariant continuous system (3.6) given by

$$\frac{dx(t)}{dt} \;=\; Ax(t) + Bu(t), \quad t \in I \;.$$

Let us assume that the complete state can be accurately measured at all times and is thus available for feedback. Then it is possible to implement a *linear control law* of the form

$$u(t) \;=\; -F(t)x(t) \;, \tag{3.50}$$

where the matrix $F(t)$ (possibly time-varying) with appropriate dimensions is called the ***feedback gain matrix***. If this control law is connected to system (3.6), we obtain a closed loop system described by

$$\frac{dx(t)}{dt} \;=\; \left(A - BF(t)\right) x(t) \;. \tag{3.51}$$

In particular, if a constant matrix F is chosen, the stability of the system is determined by the eigenvalues of $A - BF$ (see Theorem 3.2.6).

The following theorem sheds light on the concepts of controllability and stabilizability.

Theorem 3.7.1 *Consider the linear time-invariant system* (3.6) *with the time-invariant control law*

$$u(t) \;=\; -Fx(t) \;. \tag{3.52}$$

Then the following holds:

The eigenvalues of the closed loop $A - BF$ can be arbitrarily located in the complex plane (with the restriction that complex eigenvalues occur in complex conjugate pairs) by choosing F suitably if and only if the system (3.6) *is completely controllable.*

It is possible to find a constant matrix F such that the closed loop system (3.51) *is asymptotically stable if and only if the system* (3.6) *is stabilizable.*

The first part of the above theorem means that it is always possible to stabilize a completely controllable system by state feedback, or to improve its stability by locating the closed-loop poles in the left-half complex plane. However, it does not specify as to where in the left-half complex plane the closed-loop poles should be located. The second part of the theorem suggests that if the system is stabilizable but not completely controllable (not all), the unstable poles of the system can be moved to arbitrary locations by choosing appropriate gain matrix F.

3.8 The Deterministic Linear Optimal Regulator Problem

We have seen in the previous section that a complete controllable time-invariant linear system can always be stabilized by a linear feedback law. Also, since the closed-loop poles can be located anywhere in the complex plane, the system can be stabilized. Moreover, by choosing these poles far to the left in the complex plane, the convergence to the zero state can be made arbitrarily quickly. However, making the system move quickly requires large input amplitudes. In any practical problem the input amplitudes are constrained to certain maximal values. This imposes a limit of how far the closed-loop poles can be moved to the left. Thus, we need to consider both the speed of convergence of the state to zero and the magnitude of the input amplitudes. This naturally leads to an optimization problem.

Let us study the optimization problem generally by considering the linear continuous-

time system (3.1) described by

$$\frac{dx(t)}{dt} \;=\; A(t)x(t) + B(t)u(t)\ ,$$

with controlled variable

$$z(t) \;=\; D(t)x(t)\ . \tag{3.53}$$

Here we assume that the matrix $A(t)$ is continuous, the matrices $B(t)$ and $D(t)$ are piecewise continuous functions and all the matrix functions are bounded. We consider the problem to reduce the controlled variable $z(t)$ to zero as quickly as possible. One criterion to express how quickly $z(t)$ is reduced to zero during the interval $[t_0, t_1]$ is the quadratic cost functional

$$\int_{t_0}^{t_1} z^T(t)R_1z(t)\,dt\ , \tag{3.54}$$

where $R_1(t)$ is a positive-definite symmetric matrix which is piecewise continuous with respect to t. The quantity $z^T(t)R_1z(t)$ is a measure of the extent to which the controlled variable z at time t deviates from zero. The weighting matrix $R_1(t)$ determines how much weight is attached to each of the components of z. If $R_3(t)$ is diagonal (as often is the case), $z^T(t)R_1z(t)$ is the weighted sum of the deviations of each of the components of z from zero. The integral (3.54) is a criterion for cumulative deviation of $z(t)$ from zero during the interval $[t_0, t_1]$.

Now, attempting to minimize the quadratic cost criterion (3.54) will result in indefinitely large input amplitudes. Therefore, an inclusion of a second term in the criterion prevents the input from growing indefinitely. We thus consider

$$\int_{t_0}^{t_1} \left(z^T(t)R_1z(t) + u^T(t)R_2u(t)\right)\,dt\ , \tag{3.55}$$

where $R_2(t)$ is a positive-definite symmetric matrix and a piecewise continuous function of t. The relative importance of the two terms in the latter criterion (3.55) is determined by the matrices R_1 and R_2. If it is very important that the terminal state $x(t_1)$ is as close as possible to the zero state, it is useful to extend (3.55) by adding a third term as follows,

$$\int_{t_0}^{t_1} \left(z^T(t)R_1z(t) + u^T(t)R_2u(t)\right)\,dt\ + x^T(t_1)P_1x(t_1)\ , \tag{3.56}$$

where P_1 is a nonnegative-definite symmetric matrix.

As a summary to our optimization problem, we have the following definition:

Definition 3.8.1 (Deterministic Linear Optimal Regulator Problem) *Consider the state or the response of the linear control system given by equation* (3.1) *with the initial condition* $x(t_0) = x_0$*, and the controlled variable*

$$z(t) \;=\; D(t)x(t)\;. \tag{3.57}$$

Determine an input $u(t),\ t_0 \le t \le t_1$*, for which the criterion*

$$\int_{t_0}^{t_1} \left[z^T(t)R_1(t)z(t) + u^T R_2(t)u(t)\right]\, dt + x^T(t_1)P_1x(t_1) \tag{3.58}$$

is minimal. Here, P_1 *is a nonnegative-definite symmetric matrix and* $R_1(t)$ *and* $R_2(t)$ *are positive-definite symmetric matrices for* $t_0 \le t \le t_1$*.*

Remarks: It is assumed that $A(t)$ is a continuous function of t and that $B(t), D(t), R_1(t)$ and $R_2(t)$ are piecewise continuous functions of t, and that all these matrix functions are bounded. If all the matrices in the deterministic linear optimal regulator problem are constant, then it is said to be a ***time-invariant deterministic linear optimal regulator problem***.

The term "deterministic" suggests that the problem under consideration has a disturbed initial state and it is required to bring the (linear) system to the zero state as quickly as possible keeping the input amplitudes bounded. In contrast, a "stochastic" linear optimal regulator problem deals with the disturbances acting uninterruptedly upon the system that tend to drive the state away from the zero state.

The next theorem gives us the solution of the regulator problem in the form of a linear control law.

Theorem 3.8.2 *Consider the deterministic linear optimal regulator problem. Then the optimal input* $u(t)$ *can be generated through a linear control law of the form*

$$u(t) \;=\; -F(t)x(t)\;, \tag{3.59}$$

where

$$F(t) \;=\; R_2^{-1}B^T P(t)\ . \tag{3.60}$$

Here the symmetric nonnegative-definite matrix $P(t)$ satisfies the **matrix Riccati equation**

$$-\frac{dP(t)}{dt} \;=\; D^T(t)R_1(t)D(t) - P(t)B(t)R_2^{-1}(t)B^T(t)P(t) + P(t)A(t) + A^T(t)P(t)\ , \tag{3.61}$$

with the terminal condition

$$P(t_1) \;=\; P_1\ . \tag{3.62}$$

The minimal value of the cost criterion is equal to $x_0^T P(t_0)x_0$.

According to this theorem, the control law (3.59) automatically generates the optimal input for any initial state. A block diagram interpretation in Figure 3.4 illustrates the closed-loop nature of the solution.

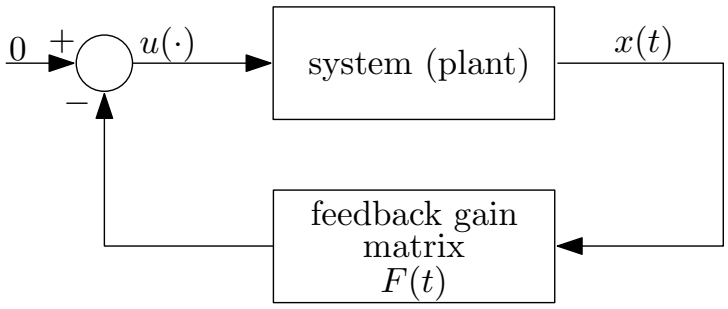

Figure 3.4: The feedback structure of the optimal linear regulator.

Remark: Under the conditions formulated in Definition 3.8.1, it can be proved that the *deterministic optimal regulator problem has a unique solution*. The existence of the solution of the regulator problem also guarantees that the matrix Riccati equation (3.61) with the terminal condition (3.62) has a unique solution. Further discussions on the existence of the solutions of the regulator problem and Riccati equations can be found at Kalman (1960) [22], Athans and Falb (1966) [1], Bucy (1967) [6, 7], Moore and Anderson (1968) [35], and Schumitzky (1968) [50].

In practical problems, it is often a natural concern to consider very long control periods $[t_0, t_1]$. The question in mind is, what happens to the asymptotic behavior

of the solution of the deterministic regulator problem as $t_1 \to \infty$? Under certain conditions (see Kwakernaak and Sivan (1972) [30], Theorem 3.5) the following results hold.

1. As $t_1 \to \infty$, the solution $P(t)$ of the matrix Riccati equation (3.61) with terminal condition (3.62) generally approaches a steady-state solution $\bar{P}(t)$ which is independent of P_1.

2. The corresponding steady state control law

$$u(t) \;=\; -\bar{F}(t)x(t) \qquad \text{with} \qquad \bar{F}(t) \;=\; R_2^{-1}B^T(t)\bar{P}(t) \tag{3.63}$$

   is asymptotically stable.

The second item can be easily understood as follows: Since the integral

$$\int_{t_0}^{\infty} \left(z^T(t)R_1(t)z(t) + u^T(t)R_2(t)u(t)\right)\, dt \tag{3.64}$$

exists for the steady-state control law, it follows that in the closed-loop system $z(t) \to 0$ and $u(t) \to 0$ as $t \to \infty$. This can be generally true only if $x(t) \to 0$, that is, the closed-loop system is asymptotically stable.

For a time-invariant system, we have the following result:

Theorem 3.8.3 *Consider the time-invariant regulator problem for the system*

$$\begin{aligned} \frac{dx(t)}{dt} &= Ax(t) + Bu(t)\ , \\ z(t) &= Dx(t)\ , \end{aligned} \tag{3.65}$$

and the criterion

$$\int_{t_0}^{t_1} \left(z^T(t)R_1z(t) + u^T(t)R_2u(t)\right)\, dt + x^T(t_1)P_1x(t_1)\ , \tag{3.66}$$

with constant matrices $A, B, D, R_1 > 0, R_2 > 0$, and $P_1 \geq 0$. The corresponding Riccati equation is given by

$$-\frac{dP(t)}{dt} \;=\; D^TR_1D - P(t)BR_2^{-1}B^TP(t) + P(t)A + A^TP(t)\ , \tag{3.67}$$

with terminal condition

$$P(t_1) \;=\; P_1 \;. \tag{3.68}$$

Assuming that the system (3.65) *is stabilizable and detectable, then the following statements hold:*

1. *As* $t_1 \to \infty$*, the solution of the Riccati equation* (3.67) *approaches the unique value* $\bar{P}$ *independent of* P_1*.*

2. $\bar{P}$ *is the unique nonnegative-definite symmetric solution of the algebraic Riccati equation given by*

$$0 \;=\; D^T R_1 D - P B R_2^{-1} B^T P + P A + A^T P \;. \tag{3.69}$$

3. *The steady-state control law described by*

$$u(t) \;=\; -\bar{F} x(t) \;, \qquad \textit{where} \qquad \bar{F} \;=\; R_2^{-1} B^T \bar{P} \tag{3.70}$$

   is asymptotically stable.

4. *The steady-state control law minimizes*

$$\lim_{t_1 \to \infty} \left\{ \int_{t_0}^{t_1} \left(z^T(t) R_1 z(t) + u^T(t) R_2 u(t) \right) \, dt + x^T(t_1) P_1 x(t_1) \right\} \;, \tag{3.71}$$

   for all $P_1 \geq 0$*. For the steady-state control law, the criterion* (3.71) *takes the value* $x^T(t_0) \bar{P} x(t_0)$*.*

Remark: Stabilizability and detectability are sufficient conditions for the Riccati equation to converge to a unique $\bar{P}$ for all $P_1 \geq 0$ and for the algebraic Riccati equation to have a unique nonnegative-definite solution.

3.9 Nonlinear Systems

For nonlinear systems, there exists no analytical closed form of a control law $u(t)$ which solves the control problem. However, there are theorems that provide local existence, uniqueness, and the possibility of linear approximation of the nonlinear feedback law. Following Theorem 5.6 in Russell (1979) [49], we have the following results:

Theorem 3.9.1 *Consider the nonlinear problem (NLCP) given by*

$$\begin{aligned} \frac{dx}{dt} &= \mathcal{F}(x,u) \ , \\ z &= Dx \ , \end{aligned} \tag{3.72}$$

and let $(\bar{x},\bar{u})$ be an equilibrium of the system such that $\mathcal{F}$ is at least two times continuously differentiable at $(\bar{x},\bar{u})$. Consider the criterion

$$J(u,x) \ = \ \int_0^\infty \Big((x-\bar{x})^T R_1 (x-\bar{x}) + (u-\bar{u})^T R_2 (u-\bar{u}) \Big) \ dt \ . \tag{3.73}$$

Furthermore, consider the linearized system around $(\bar{x},\bar{u})$ described by

$$\begin{aligned} \frac{dx}{dt} &= A(x-\bar{x}) + B(u-\bar{u}) \ , \\ z &= D(x-\bar{x}) \ , \end{aligned} \tag{3.74}$$

where A and B denotes the Jacobian of $\mathcal{F}(x,u)$ with respect to x and u at $(\bar{x},\bar{u})$, respectively. Supposed that the linearized system (3.74) is stabilizable and observable. Then there exists a neighborhood $\mathcal{N}$ of $(\bar{x},\bar{u})$ such that the following holds:

1. *A unique feedback law $u = \mathcal{K}(x)$ which solves the NLCP for $x \in \mathcal{N}$ exists.*

2. *The stationary solution $x = \bar{x}$ is asymptotically stable for the closed-loop system*

$$\frac{dx}{dt} \ = \ \mathcal{F}(x,\mathcal{K}(x)) \, , \ x(0) \in \mathcal{N} \ . \tag{3.75}$$

3. *The feedback $\mathcal{K}$ has the form*

$$\mathcal{K} \ = \ K(x-\bar{x}) + \bar{u} + o(\|x-\bar{x}\|) \ , \tag{3.76}$$

   where K is the optimal feedback matrix for the linearized system.

4. *The feedback law*

$$u_\ell \ = \ K(x-\bar{x}) + \bar{u} \ , \tag{3.77}$$

   also stabilizes the nonlinear system for $x(0) \in \mathcal{N}$.

Chapter 4

The Model Equations and the Control Formulation

In this chapter we will present the full cardiovascular system model developed in Chapter 2 and the control problem. The focus is to obtain a stabilizing control for the nonlinear full system which is suboptimal via constructing an optimal control for the corresponding simplified model. Model modifications and the corresponding linearization will be discussed to achieve a linear feedback control.

4.1 The Cardiovascular System Model

Our full system cardiovascular model is depicted in Figure 4.1. The model can be described as a system of coupled first order ordinary differential equations with state vector

$$\tilde{x} = (P_{sa}, P_{fa}, P_{as}, P_{vs}, P_{ap}, P_{vp}, P_{\ell v}, R_{sp}, S_{rv}, \sigma_{rv}, H)^T \in \mathbb{R}^{11} \ , \tag{4.1}$$

representing pressures in the systemic aorta, finger arteries, arterial systemic, venous systemic, arterial pulmonary venous pulmonary and left ventricle compartments, systemic peripheral resistance, right ventricular contractility and its derivative, and

the heart rate, respectively. The parameter vector of the system is

$$\begin{aligned}\tilde{p} \;=\; (&c_{sa}, c_{fa}, c_{as}, c_{vs}, c_{rv}, c_{ap}, c_{vp}, V_{\mathrm{tot}}, V_{\mathrm{d}},\\ &R_{mv,open}, R_{av,open}, R_{sc_1}, R_{sc_2}, R_{sp_f}, R_{rv}, R_{pp}, a, b, c,\\ &E_m, T_{r,frac}, \kappa, C_{a,O_2}, K, A_{\mathrm{pesk}}, M_0, \rho, \alpha_{rv}, \gamma_{rv}, \beta_{rv})^T \in \mathbb{R}^{30}\ .\end{aligned} \tag{4.2}$$

The system of differential equations describing the full system is given by

$$\begin{aligned}
\frac{dP_{sa}(t)}{dt} &= \frac{1}{c_{sa}}\left(\frac{P_{\ell v}(t)-P_{sa}(t)}{R_{av}(t)} - \frac{P_{sa}(t)-P_{fa}(t)}{R_{sc_1}} - \frac{P_{sa}(t)-P_{as}(t)}{R_{sc_2}}\right)\ ,\\
\frac{dP_{fa}(t)}{dt} &= \frac{1}{c_{fa}}\left(\frac{P_{sa}(t)-P_{fa}(t)}{R_{sc_1}} - \frac{P_{fa}(t)-P_{vs}(t)}{R_{sp_f}}\right)\ ,\\
\frac{dP_{as}(t)}{dt} &= \frac{1}{c_{as}}\left(\frac{P_{sa}(t)-P_{as}(t)}{R_{sc_2}} - \frac{P_{as}(t)-P_{vs}(t)}{R_{sp}(t)}\right)\ ,\\
\frac{dP_{vs}(t)}{dt} &= \frac{1}{c_{vs}}\left(\frac{P_{as}(t)-P_{vs}(t)}{R_{sp}(t)} + \frac{P_{fa}(t)-P_{vs}(t)}{R_{sp_f}} - Q_{rv}(t)\right)\ ,\\
\frac{dP_{ap}(t)}{dt} &= \frac{1}{c_{ap}}\left(Q_{rv}(t) - \frac{P_{ap}(t)-P_{vp}(t)}{R_{pp}}\right)\ ,\\
\frac{dP_{vp}(t)}{dt} &= \frac{1}{c_{vp}}\left(\frac{P_{ap}(t)-P_{vp}(t)}{R_{pp}} - \frac{P_{vp}(t)-P_{lv}(t)}{R_{mv}(t)}\right)\ ,\\
\frac{dP_{\ell v}(t)}{dt} &= E_{\ell v}(t)\left(\frac{\frac{dE_{\ell v}(t)}{dt}P_{\ell v}(t)}{E_{\ell v}(t)^2} + \frac{P_{vp}(t)-P_{\ell v}(t)}{R_{mv}(t)} - \frac{P_{\ell v}(t)-P_{sa}(t)}{R_{av}(t)}\right)\ ,\\
\frac{dR_{sp}(t)}{dt} &= \frac{1}{K}\left(A_{pesk}\left(\frac{P_{as}(t)-P_{vs}(t)}{R_{sp}(t)}C_{a,O_2} - M_T\right) - (P_{as}(t)-P_{vs}(t))\right)\ ,\\
\frac{dS_{rv}(t)}{dt} &= \sigma_{rv}(t)\ ,\\
\frac{d\sigma_{rv}(t)}{dt} &= -\alpha_{rv}S_{rv}(t) - \gamma_r\sigma_{rv}(t) + \beta_{rv}H(t)\ ,\\
\frac{dH}{dt} &= u(t)\ .
\end{aligned} \tag{4.3}$$

The cardiac output of the right ventricle $Q_{rv}(t)$ is given by

$$Q_{rv}(t) \;=\; H\frac{c_{rv}P_{vs}(t)a_r(H)f(S_{rv}(t),P_{ap}(t))}{a_r(H)P_{ap}(t) + k_r(H)f(S_{rv}(t),P_{ap}(t))}\ , \tag{4.4}$$

where

$$k_r(H) \;=\; e^{-t_d(H)(c_{rv}R_{rv})^{-1}} \quad \text{and} \quad a_r(H) \;=\; 1-k_r(H)\ , \tag{4.5}$$

and

$$f(S_{rv}(t),P_{ap}(t)) \;=\; 0.5\,(S_{rv}(t)+P_{ap}(t)) - 0.5\left((P_{ap}(t)-S_{rv}(t))^2 + 0.001\right)^{1/2}\ , \tag{4.6}$$

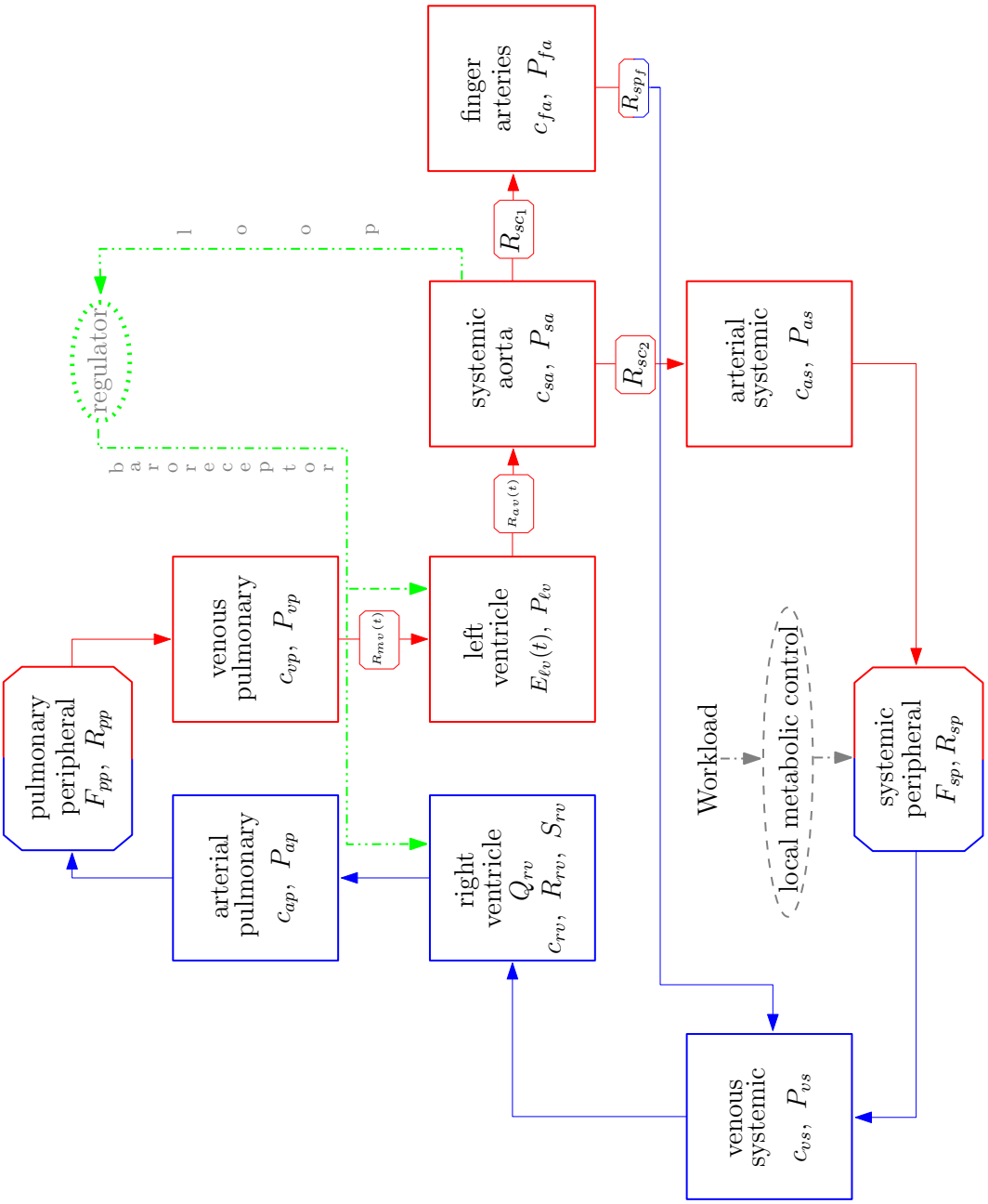

Figure 4.1: The block diagram of the full cardiovascular system model.

is a smooth function that chooses the minimum between S_{rv} and P_{ap} at a time instant t. The time varying resistances, $R_{mv}(t)$ and $R_{av}(t)$ are defined by

$$\begin{aligned} R_{mv}(t) &= \begin{cases} \infty & \text{for } P_{\ell v}(t) > P_{vp}(t) \ , \\ R_{mv,open} & \text{for } P_{\ell v}(t) \leq P_{vp}(t) \ , \end{cases} \\ R_{av}(t) &= \begin{cases} \infty & \text{for } P_{\ell v}(t) < P_{sa}(t) \ , \\ R_{av,open} & \text{for } P_{\ell v}(t) \geq P_{sa}(t) \ . \end{cases} \end{aligned} \tag{4.7}$$

Moreover, the time-varying elastance $E_{\ell v}(t)$ and its derivative $\dfrac{E_{\ell v}(t)}{dt}$ are given, respectively, as

$$E_{\ell v}(t) = \begin{cases} E_m + \dfrac{E_M - E_m}{2}\left[1 - \cos\left(\dfrac{\pi t}{T_M}\right)\right], & 0 \leq t \leq T_M \\ E_m + \dfrac{E_M - E_m}{2}\left[\cos\left(\dfrac{\pi}{T_r}\left(t - T_M\right)\right) + 1\right], & T_M \leq t \leq T_M + T_r \\ E_m, & T_M + T_r \leq t < T \ , \end{cases} \tag{4.8}$$

and

$$\frac{dE_{\ell v}(t)}{dt} = \begin{cases} \dfrac{E_M - E_m}{2}\left[\dfrac{\pi}{T_M}\sin\left(\dfrac{\pi t}{T_M}\right)\right], & 0 \leq t \leq T_M \\ \dfrac{E_M - E_m}{2}\left[-\dfrac{\pi}{T_r}\sin\left(\dfrac{\pi}{T_r}\left(t - T_M\right)\right)\right], & T_M \leq t \leq T_M + T_r \\ 0, & T_M + T_r \leq t < T \ , \end{cases} \tag{4.9}$$

where the maximum elastance function value E_M is a function of H described by

$$E_M(H) = a\exp(-b\exp(-cH)) \ , \tag{4.10}$$

and the time of peak elastance T_M is expressed using Bazett's formula as

$$T_M = \frac{\kappa}{H^{1/2}} \ . \tag{4.11}$$

See Chapter 2 for detailed explanation of these auxiliary equations. The values for all the parameters used is listed in the tables in Appendix A.

The last equation in (4.3) is an equation for the feedback law which controls the heart rate, where $u(t)$ is constructed as a function of the state variables. Details will be discussed in the next section.

Adding the first seven equations in (4.3) will yield

$$c_{sa}P_{sa} + c_{fa}P_{fa} + c_{as}P_{as} + c_{vs}P_{vs} + c_{ap}P_{ap} + c_{vp}P_{vp} + \frac{1}{E_{\ell v}}P_{\ell v} + V_d \equiv V_{\text{tot}} \ , \quad (4.12)$$

where V_{tot} denotes the total blood volume, which remains constant. This suggests that there is no exchange of volume between the cardiovascular system and the interstitium. Also, for given $V_{\text{tot}}, c_{sa}, c_{fa}, c_{as}, c_{vs}, c_{ap}, c_{vp}, E_{\ell v}$, and V_d, equation (4.12) defines a hyperplane in $\mathbb{R}^7$ which is invariant for system (4.3). From equation (4.12), we can express one of the pressures in terms of the others. For instance, we can choose

$$\begin{aligned} P_{vp} = \ & P_{vp}\left(P_{sa}, P_{fa}, P_{as}, P_{vs}, P_{ap}, P_{\ell v}\right) \\ := \ & \frac{1}{c_{vp}}\left(V_{\text{tot}} - c_{sa}P_{sa} - c_{fa}P_{fa} - c_{as}P_{as} - c_{vs}P_{vs} - c_{ap}P_{ap} - \frac{1}{E_{\ell v}}P_{\ell v} - V_d\right) \ . \end{aligned} \quad (4.13)$$

With the above argument on the invariance of (4.12) for the full system, we can reduce the dimension of the system by one. This can be done by replacing P_{vp} by the expression in (4.13), and eliminate the sixth equation of the full system (4.3). This system reduction plays an important role in obtaining a stabilizing feedback control. Now, for the reduced state

$$x = (P_{sa}, P_{fa}, P_{as}, P_{vs}, P_{ap}, P_{\ell v}, R_{sp}, S_{rv}, \sigma_r, H)^T \in \mathbb{R}^{10} \ , \quad (4.14)$$

and the parameter vector of the system,

$$\begin{aligned} p \ = \ & (c_{sa}, c_{fa}, c_{as}, c_{vs}, c_{rv}, c_{ap}, V_{\text{tot}}, V_{\text{d}}, \\ & R_{mv,open}, R_{av,open}, R_{sc_1}, R_{sc_2}, R_{sp_f}, R_{rv}, R_{pp}, a, b, c, \\ & E_m, T_{r,frac}, \kappa, C_{a,O_2}, K, A_{\text{pesk}}, M_0, \rho, \alpha_{rv}, \gamma_{rv}, \beta_{rv})^T \in \mathbb{R}^{29} \ . \end{aligned} \quad (4.15)$$

Letting W be the ergometric workload introduced in Chapter 2, Section 2.6, we can write the system of first order differential equations as follows:

$$\frac{dx}{dt} \ = \ \mathcal{G}\left(x(t), p, W, u(t)\right), \qquad t \geq 0 \ . \quad (4.16)$$

Omitting t for brevity, the coordinates of $\mathcal{G}$ are given by

$$\begin{aligned}
\mathcal{G}_1 &= \frac{1}{c_{sa}}\left(\frac{P_{\ell v}-P_{sa}}{R_{av}}-\frac{P_{sa}-P_{fa}}{R_{sc_1}}-\frac{P_{sa}-P_{as}}{R_{sc_2}}\right)\ ,\\
\mathcal{G}_2 &= \frac{1}{c_{fa}}\left(\frac{P_{sa}-P_{fa}}{R_{sc_1}}-\frac{P_{fa}-P_{vs}}{R_{sp_f}}\right)\ ,\\
\mathcal{G}_3 &= \frac{1}{c_{as}}\left(\frac{P_{sa}-P_{as}}{R_{sc_2}}-\frac{P_{as}-P_{vs}}{R_{sp}}\right)\ ,\\
\mathcal{G}_4 &= \frac{1}{c_{vs}}\left(\frac{P_{as}-P_{vs}}{R_{sp}}+\frac{P_{fa}-P_{vs}}{R_{sp_f}}-Q_{rv}\right)\ ,\\
\mathcal{G}_5 &= \frac{1}{c_{ap}}\left(Q_{rv}-\frac{P_{ap}-P_{vp}\left(P_{sa},P_{fa},P_{as},P_{vs},P_{ap},P_{\ell v}\right)}{R_{pp}}\right)\ ,\\
\mathcal{G}_6 &= E_{\ell v}\left(\frac{\frac{dE_{\ell v}}{dt}P_{\ell v}}{{E_{\ell v}}^2}+\frac{P_{vp}\left(P_{sa},P_{fa},P_{as},P_{vs},P_{ap},P_{\ell v}\right)-P_{\ell v}}{R_{mv}}-\frac{P_{\ell v}-P_{sa}}{R_{av}}\right)\ ,\\
\mathcal{G}_7 &= \frac{1}{K}\left(A_{pesk}\left(\frac{P_{as}-P_{vs}}{R_{sp}}C_{a,O_2}-M_T\right)-\left(P_{as}-P_{vs}\right)\right)\ ,\\
\mathcal{G}_8 &= \sigma_{rv}\ ,\\
\mathcal{G}_9 &= -\alpha_{rv}S_{rv}-\gamma_{rv}\sigma_{rv}+\beta_{rv}H\ ,\\
\mathcal{G}_{10} &= u\ ,
\end{aligned} \tag{4.17}$$

where the auxiliary equations are the same as in the full system (4.3) mentioned above .

In the following sections, we will present the control problem and its formulation. We will proceed as in Batzel et al. (2007) [2], Chapter 1, where we replaced the arterial systemic pressure P_{as} by the systemic aortic P_{sa} in the control formulation.

4.2 The Control Problem

Many physiologists proceed from the assumption that optimization is a fundamental concept in the evolution of biological systems (see Kenner (1979) [27] or Swan (1984) [53]). That is, cells, tissues, organs, systems of organs, etc. function in such a way, that for instance, consumption of energy is minimized. Applying the principle

of economical use of energy to the cardiovascular system means that the work done by the heart, which is essentially ejection of the stroke volume, is minimized.

Now, let us talk more about the control variable. We consider the variation of the heart rate to be the control variable and is given by

$$\frac{dH}{dt} \;=\; u(t)\;. \tag{4.18}$$

This control represents the baroreceptor loop including the action of the baroreceptors which measure the aortic pressure P_{sa}. Control signals are then generated in the medulla and are transmitted by the autonomic nervous system. The baroreceptor loop also includes the action of the control signals on the pacemaker cells in the sine node which in turn change the heart frequency. It should be noted that we do not consider the fact that these signals also influence the systemic peripheral resistance, the compliance of the venous systemic compartment and the contractilities respectively, elastances of the ventricles. We assume that the latter are controlled indirectly via the heart frequency. We do not know the exact details of how the signals from the baroreceptors are transformed in the medulla into the signals transmitted by the sympathetic and parasympathetic nervous system. With this limitation, our approach is based on the optimal control theory. The idea is to construct a stabilizing feedback control which drives the system from one equilibrium state to another equilibrium state.

In our case, we consider a situation where a constant workload is imposed on the cardiovascular system assuming that the control mechanism works in an optimal way. This means, that we are interested in the system transitions from the equilibrium "rest" state x^{rest} corresponding to zero workload, $M_{\text{T}} = M^{\text{rest}} = M_0$ to the equilibrium "exercise" state x^{exer} corresponding to the imposed constant workload W^{exer}, $M_{\text{T}} = M^{\text{exer}} = M_0 + \rho W^{\text{exer}}$. Mathematically, we assume that the control $u(t)$ is chosen such that the quadratic cost functional

$$J\left(u(\cdot), x^{\text{rest}}\right) \;=\; \int_0^\infty \left(q_{sa}^2 \left(P_{sa}(t) - P_{sa}^{\text{exer}}\right)^2 + u(t)^2\right)\, dt \tag{4.19}$$

is minimized. Quadratic terms are used instead of absolute values due to continuity

reasons. The positive scalar q_{sa}^2 is a weighting factor. In the cost functional (4.19), deviations of the aortic pressure from the equilibrium value and large values of the control function are penalized. Notice also that only P_{sa} (i.e., first component of the solution $x(t)$ of the system (4.16) with initial condition $x(0) = x^{\text{rest}}$ and $W = W^{\text{exer}}$) enters the cost functional. This reflects the assumption that only the aortic pressure is sensed in the system.

Moreover, in addition to system (4.16) we have the output equation

$$y(t) \;=\; q_{sa}\,(P_{sa}(t) - P_{sa}^{\text{exer}}) \;=\; (q_{sa}, 0, \ldots, 0)\,(x(t) - x^{\text{exer}})\,, \quad t \geq 0\ . \tag{4.20}$$

Hence, the cost functional (4.19) can be written as

$$J\left(u(\cdot), x^{\text{rest}}\right) \;=\; \int_0^\infty \left(y(t)^2 + u(t)^2\right)\, dt\ . \tag{4.21}$$

4.3 Determination of Equilibria

In this study, we are considering cardiovascular system model (4.3) which generates pulsatile pressures. The left ventricle is the source of pulse waves in the system. We pointed out in the previous section that we will consider the system transitions from equilibrium rest state to equilibrium exercise state. The question now is, what does the equilibrium state means, in the case of pulsatile pressures?

Before we answer the question, let us first recall the definition of a periodic solution of a system (cf. Boyce and DiPrima (2001) [4] and Hirsch et al. (2004) [18]).

Definition 4.3.1 *A* **periodic solution** *for the system*

$$\frac{dx}{dt} \;=\; f(x)\ , \tag{4.22}$$

satisfies the relation

$$x(t+\tau) \;=\; x(t)\ . \tag{4.23}$$

for all t and some nonnegative constant τ. The least such τ is called the period *of the solution.*

It can be verified numerically, that our full system (4.3) generates a periodic solution (see next chapter). Going back to our problem, we need to specify equilibrium rest and equilibrium exercise values. These would be the initial conditions, respectively, the terminal values in which the system tends, in our control formulation. To determine the "*equilibrium values*", we consider taking the *mean values* of the pressures of the corresponding periodic solutions, using

$$P_{\text{mean}} \;=\; P_{\text{dias}} + \frac{1}{3}\left(P_{\text{sys}} - P_{\text{dias}}\right) \;, \tag{4.24}$$

where P_{dias} and P_{sys} are the end-diastolic and end-systolic pressures, respectively, and P_{mean} denotes the computed mean pressure. Two separate computations are done to obtain equilibrium "*mean*" values. One for the rest condition and the other for the exercise condition. To do this, we choose to fix the values for the controlled parameters namely, the heart rate H, workload W and Peskin's constant A_{pesk}. Thus we have, $H^{\text{rest}}, W^{\text{rest}}$, and $A^{\text{rest}}_{\text{pesk}}$ corresponding to rest condition and respectively, $H^{\text{exer}}, W^{\text{exer}}$, and $A^{\text{exer}}_{\text{pesk}}$ for exercise condition. The set of values are listed in table A.5. In both cases, the baroreceptor loop control $\frac{dH}{dt} = u(t)$ is not considered. Numerical implementation in determining these equilibria is presented in the next chapter.

4.4 System Modifications and Reductions

Our full system (4.3) is a set of nonlinear coupled ordinary differential equations. Also, the right hand side of the system involves terms which are time dependent aside from the states. These include the time-varying resistances $R_{mv}(t)$ and $R_{av}(t)$, elastance function $E_{\ell v}(t)$ and its derivative $\dfrac{dE_{\ell v}(t)}{dt}$, and indirectly the Gompertz function (H-dependent) which is inherent in the computation of the left ventricular elastance. Instead of dealing with this non-autonomous nonlinear system which will give us difficulty in linearizing, we consider another system where the left ventricle is modeled similar to the right ventricle. This leads us to a system similar to the Kappel model (cf. Batzel (2007) [2], Chapter 1) with additional systemic aorta and finger arteries compartment. Figure 4.2 shows the block diagram of this model.

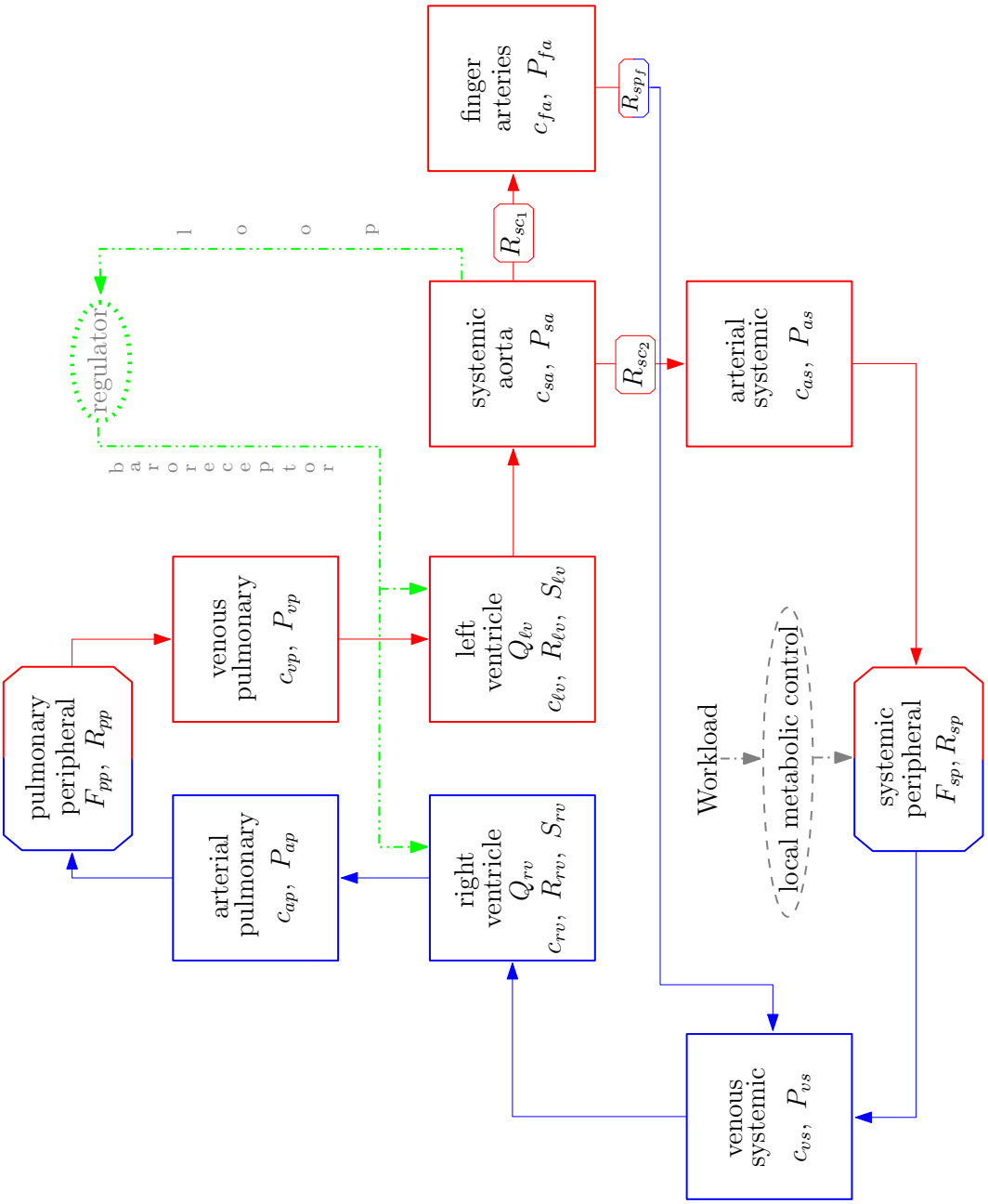

Figure 4.2: The block diagram of the modified linear cardiovascular system model.

The time varying left ventricular elastance $E_{\ell v}(t)$ and resistances $R_{mv}(t)$ and $R_{av}(t)$ do not appear in this modified model. However, introduction of new variables and parameters are inevitable. As in [2], we have the left ventricular cardiac output $Q_{\ell v}$ as

$$Q_{\ell v} \;=\; H\frac{c_{\ell v}P_{vp}a_{\ell}(H)f(S_{\ell v},P_{as})}{a_{\ell}(H)P_{as}+k_{\ell}(H)f(S_{\ell v},P_{as})}\;, \tag{4.25}$$

where

$$k_{\ell}(H) \;=\; e^{-t_d(H)(c_{\ell v}R_{\ell v})^{-1}} \quad \text{and} \quad a_{\ell}(H) \;=\; 1-k_{\ell}(H)\;, \tag{4.26}$$

and

$$f(S_{\ell v},P_{as}) \;=\; 0.5\,(S_{\ell v}+P_{as})-0.5\left((P_{as}-S_{\ell v})^2+0.001\right)^{1/2}\;. \tag{4.27}$$

$c_{\ell v}$ and $R_{\ell v}$ are the compliance and resistance of the left ventricle, respectively. Furthermore, the contractility of the left ventricle $S_{\ell v}$ is described by the second order differential equation

$$\frac{d^2S_{\ell v}}{dt^2}+\gamma_{\ell v}\frac{dS_{\ell v}}{dt}+\alpha_{\ell v}S_{\ell v}=\beta_{\ell v}H\;, \tag{4.28}$$

where $\alpha_{\ell v},\beta_{\ell v}$ and $\gamma_{\ell v}$ are constants. Transforming this system to system of first order differential equation and introducing $\sigma_{\ell v}=\frac{dS_{\ell v}}{dt}$ gives us

$$\begin{aligned}\frac{dS_{\ell v}}{dt}&=\sigma_{\ell v}\;,\\ \frac{d\sigma_{\ell v}}{dt}&=-\alpha_{\ell v}S_{\ell v}-\gamma_{\ell v}\sigma_{\ell v}+\beta_{\ell v}H\;.\end{aligned} \tag{4.29}$$

We hope that a stabilizing control for the modified model would work for the full system (4.17) as well (which it does!). It can also be verified that neglecting the finger arteries compartment in the modified model also stabilizes the system (4.17). Figure 4.3 illustrates the modified model neglecting the finger arteries compartment. The next chapter will provide simulations taking the modified model with and without finger arteries compartment for the computation of gain matrix in the control problem.

Our modified system with finger arteries can now be expressed as a system of differential equation as

$$\frac{d\hat{x}}{dt} \;=\; \mathcal{F}\left(\hat{x}(t),\hat{p},W,u(t)\right),\qquad t\geq 0\;. \tag{4.30}$$

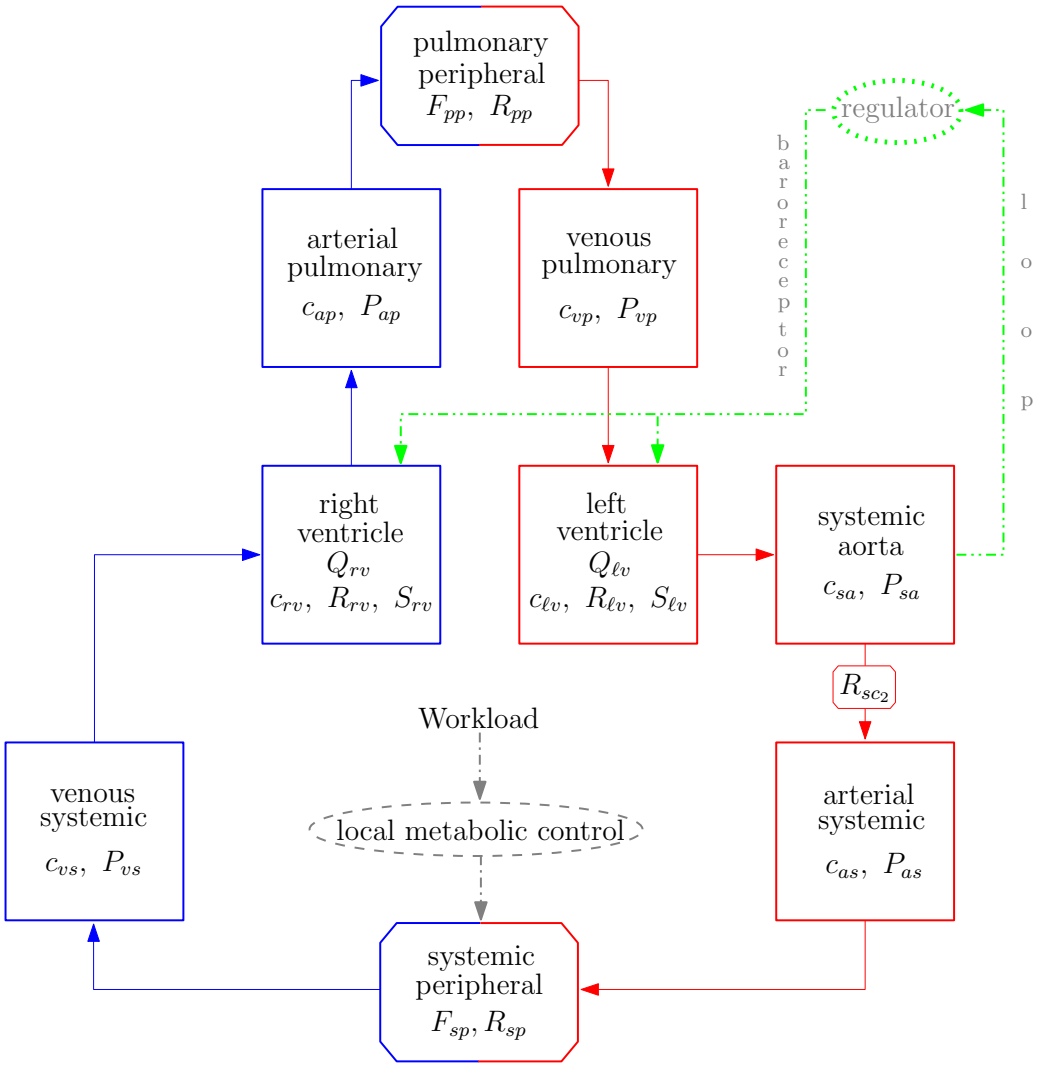

Figure 4.3: The block diagram of the modified linear cardiovascular system model without the finger arteries compartment.

with the state vector

$$\hat{x} = (P_{sa}, P_{fa}, P_{as}, P_{vs}, P_{ap}, R_{sp}, S_{\ell v}, \sigma_{\ell v}, S_{rv}, \sigma_{rv}, H)^T \in \mathbb{R}^{11} \ , \tag{4.31}$$

and the parameter vector

$$\begin{aligned} \hat{p} \ = \ & (c_{sa}, c_{fa}, c_{as}, c_{vs}, c_{\ell v}, c_{rv}, c_{ap}, V_{\text{tot}}, R_{mv,open}, R_{av,open}, R_{sc_1}, \\ & R_{sc_2}, R_{sp_f}, R_{\ell v}, R_{rv}, R_{pp}, a, b, c, E_m, T_{r,frac}, \kappa, C_{a,O_2}, \\ & K, A_{\text{pesk}}, M_0, \rho, \alpha_{\ell v}, \gamma_{\ell v}, \beta_{\ell v}, \alpha_{rv}, \gamma_{rv}, \beta_{rv})^T \in \mathbb{R}^{33} \ . \end{aligned} \tag{4.32}$$

The coordinates of $\mathcal{F}$ are given by

$$\begin{aligned} \mathcal{F}_1 = \ & \frac{1}{c_{sa}} \left(Q_{\ell v} - \frac{P_{sa} - P_{fa}}{R_{sc_1}} - \frac{P_{sa} - P_{as}}{R_{sc_2}} \right) \ , \\ \mathcal{F}_2 = \ & \frac{1}{c_{fa}} \left(\frac{P_{sa} - P_{fa}}{R_{sc_1}} - \frac{P_{fa} - P_{vs}}{R_{sp_f}} \right) \ , \\ \mathcal{F}_3 = \ & \frac{1}{c_{as}} \left(\frac{P_{sa} - P_{as}}{R_{sc_2}} - \frac{P_{as} - P_{vs}}{R_{sp}} \right) \ , \\ \mathcal{F}_4 = \ & \frac{1}{c_{vs}} \left(\frac{P_{as} - P_{vs}}{R_{sp}} + \frac{P_{fa} - P_{vs}}{R_{sp_f}} - Q_{rv} \right) \ , \\ \mathcal{F}_5 = \ & \frac{1}{c_{ap}} \left(Q_{rv} - \frac{P_{ap} - P_{vp}\left(P_{sa}, P_{fa}, P_{as}, P_{vs}, P_{ap}\right)}{R_{pp}} \right) \ , \\ \mathcal{F}_6 = \ & \frac{1}{K} \left(A_{pesk} \left(\frac{P_{as} - P_{vs}}{R_{sp}} C_{a,O_2} - M_T \right) - (P_{as} - P_{vs}) \right) \ , \\ \mathcal{F}_7 = \ & \sigma_{\ell v} \ , \\ \mathcal{F}_8 = \ & -\alpha_{\ell v} S_{\ell v} - \gamma_{\ell v} \sigma_{\ell v} + \beta_{\ell v} H \ , \\ \mathcal{F}_9 = \ & \sigma_{rv} \ , \\ \mathcal{F}_{10} = \ & -\alpha_{rv} S_{rv} - \gamma_{rv} \sigma_{rv} + \beta_{rv} H \ , \\ \mathcal{F}_{11} = \ & u \ , \end{aligned} \tag{4.33}$$

with

$$\begin{aligned} Q_{\ell v} = \ & H \frac{c_{\ell v} P_{vp} a_\ell(H) f(S_{\ell v}, P_{as})}{a_\ell(H) P_{as} + k_\ell(H) f(S_{\ell v}, P_{as})} \ , \\ Q_{rv} = \ & H \frac{c_{rv} P_{vs} a_r(H) f(S_{rv}, P_{ap})}{a_r(H) P_{ap} + k_r(H) f(S_{rv}, P_{ap})} \ , \end{aligned} \tag{4.34}$$

and

$$P_{vp} \ = \ \frac{1}{c_{vp}} \left(V_{\text{tot}} - c_{sa} P_{sa} - c_{fa} P_{fa} - c_{as} P_{as} - c_{vs} P_{vs} - c_{ap} P_{ap} \right) \ . \tag{4.35}$$

Now, without the finger arteries compartment, we consider the further modified and reduced system as follows:

$$\frac{d\check{x}}{dt} \;=\; \mathcal{B}\left(\check{x}(t), \check{p}, W, u(t)\right), \qquad t \geq 0 \;. \tag{4.36}$$

with the state vector

$$\check{x} = (P_{sa}, P_{as}, P_{vs}, P_{ap}, R_{sp}, S_{\ell v}, \sigma_{\ell v}, S_{rv}, \sigma_{rv}, H)^T \in \mathbb{R}^{10} \;, \tag{4.37}$$

and the parameter vector

$$\begin{aligned} \check{p} \;=\; (&c_{sa}, c_{as}, c_{vs}, c_{\ell v}, c_{rv}, c_{ap}, V_{\text{tot}}, R_{mv,open}, R_{av,open}, \\ &R_{sc_2}, R_{\ell v}, R_{rv}, R_{pp}, a, b, c, E_m, T_{r,frac}, \kappa, C_{a,O_2}, \\ &K, A_{\text{pesk}}, M_0, \rho, \alpha_{\ell v}, \gamma_{\ell v}, \beta_{\ell v}, \alpha_{rv}, \gamma_{rv}, \beta_{rv})^T \in \mathbb{R}^{30} \;. \end{aligned} \tag{4.38}$$

The coordinates of $\mathcal{B}$ are given by

$$\begin{aligned} \mathcal{B}_1 =\;& \frac{1}{c_{sa}}\left(Q_{\ell v} - \frac{P_{sa} - P_{as}}{R_{sc_2}}\right) \;, \\ \mathcal{B}_2 =\;& \frac{1}{c_{as}}\left(\frac{P_{sa} - P_{as}}{R_{sc_2}} - \frac{P_{as} - P_{vs}}{R_{sp}}\right) \;, \\ \mathcal{B}_3 =\;& \frac{1}{c_{vs}}\left(\frac{P_{as} - P_{vs}}{R_{sp}} - Q_{rv}\right) \;, \\ \mathcal{B}_4 =\;& \frac{1}{c_{ap}}\left(Q_{rv} - \frac{P_{ap} - P_{vp}\left(P_{sa}, P_{as}, P_{vs}, P_{ap}\right)}{R_{pp}}\right) \;, \\ \mathcal{B}_5 =\;& \frac{1}{K}\left(A_{pesk}\left(\frac{P_{as} - P_{vs}}{R_{sp}} C_{a,O_2} - M_T\right) - \left(P_{as} - P_{vs}\right)\right) \;, \\ \mathcal{B}_6 =\;& \sigma_{\ell v} \;, \\ \mathcal{B}_7 =\;& -\alpha_{\ell v} S_{\ell v} - \gamma_{\ell v}\sigma_{\ell v} + \beta_{\ell v} H \;, \\ \mathcal{B}_8 =\;& \sigma_{rv} \;, \\ \mathcal{B}_9 =\;& -\alpha_{rv} S_{rv} - \gamma_{rv}\sigma_{rv} + \beta_{rv} H \;, \\ \mathcal{B}_{10} =\;& u \;, \end{aligned} \tag{4.39}$$

with

$$\begin{aligned} Q_{\ell v} =\;& H\frac{c_{\ell v} P_{vp} a_\ell(H) f(S_{\ell v}, P_{as})}{a_\ell(H) P_{as} + k_\ell(H) f(S_{\ell v}, P_{as})} \;, \\ Q_{rv} =\;& H\frac{c_{rv} P_{vs} a_r(H) f(S_{rv}, P_{ap})}{a_r(H) P_{ap} + k_r(H) f(S_{rv}, P_{ap})} \;, \end{aligned} \tag{4.40}$$

and

$$P_{vp} \;=\; \frac{1}{c_{vp}}\left(V_{\text{tot}} - c_{sa}P_{sa} - c_{as}P_{as} - c_{vs}P_{vs} - c_{ap}P_{ap}\right) \;. \tag{4.41}$$

4.5 The Linear-Quadratic Regulator Problem

In this section, we will present the linearization of the modified model (4.30) and the corresponding linear-quadratic regulator problem (LQRP). Analogously, one can obtain the linearization and LQRP of the further modified model without finger arteries compartment given by system (4.36).

We perform a transformation of our control system by introducing

$$\xi(t) = \hat{x}(t) - \hat{x}^{\text{exer}} \tag{4.42}$$

and linearizing the model equations around $\xi = 0$. This gives the linear system

$$\begin{aligned} \frac{d\xi}{dt} &= \hat{A}\xi(t) + \hat{B}u(t), \quad t \geq 0 \ , \\ \xi(0) &= \hat{x}^{\text{rest}} - \hat{x}^{\text{exer}} \ , \end{aligned} \tag{4.43}$$

where

$$\begin{aligned} \hat{A} &= \frac{\partial \mathcal{F}}{\partial \hat{x}} (\hat{x}^{\text{exer}}, \hat{p}, W^{\text{exer}}, 0) \in \mathbb{R}^{11\times 11} \ , \\ \hat{B} &= (0, \ldots, 0, 1)^T \in \mathbb{R}^{11} \ . \end{aligned} \tag{4.44}$$

The matrix $\hat{A} \in \mathbb{R}^{11\times 11}$ is the Jacobian with respect to the states $\hat{x}$ evaluated at the equilibrium mean exercise values $\hat{x} = \hat{x}^{\text{exer}}$. The structure of A is given by

$$\hat{A} = \begin{bmatrix} * & * & * & * & * & 0 & 0 & 0 & 0 & 0 & * \\ * & * & 0 & * & 0 & 0 & 0 & 0 & 0 & 0 & 0 \\ * & 0 & * & * & 0 & * & 0 & 0 & 0 & 0 & 0 \\ 0 & * & * & * & * & * & 0 & 0 & * & 0 & * \\ * & * & * & * & * & 0 & 0 & 0 & * & 0 & * \\ 0 & 0 & * & * & 0 & * & 0 & 0 & 0 & 0 & 0 \\ 0 & 0 & 0 & 0 & 0 & 0 & 0 & 1 & 0 & 0 & 0 \\ 0 & 0 & 0 & 0 & 0 & 0 & -\alpha_{\ell v} & -\gamma_{\ell v} & 0 & 0 & \beta_{\ell v} \\ 0 & 0 & 0 & 0 & 0 & 0 & 0 & 0 & 0 & 1 & 0 \\ 0 & 0 & 0 & 0 & 0 & 0 & 0 & 0 & -\alpha_{rv} & -\gamma_{rv} & \beta_{rv} \\ 0 & 0 & 0 & 0 & 0 & 0 & 0 & 0 & 0 & 0 & 0 \end{bmatrix} , \tag{4.45}$$

where "$*$" indicates an entry evaluated at specific equilibrium mean exercise values. Appendix B provides the entire formula for the matrix $\hat{A}$ (and $\check{A}$, corresponding to the Jacobian of the further modified model without the finger arteries compartment).

Using the transformation $\hat{x} \to \xi$ the quadratic cost functional J takes the form

$$J\left(u(\cdot), \hat{x}^{\text{rest}} - \hat{x}^{\text{exer}}\right) \;=\; \int_0^\infty \left(\eta(t)^2 + u(t)^2\right)\, dt \;, \tag{4.46}$$

where

$$\eta(t) \;=\; \hat{C}\xi(t), \quad t \geq 0 \;, \tag{4.47}$$

with $\hat{C} = (q_{sa}, 0, \ldots, 0) \in \mathbb{R}^{11}$ and $\xi(t)$ is the solution of the initial value problem (4.43) with the given control $u(t)$. Thus far, we have the linear system (4.43), (4.47) and the quadratic cost functional (4.46) which constitute the ***linear-quadratic regulator problem (LQRP)***.

4.6 Optimal Linear Feedback Control

The LQRP presented in the preceding section requires that we find a function $\hat{u} \in \mathscr{L}^2\,(0, \infty; \mathbb{R})$ such that

$$J\left(\hat{u}, \hat{x}^{\text{rest}} - \hat{x}^{\text{exer}}\right) \;=\; \min_{u \in \mathscr{L}^2(0,\infty;\mathbb{R})} J\left(u, \hat{x}^{\text{rest}} - \hat{x}^{\text{exer}}\right) \;. \tag{4.48}$$

From control theory, the solution of the linear-quadratic regulator problem is given by a linear feedback law (see for instance Kwakernaak and Sivan (1972) [30]). That is, we have

$$\hat{u}(t) \;=\; -F\xi^*(t), \quad t \geq 0 \;, \tag{4.49}$$

where $\xi^*(t)$ is the solution of the closed loop system

$$\begin{aligned} \frac{d\xi}{dt} &= \; (\hat{A} - \hat{B}F)\xi(t), \quad t \geq 0 \;, \\ \xi(0) &= \; \hat{x}^{\text{rest}} - \hat{x}^{\text{exer}} \;. \end{aligned} \tag{4.50}$$

with the feedback matrix $F = \hat{B}^T X \in \mathbb{R}^{1\times 11}$ and X is the solution of the Riccati matrix equation

$$X\hat{A} + \hat{A}^T X - X\hat{B}\hat{B}^T + \hat{C}^T\hat{C} \;=\; 0 \;. \tag{4.51}$$

If the pair $(\hat{A}, \hat{B})$ is stabilizable and the pair $(\hat{C}, \hat{A})$ is detectable, then the Riccati equation (4.51) has a unique positive definite solution X. Controllability of $(\hat{A}, \hat{B})$ and observability of $(\hat{C}, \hat{A})$ provide stronger conditions requiring

$$\text{rank}\left(\hat{B}, \hat{A}\hat{B}, \ldots, \hat{A}^{10}\hat{B}\right) = 11 \qquad \text{and} \qquad \text{rank}\left(\hat{C}^T, \hat{A}^T\hat{C}^T, \ldots, \left(\hat{A}^T\right)^{10}\hat{C}^T\right) = 11 \ .$$

4.7 The Nonlinear Control Problem

To conclude this chapter, let us reemphasize our nonlinear control problem and how the corresponding linear system provides the stabilizing control feedback to this problem. Our objective is to find a control function $u(t)$ that minimizes the quadratic cost functional criterion

$$J\left(u(\cdot), x^{\text{rest}}\right) \ = \ \int_0^\infty \left(q_{sa}^2 \left(P_{sa}(t) - P_{sa}^{\text{exer}}\right)^2 + u(t)^2\right) \, dt \tag{4.52}$$

subject to the state equations

$$\frac{dx}{dt} \ = \ \mathcal{G}\left(x(t), p, W^{\text{exer}}, u(t)\right), \qquad x(0) \ = \ x^{\text{rest}} \ . \tag{4.53}$$

The previous sections talked about the model simplifications and linearization. It neglects some of the essential variable state(s) in the full system such as left ventricle pressure (finger arterial pressure). The LQRP and its solution provides additional states including $S_{\ell v}$ and $\sigma_{\ell v}$ which are not in the original model. These terms only appear to compute for the gain matrix of the modified model. However, in the numerical implementation, only the elements corresponding to the states in the original model influences the solution.

Chapter 5

Numerical Experiments and Simulations

In this chapter, we will present the numerical computations and simulation results of the cardiovascular model. The set of all the parameters used are given in the tables in Appendix A. These parameter values are chosen from the identified parameters from Kappel and Peer (1993) [26], from the literature, and some are estimated to obtain reasonable values (for instance, a normal rest finger arterial pulsatile pressure of 120/90 mmHg). Numerical simulations on the left ventricular pressure and volume, the states rest and exercise equilibrium behaviors, and the dynamics of controlling the system from rest to exercise conditions will be presented.

5.1 The Left Ventricle

In our model, the left ventricle is the source of pulse waves in the cardiovascular system. In this section we will present the computed left ventricular pressure and volume curves during rest condition.

In Chapter 2, Section 2.4, we discussed the opening and closing of the mitral and aortic valves. Starting at the relaxation phase, the pressure in the ventricle $P_{\ell v}$ drops down to the level of the venous pressure P_{vp}. Then the mitral valve opens which is the start of the filling process. $P_{\ell v}$ continues to decease in a short while and

starts to increase until it again reaches P_{vp}. Here the filling process ends and the mitral valve closes. At this point, we can measure the end-diastolic left ventricular pressure. $P_{\ell v}$ continues to increase until it reaches the systemic aortic pressure P_{sa}. The aortic valve opens and the ejection process starts. $P_{\ell v}$ continues to increase further and after some time it decreases to the same level of P_{sa} in which the aortic valve closes. This time we measure the end-systolic left ventricular pressure.

We are interested in determining the four time points for one heart cycle. These are the time when the filling process starts, when it ends, the time when the ejection process starts, and when it ends. To find these time points, we incorporated in the *option* for the `odesolver` a function called ***'Events'*** (see Matlab help for details). In this function, we specify the four instances that we want to determine. Figure 5.1 depicts these four time points which are of importance to us. It shows the plots of the venous (P_{vp}), aortic pressure (P_{sa}) and left ventricular pressures ($P_{\ell v}$) and their points of intersections. The points for which end-diastolic and end-systolic pressures occur are also specified. The simulation runs for 1500 seconds and the plots are taken from the last full heart cycle.

Figures 5.14 (a) and (b) are the computed left ventricular pressure and volume curves, respectively, showing the behavior of the pressure, respectively, volume in the left ventricle during phases of isovolumetric contraction and isovolumetric relaxation. It also specifies the region for the duration of the diastole and systole. As shown in the figures, during isovolumetric contraction, the pressure in the left ventricle is increasing while the volume remains constant. At the start of ejection, the pressure still increases and the volume drops. During isovolumetric relaxation, the pressure is decreasing while the volume remains the same. The time points for these phases are numerically obtained using the '*Events*' specified earlier. The simulations are from one of the last complete pressure and volume cycles running for 1500 seconds.

To complete the numerical computations for the left ventricle dynamics, we in-

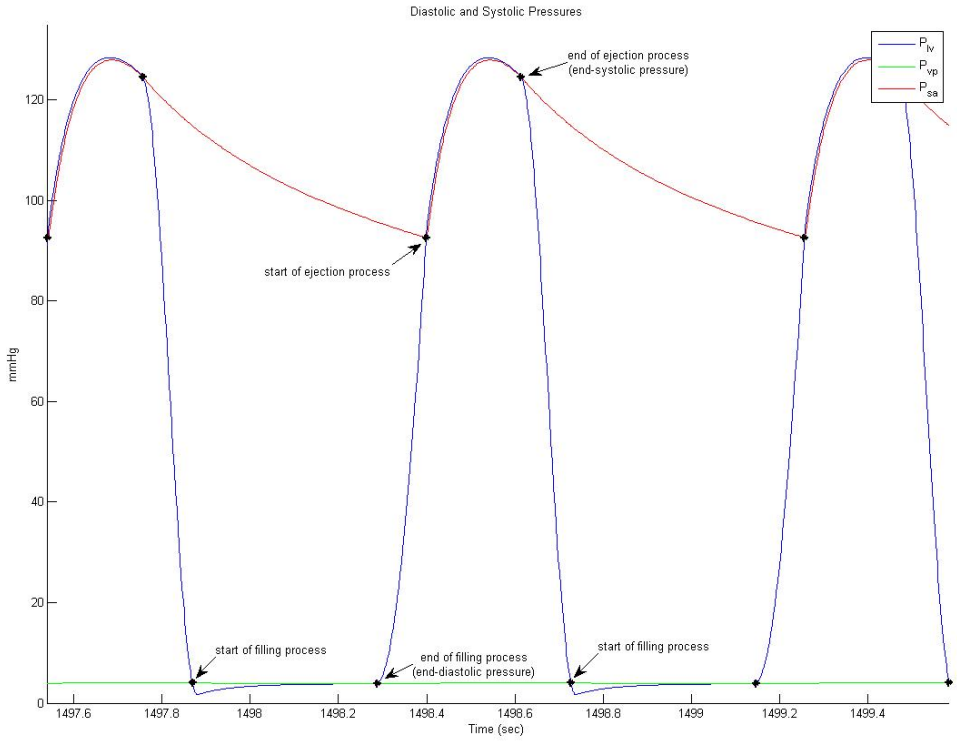

Figure 5.1: The left ventricular, venous and aortic pressures showing the time points for the start and end of filling process, start and end of ejection process.

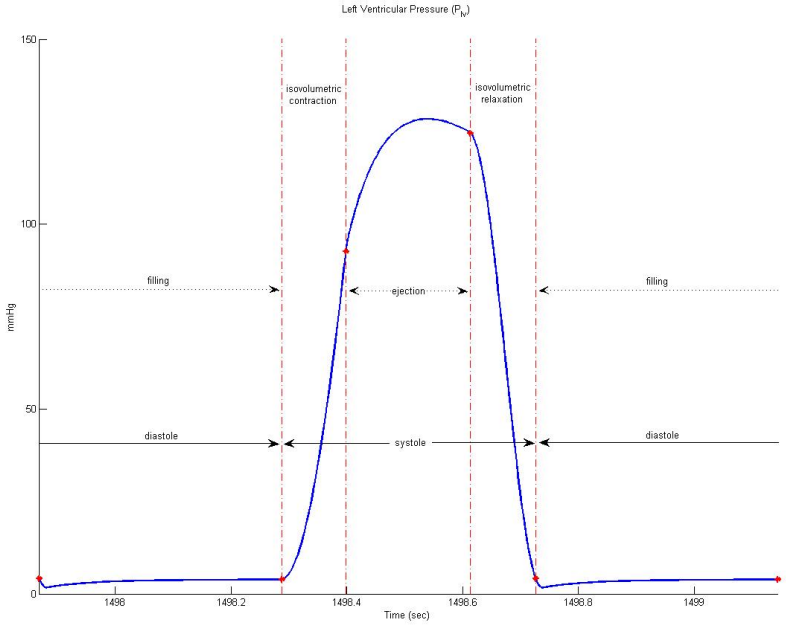

(a)

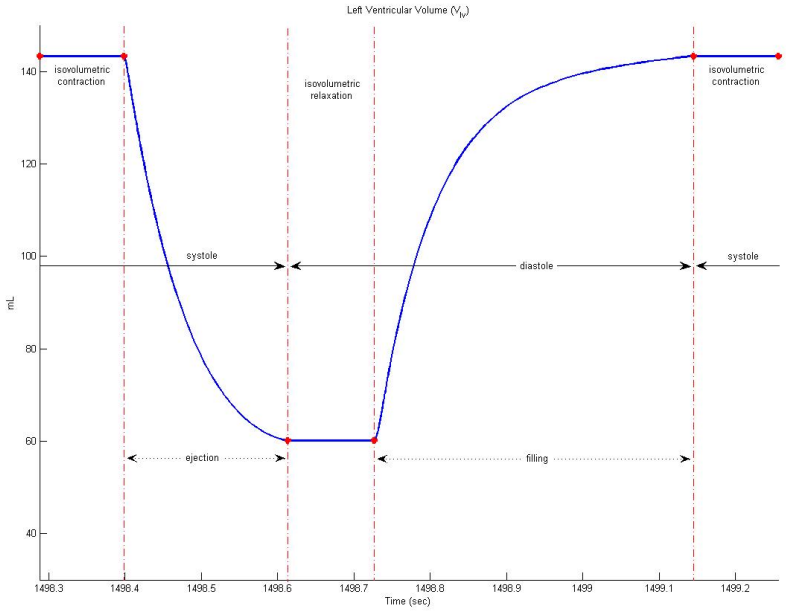

(b)

Figure 5.2: (a) The time course of the left ventricular pressure. (b) The time course of the left ventricular volume.

clude the pressure-volume diagram as shown in figure 5.3. The time instances for which the start and end of filling process and start and end of ejection process occur are depicted as well. As above, the simulation is taken from the last complete cycle.

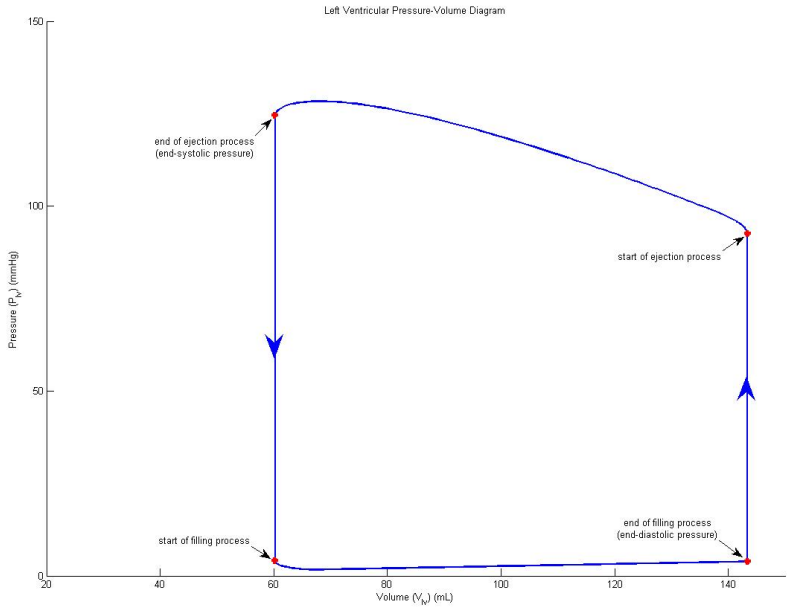

Figure 5.3: The pressure-volume diagram for the left ventricle.

5.2 Computation of the Mean Values

In Section 4.5, we presented how to compute the equilibria. In this section, we will provide the numerical implementation and the plots of the whole cardiovascular system depicting rest and exercise conditions. It should be noted that the computations for equilibria are taken from the last full cycle of the simulation. In our case, we run the program for 1500 seconds in which stabilities are observed in the states behavior.

In our numerical experiments, we first consider the system (4.3) without control equation $\frac{dH}{dt} = u(t)$. Two simulation runs are done to obtain the mean values for both rest and exercise conditions. For the rest phase, we started at an initial condition given in A.7 and run the program for 1500 seconds. The mean values

are computed using equation (4.24) during the last full cycle. The values obtained after the first simulation are used as initial conditions for the second run ($P_{\ell v}$ is held constant at 2.4 mmHg). Then, the mean values are again computed in a similar way after the run. These values are considered to be the 'rest equilibrium values' (except for $P_{\ell v}$ in which its value is fixed to be 2.4 mmHg). Figure 5.4 (a) and (b) show the behavior of the states during rest condition for the first and second simulation runs, respectively. Table A.7 lists all the initial values of the states and the computed mean and equilibrium values for the first and second runs.

For the exercise phase, the computed rest equilibrium values are used as initial conditions (with $P_{\ell v} = 2.4$ mmHg). The mean values are computed as before after the first simulation run for 1500 seconds. Again these values serve as the initial condition for the next run (again holding $P_{\ell v} = 2.4$ mmHg). Finally, the 'exercise equilibrium values' are computed from the last full cycle of the system. The initial, mean and equilibrium values for the two simulation runs are given in table A.8. Figure 5.5 (a) and (b) show the behavior of the states during exercise phase for the first and second simulation runs, respectively.

5.3 Comparison of the Rest and Exercise Equilibrium Conditions

Now, let us look more closely at the behavior of the states during rest and exercise conditions (no baroreceptor loop control). For the following simulations, the initial values for the rest condition are the computed mean values from the first simulation run (see previous section and table A.7) and the initial values for the exercise condition are the computed mean values after the first run (see table A.8). Each plot has two subplots, the top subplot for the whole duration (0-1500 seconds) and bottom subplot for at least the last 7.5% of the total time duration of the simulations. Also, the red lines for all the bottom subplots denote the mean values of the states following equation (4.24) obtained from the last full heart cycle. The blown-up subplots for both rest and exercise are adjusted for comparison purposes. The values for the

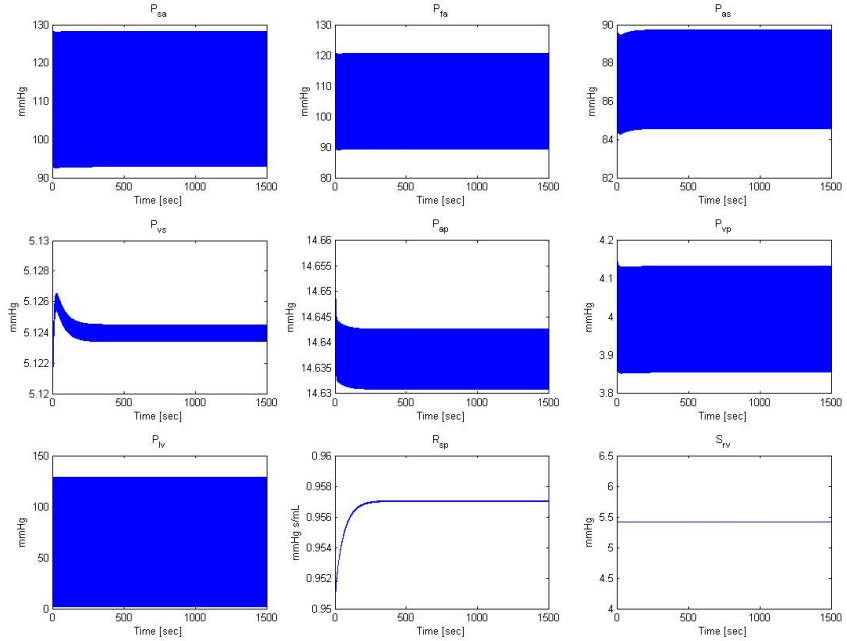

(a)

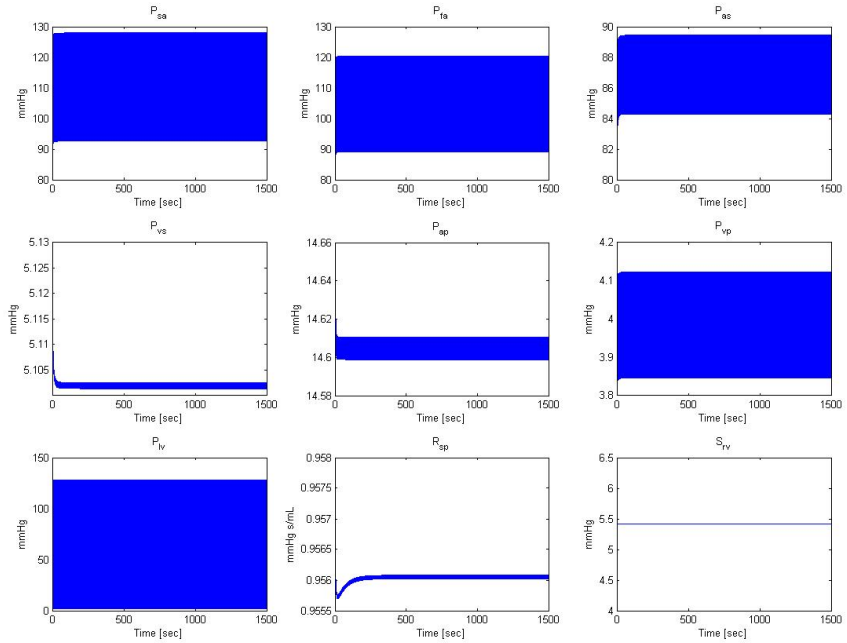

(b)

Figure 5.4: (a) First simulation results during rest condition. (b) Second simulation results during rest condition obtaining 'rest equilibrium values' using the computed mean values in the first simulation.

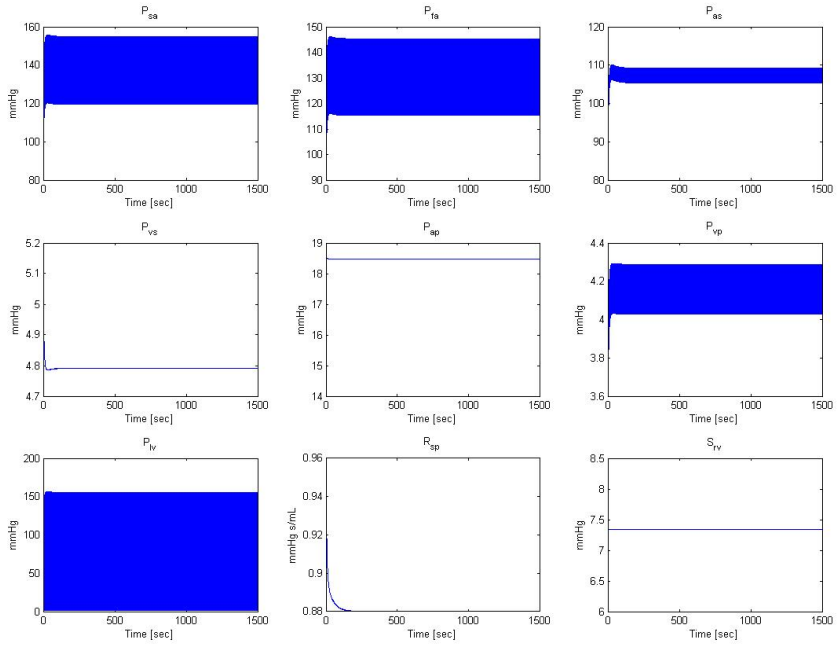

(a)

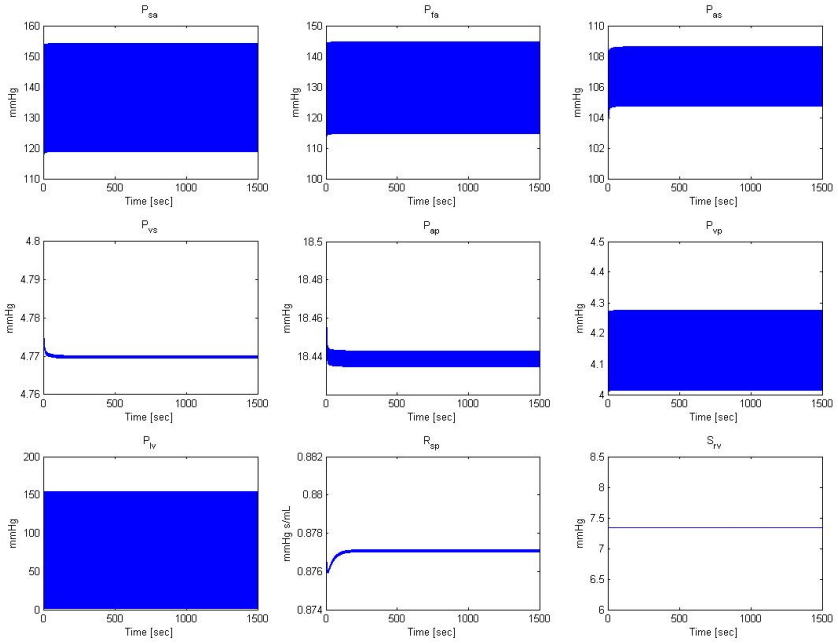

(b)

Figure 5.5: (a) First simulation results during exercise condition. (b) Second simulation results during exercise condition obtaining 'exercise equilibrium values' using the computed mean values in the first simulation.

controlled variables, namely, H, W, and A_{pesk} for rest and exercise phases are listed in table A.5.

From Figures 5.6-5.12, it can be deduced (except for the P_{vs}) that increasing the controlled variables (mainly the heart rate, H) causes an increase in the corresponding pressure values (and of course, the corresponding mean values). The decrease of P_{vs} while increasing the heart rate may be attributed the Frank Starling mechanism which is assumed in the filling process of the right ventricle. It can be clearly seen from the figures that pulsatility is also increased. Notice also the decrease in the range of pulsatility in the arterial systemic compartment (see figure 5.8). Furthermore, pulsatility is somehow damped out (almost linear) in the venous systemic and arterial pulmonary compartments which are physiologically observable. These behaviors can be seen in figures 5.9 and 5.10 (please note the scalings used). The venous pulmonary pressure is again pulsatile since it is attached to the left ventricle compartment in which pulsatility is generated. However, the pulsatility range is small (see figure 5.11). Figure 5.13 depicts the behavior of the systemic peripheral resistance. Pulsatility of R_{sp} is not so pronounced (take note of the scalings). Rest condition has a higher equilibrium R_{sp} compared to the exercise condition.

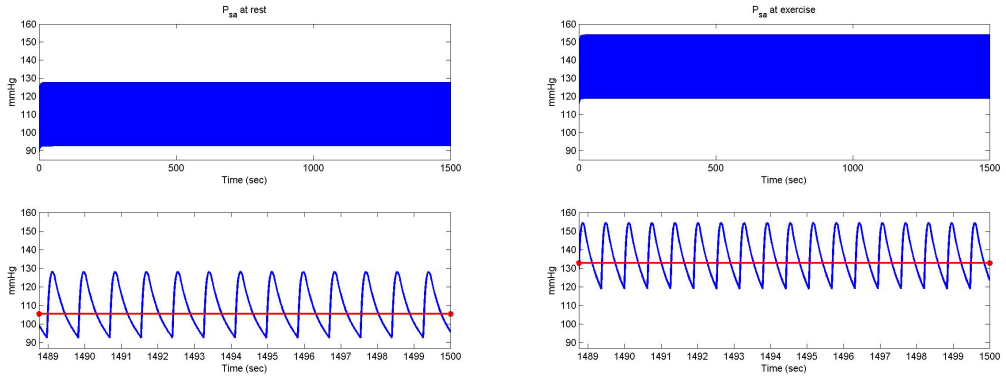

(a) (b)

Figure 5.6: The aortic pressure P_{sa} during (a) rest and (b) exercise conditions.

The figures below show the elastance function of the left ventricle during rest and exercise phases. Observe that the maximum elastance value E_M which is the

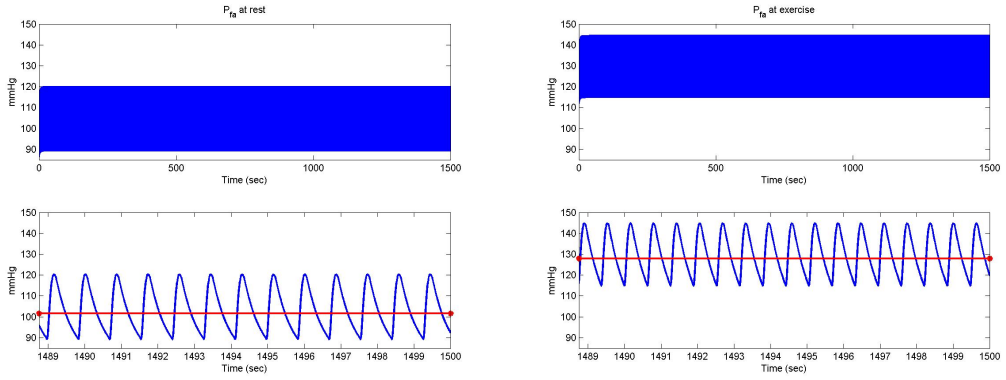

(a) (b)

Figure 5.7: The finger arterial pressure P_{fa} during (a) rest and (b) exercise conditions.

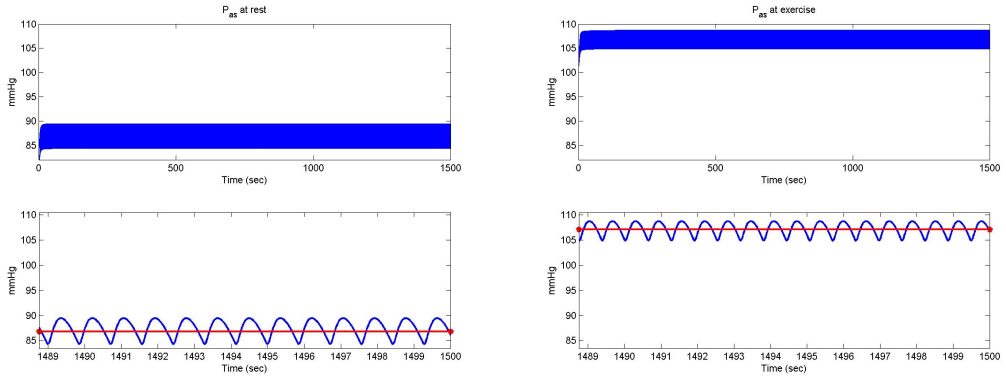

(a) (b)

Figure 5.8: The arterial systemic pressure P_{as} during (a) rest and (b) exercise conditions.

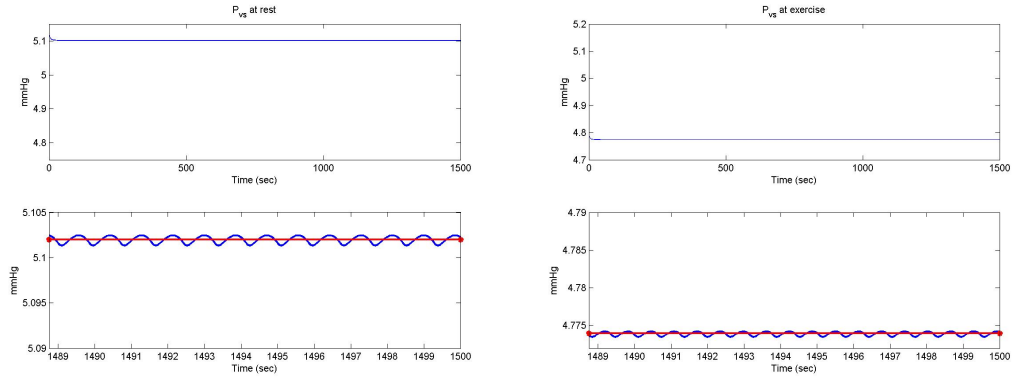

(a) (b)

Figure 5.9: The venous systemic pressure P_{vs} during (a) rest and (b) exercise conditions.

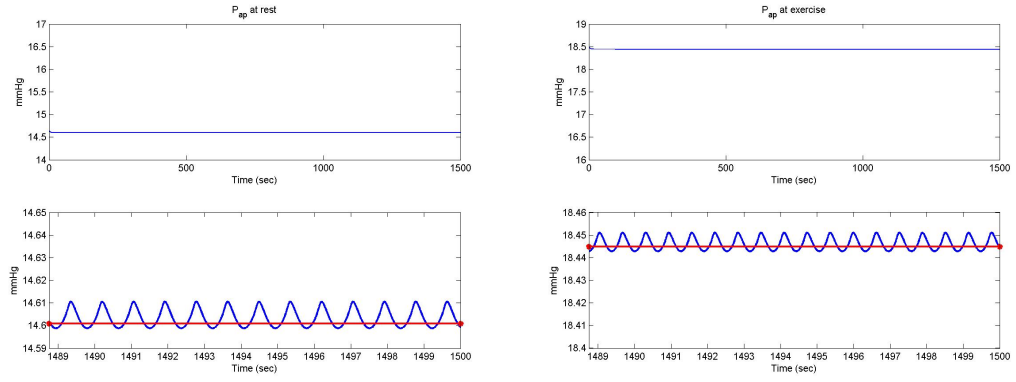

(a) (b)

Figure 5.10: The arterial pulmonary pressure P_{ap} during (a) rest and (b) exercise conditions.

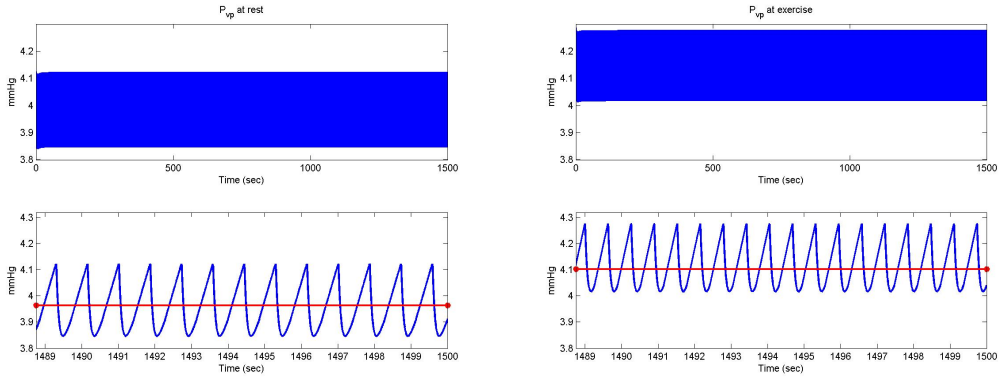

(a) (b)

Figure 5.11: The venous pulmonary pressure P_{vp} during (a) rest and (b) exercise conditions.

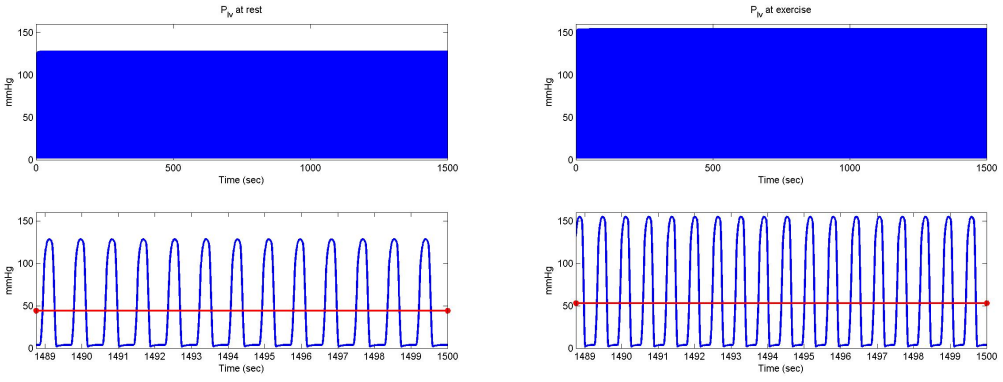

(a) (b)

Figure 5.12: The left ventricular pressure $P_{\ell v}$ under (a) rest and (b) exercise conditions.

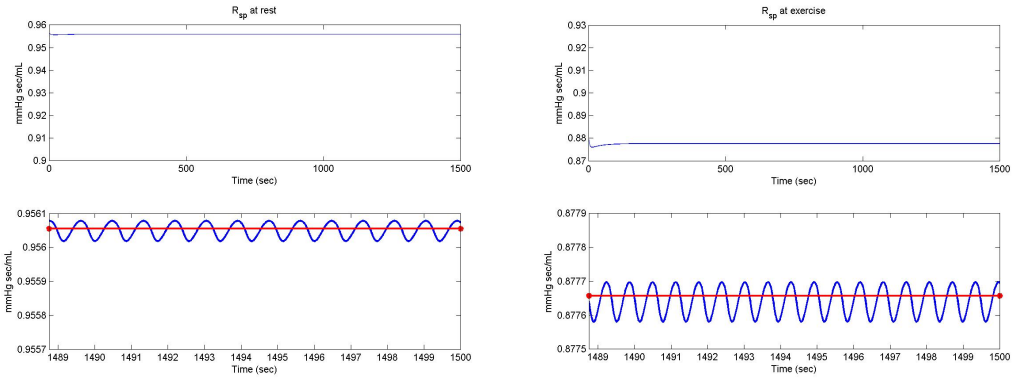

(a) (b)

Figure 5.13: The systemic peripheral resistance R_{sp} under (a) rest and (b) exercise conditions.

peak of the elastance function increases as heart rate is increased during exercise. Also, there is a time shift of the elastance function from rest to exercise conditions (see Figure 5.14 (c)). These plots are generated from the last few complete cycles of the system at equilibria.

Finally, Figure 5.15 (a) and (b) show the systemic and pulmonary flows during rest and exercise conditions. The flows are computed as given in equation (2.5) where R_{sp} is taken to be the mean equilibrium value. As expected, flows are elevated during the exercise phase. Looking at the plots carefully, one can notice a time shift of the flows during exercise.

5.4 Dynamics of the Controlled System

In this section, we will provide numerical simulations for the controlled system. Two sets of simulations will be presented. One using the modified linearized model with finger arterial compartment for control formulation and the other without this compartment (as discussed in the previous chapter).

Let us now summarize the steps for calculating the stabilizing control for our

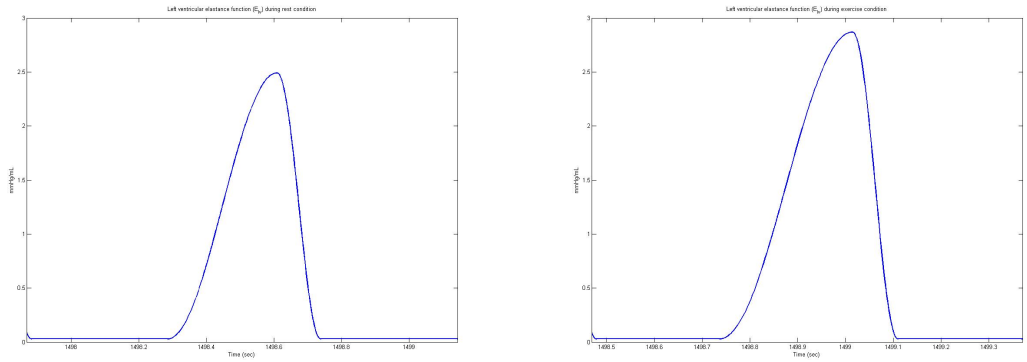

(a) (b)

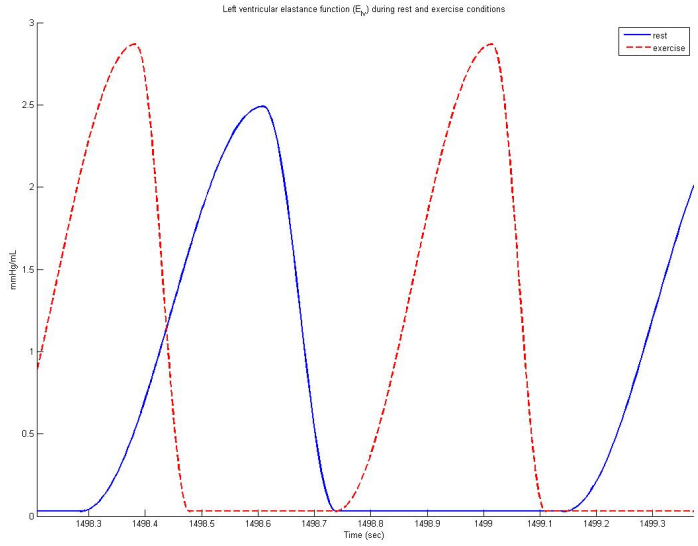

(c)

Figure 5.14: The left ventricular elastance function $E_{\ell v}$ during (a) rest and (b) exercise conditions. (c) $E_{\ell v}$ during rest and exercise in the same coordinates.

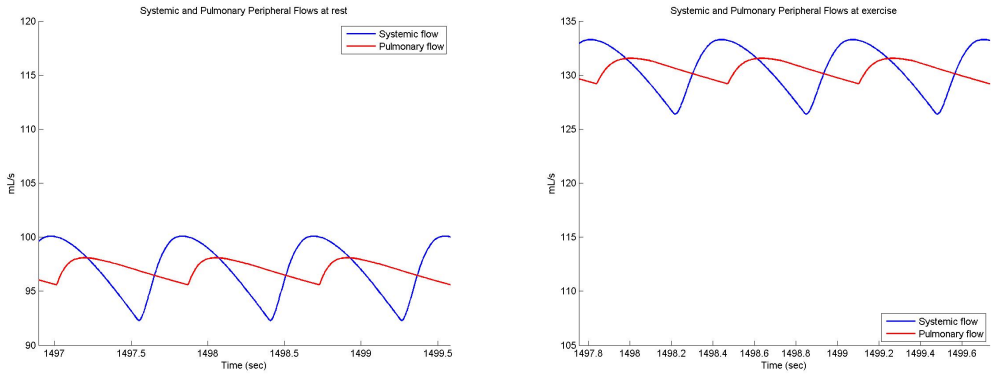

(a) (b)

Figure 5.15: The systemic and pulmonary flows during (a) rest and (b) exercise conditions.

reduced cardiovascular model (4.17).

Step 1: Compute the "initial" equilibrium state x^{initial} defined by the parameter choices from which the system starts. Compute the "final" equilibrium state x^{final} determined by the choice of parameters characterizing the final state. The initial state is the initial condition for the simulation and the control is designed to steer the system from initial to final state. The initial and final equilibrium states correspond to the equilibrium rest x^{rest} and equilibrium exercise x^{exer}, respectively. (See Sections 4.3 and 5.2 for further details).

Step 2: Simplify the model and linearize the system around the final steady state. (See Section 4.4 and 4.5.)

Step 3: Calculate the feedback gain matrix for the linear quadratic regulator problem that will transfer the linearized system to the final state. This minimizes the cost functional (4.52).

Step 4: The feedback gain matrix will provide a control for the nonlinear system that is suboptimal but stabilizing.

Generally speaking, with or without the finger arterial compartment in the model simplification and control formulation, both provide a stabilizing control for the

nonlinear problem. This is depicted in the following figures below. It can be seen from Figures 5.16, 5.17, 5.18, 5.19, and 5.21 that the pressures drop for a short time before going up and tending to the final states. This can be attributed to the autoregulation which is manifested in the dynamics of the systemic peripheral resistance R_{sp} in Figure 5.22. R_{sp} suddenly drops increasing the blood flow, thus reducing the pressure for a short time duration. Then it increases and levels off at some value influencing the pressures in a similar fashion.

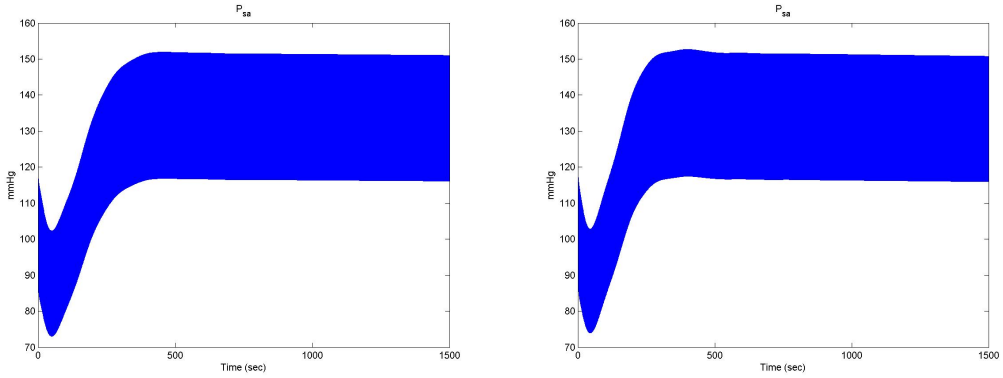

(a) (b)

Figure 5.16: Controlled systemic aortic pressure P_{sa} (a) with (b) without finger arterial compartment in the control formulation.

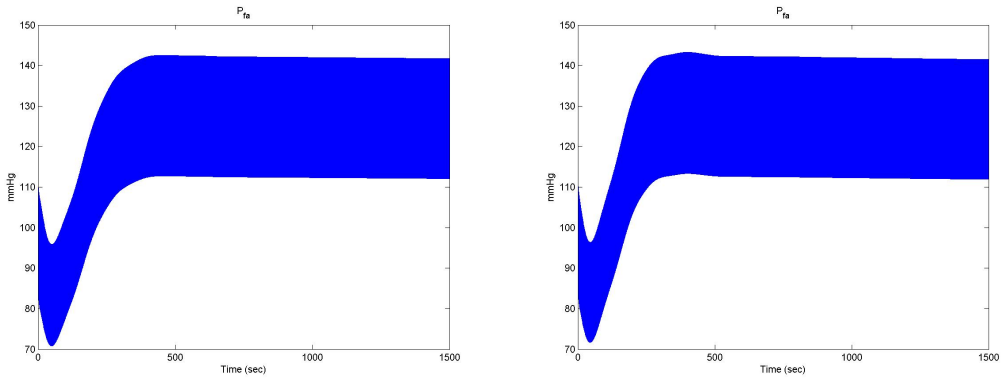

(a) (b)

Figure 5.17: Controlled finger arterial pressure P_{fa} (a) with (b) without finger arterial compartment in the control formulation.

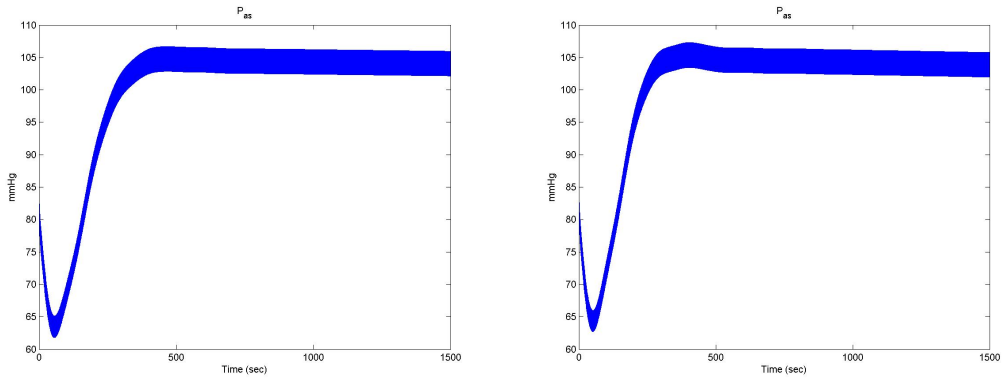

(a) (b)

Figure 5.18: Controlled arterial systemic pressure P_{as} (a) with (b) without finger arterial compartment in the control formulation.

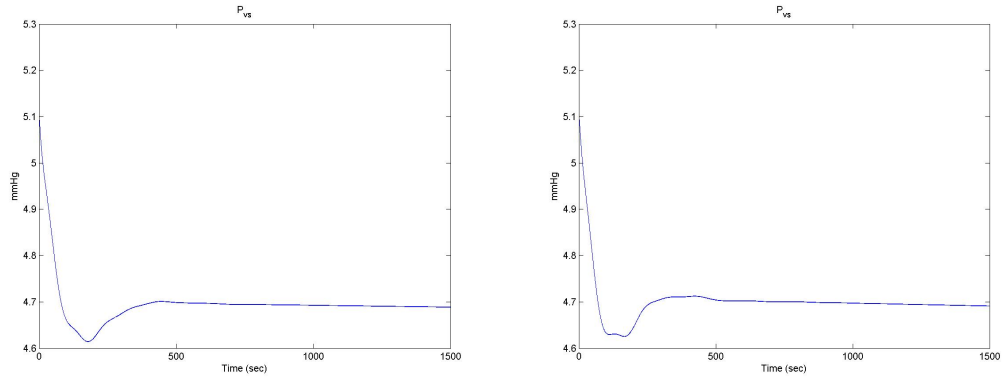

(a) (b)

Figure 5.19: Controlled venous systemic pressure P_{vs} (a) with (b) without finger arterial compartment in the control formulation.

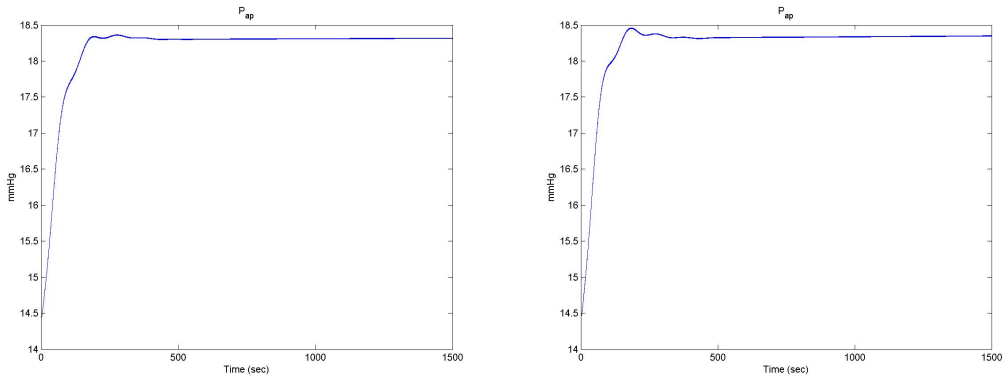

(a) (b)

Figure 5.20: Controlled arterial pulmonary pressure P_{ap} (a) with (b) without finger arterial compartment in the control formulation.

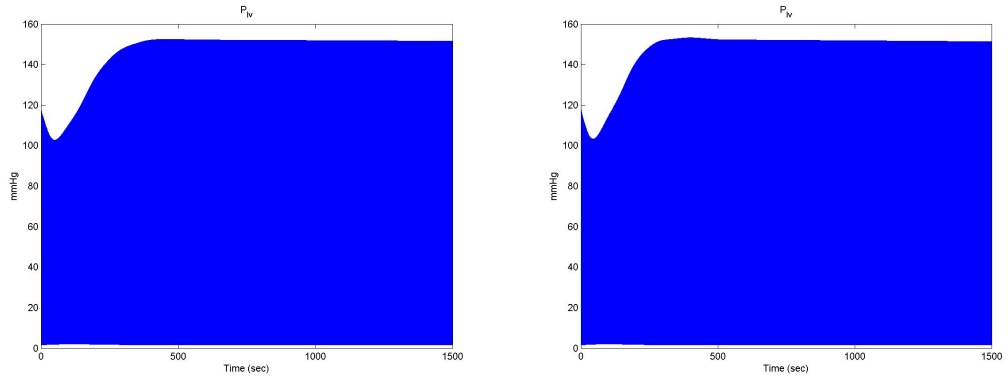

(a) (b)

Figure 5.21: Controlled left ventricular pressure $P_{\ell v}$ (a) with (b) without finger arterial compartment in the control formulation.

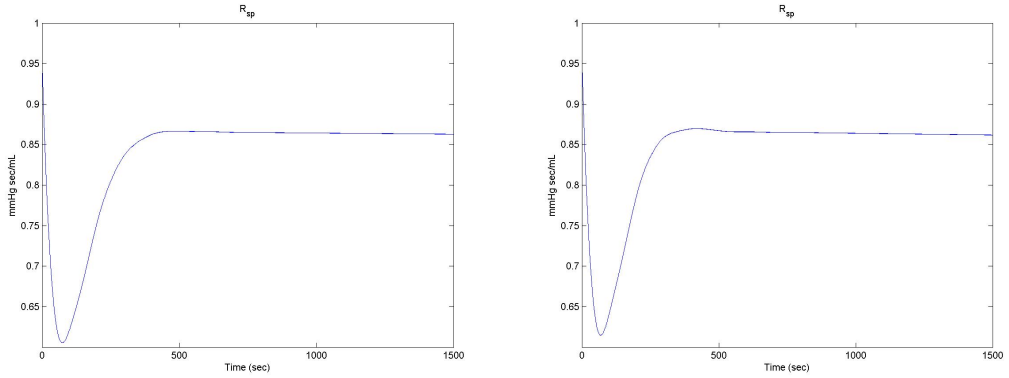

(a) (b)

Figure 5.22: Controlled systemic peripheral resistance R_{sp} (a) with (b) without finger arterial compartment in the control formulation.

Figures 5.23, 5.24, 5.25, and 5.26 show the dynamics of the left $S_{\ell v}$ and right S_{rv} ventricular contractilities and the corresponding derivatives $\sigma_{\ell v}$ and σ_{rv}. Focusing our attention to S_{rv} which is one of the original state variables, it can be observed that the control immediately increases the contractility of the right ventricle. However, it fluctuates for some time before it tends to the equilibrium final state.

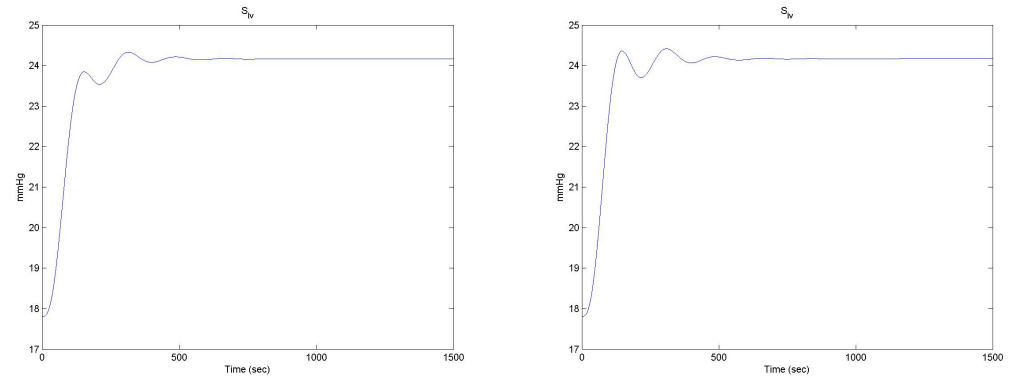

(a) (b)

Figure 5.23: Controlled left ventricular contractility $S_{\ell v}$ (a) with (b) without finger arterial compartment in the control formulation.

Figure 5.27 depict the behavior of the heart rate H. With the weight (equal to 1) that is attached on the control $u(t)$, H immediately tends to the equilibrium final

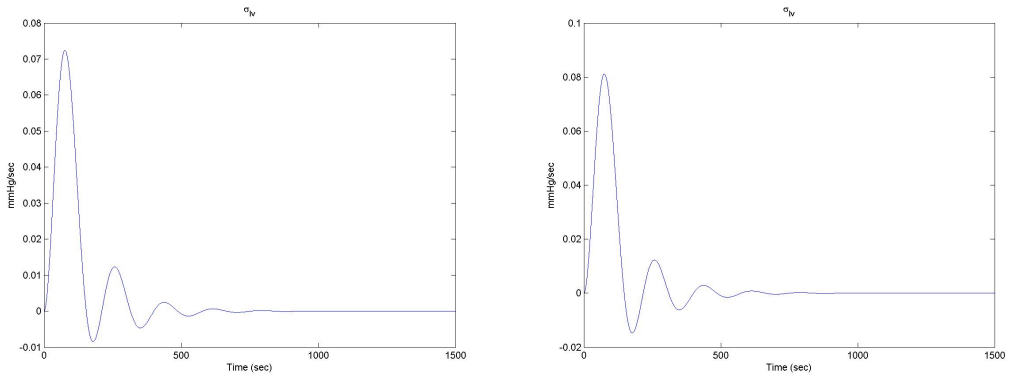

(a) (b)

Figure 5.24: The dynamics of $\sigma_{\ell v}$ (a) with (b) without finger arterial compartment in the control formulation.

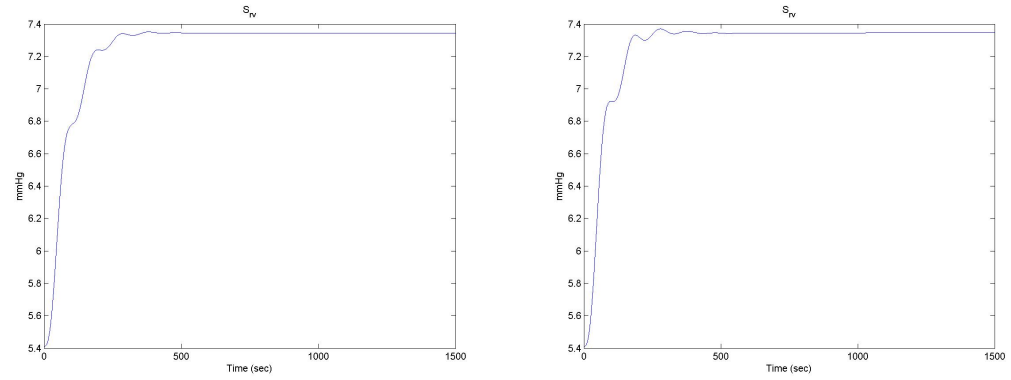

(a) (b)

Figure 5.25: Controlled right ventricular contractility S_{rv} (a) with (b) without finger arterial compartment in the control formulation.

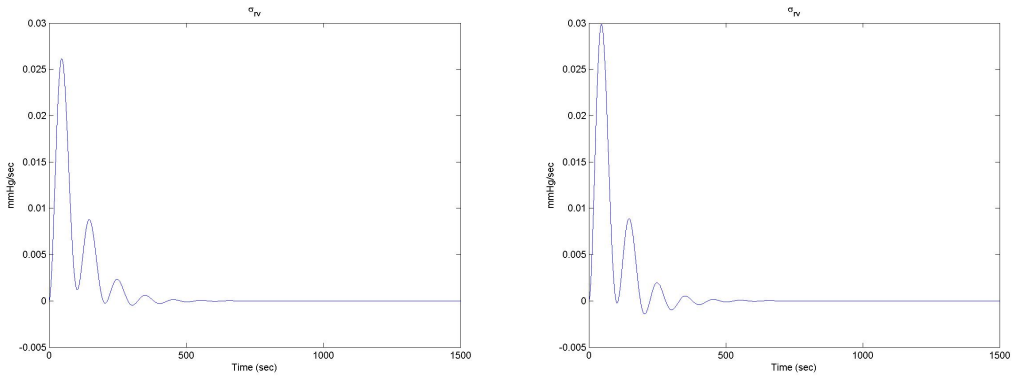

(a) (b)

Figure 5.26: The dynamics of σ_{rv} (a) with (b) without finger arterial compartment in the control formulation.

state.

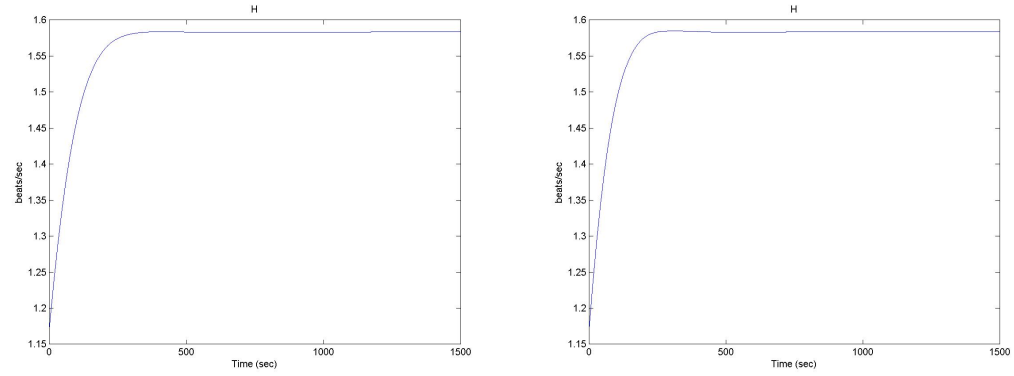

(a) (b)

Figure 5.27: The heart rate H dynamics (a) with (b) without finger arterial compartment.

Finally, Figure 5.28 shows the dynamics of the control $u(t)$ stabilizing to the zero state. An oscillatory behavior in the control is almost negligible.

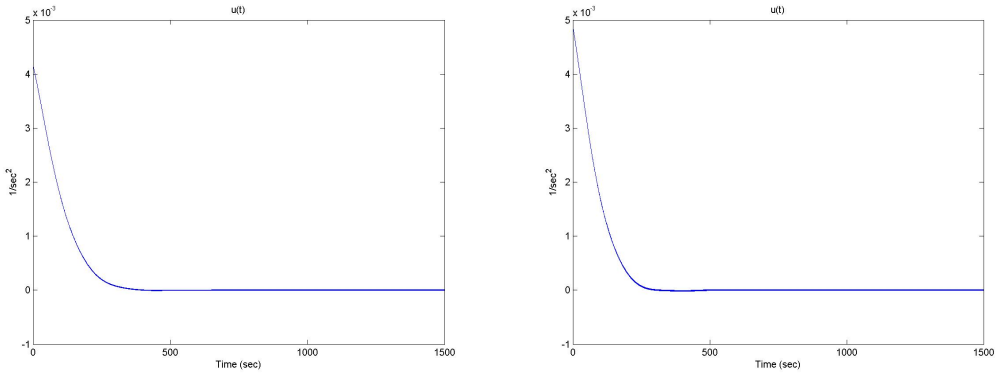

(a) (b)

Figure 5.28: The dynamics of the control $u(t)$ (a) with (b) without finger arterial compartment.

Chapter 6

Discussions and Remarks

The results of this thesis can be summarized into two parts. First is the mathematical modeling of a global pulsatile human cardiovascular system. We have shown, that a pulsatile model can be obtained by considering the left ventricle as the source of the pulse waves in the system while keeping the model flow in the other compartments as simple as possible. That is, we incorporated the pulsatile left ventricle model in the existing nonpulsatile cardiovascular model developed by Kappel and Peer (1993) [26] and previous works. We have used the left ventricle model developed by Olufsen, et al. [46] and other related studies. We have simplified the time-varying resistances $R_{mv}(t)$ and $R_{av}(t)$ into piecewise functions which are constant at certain conditions and "infinitely large" at some instances (cf. Section 2.4, equation (2.26)). The simulation results in Section 5.1 present satisfactory dynamics of the pressure and volume curves of the left ventricle at rest. Modifications were made in the elastance function of the left ventricle to allow changes under exercise activities.

The second main result of the thesis is the construction of the feedback control law which transfers the pulsatile model from equilibrium rest to equilibrium exercise condition. In the previous chapter, we presented two simplified models (one with the finger arterial compartment and the other without) in which the linearized system more ore less approximates the nonlinear pulsatile model. It has been shown that the control formulation provides a suboptimal but stabilizing control for the nonlinear system.

The numerical simulations presented in Chapter 5 provide a satisfactory description of the regulatory mechanisms in the cardiovascular system in response to a submaximal workload by considering only one control variable. Also, it is sufficient to consider the systemic aortic pressure P_{sa} in the cost functional to obtain a feedback law. Hence, the short-term reaction of the cardiovascular system to a submaximal workload can be modeled by a single input/single output control system. Moreover, we approximated the feedback law by the solution of a linear quadratic regulator problem.

As far as the work is concerned in this study, it is mainly theoretical modeling. Model validation can be done through performing experiments and obtaining real-time data. In this way, extensive parameter estimation can be done. Sensitivity analysis can be performed to determine parameters which are sensitive to model output. Then, model improvement can be obtained. Furthermore, there are a number of details which need thorough investigation.

- The role of the unstressed volumes in the compartments.
- The relationship between the right ventricle contractility S_{rv} and the left ventricle elastance E_M should be further investigated.
- The current model includes the process of autoregulation involving the constants K and A_{pesk}. An improved model providing more insights in metabolic mechanisms can be included. For instance, the influence of the vasodilator can be taken into account.
- Investigation of the influence of the sympathetic nervous system on compliance, respectively on the elastance of the ventricles during exercise should be considered.
- The compliance of the venous systemic compartment could be modeled to reflect the mechanism of active modification of the venous tone during periods of exercising.
- The significance of the pulmonary baroreceptor loop (which is not included in

the present model) for the control formulation needs further studies.

- Only short-term regulatory effects are considered in the current model. Long-term control mechanisms such as control of blood volume by the kidneys can be incorporated to model hemodynamics during a dialysis process.

- A model modification can be done to study the case of hemorrhage or transfusion. Suppose that the arterial compartment is the source of hemorrhage, then we could model the blood loss at the rate F_{hem} by

$$\frac{dP_{as}}{dt} = \frac{1}{c_{as}}\left(\frac{P_{sa}-P_{as}}{R_{sc_2}} - \frac{P_{as}-P_{vs}}{R_{sp}} - F_{\text{hem}}\right) . \tag{6.1}$$

- The current model can be used to model the dynamics of the cardiovascular system under orthostatic stress. In particular, the arterial systemic and venous systemic compartments can be further subdivided to upper and lower parts. These will give room to the rib and hips compartment in which orthostatic stress induced by lower body negative pressure can be investigated. See for example Kappel, et al. (2007) [24] and Fink et al. (2004) [34].

- The respiratory system and the corresponding control regulation can be included to have a more global pulsatile cardiovascular-respiratory model.

- In addition to respiratory, the brain compartment can be treated separately. See for instance, Fincham and Tehrani (1983) [10], Grodins, et.al (1967) [14], and Milhorn, et al. (1965) [20].

Appendix A

Table of Variables and Parameter Values

This appendix will provide the meanings, values and units of all parameters and state variables used in the model. Equilibrium mean values for the rest and exercise conditions will also be given.

Table A.1: The table for compliances.

Compliance	**Compartment**	**Value [mL/mmHg]**
c_{sa}	systemic aorta	1.5
c_{fa}	finger arteries	0.085
c_{as}	arterial systemic	3.25
c_{vs}	venous systemic	850.95
c_{rv}	relaxed right ventricle	44.131
c_{ap}	arterial pulmonary	25.15
c_{vp}	venous pulmonary	200.75
$c_{\ell v}$	relaxed left ventricle	25

Table A.2: The table for resistances.

Resistance	**Meaning**	**Value [mmHg sec/mL]**
$R_{mv,open}$	Resistance when the mitral valve is open	0.0025
$R_{av,open}$	Resistance when the aortic valve is open	0.0025
R_{sc_1}	Resistance between systemic aorta and finger arteries	0.4745
R_{sc_2}	Resistance between systemic aorta and arterial systemic	0.25
R_{sp_f}	Resistance between finger and venous systemic compartment	9
R_{rv}	Inflow resistance of the right ventricle	0.002502
R_{pp}	Resistance in the peripheral region of the pulmonary circuit	0.1097
$R_{\ell v}$	Inflow resistance of the left ventricle	0.02502

Table A.3: The table for the coefficients of the differential equation involving S_{rv} and $S_{\ell v}$.

Parameter	**Meaning**	**Value**	**Unit**
α_{rv}	Coefficient of S_{rv} in the differential equation for S_{rv}	0.003969	sec^{-2}
γ_{rv}	Coefficient of $\frac{dS_{rv}}{dt}$ in the differential equation for S_{rv}	0.021125	sec^{-1}
β_{rv}	Coefficient of H in the differential equation for S_{rv}	0.01841	mmHg/sec
$\alpha_{\ell v}$	Coefficient of $S_{\ell v}$ in the differential equation for $S_{\ell v}$	0.0013006	sec^{-2}
$\gamma_{\ell v}$	Coefficient of $\frac{dS_{\ell v}}{dt}$ in the differential equation for $S_{\ell v}$	0.0149367	sec^{-1}
$\beta_{\ell v}$	Coefficient of H in the differential equation for $S_{\ell v}$	0.01985	mmHg/sec

Table A.4: The table for other parameters used.

Parameter	Meaning	Value	Unit
a	Constant in the Gompertz function	3	mmHg/mL
b	Constant in the Gompertz function	10	1
c	Constant in the Gompertz function	3.415	sec^{-1}
E_m	Minimum elastance value of the left heart	0.029	mmHg/mL
$T_{r,frac}$	Quotient between T_r and T, i.e. $T_{r,frac} = \frac{T_r}{T}$	0.15	1
V_{tot}	Total blood volume	5940	mL
V_d	Unstressed blood volume in the left ventricle	10	mL
κ	Constant in the Bazett's formula	0.35	sec
$C_{\text{a,O}_2}$	O_2 concentration in arterial systemic blood	0.2	1
K	Constant in the formula for the biochemical energy flow	5465.9	mL
M_0	Metabolic rate in the systemic tissue region with zero workload	5.83	mL/sec
ρ	Coefficient of W in (2.34)	0.183	mL/(sec Watt)

Table A.5: The controlled parameters.

State	Meaning	Value		Unit
		rest	***exercise***	
H	Heart rate	70/60	95/60	beat/sec
W	Workload	0	50	Watt
A_{pesk}	Peskin's constant	7.2276	12.25	mmHg sec/mL

Table A.6: The state variables and other auxiliary variables of the model.

Variable	Meaning	Unit
P_{sa}	Pressure in the systemic aorta compartment	mmHg
P_{fa}	Pressure in the finger arteries compartment	mmHg
P_{as}	Pressure in the arterial systemic compartment	mmHg
P_{vs}	Pressure in the venous systemic compartment	mmHg
P_{ap}	Pressure in the arterial pulmonary compartment	mmHg
P_{vp}	Pressure in the venous pulmonary compartment	mmHg
$P_{\ell v}$	Pressure in the left ventricle compartment	mmHg
S_{rv}	Contractility of the right ventricle	mmHg
$S_{\ell v}$	Contractility of the left ventricle	mmHg
$E_{\ell v}$	Elastance of the left ventricle	mmHg/mL
Q_{rv}	Cardiac output of the right ventricle	mL/sec
$Q_{\ell v}$	Cardiac output of the right ventricle	mL/sec

Table A.7: Initial and equilibrium mean values during rest condition.

State	Initial Value	Mean Value	
		(1st run)	(2nd run)
P_{sa}	120	105.6634	105.3509
P_{fa}	$0.99(P_{sa})$	101.8399	101.5397
P_{as}	86.5	87.0774	86.8040
P_{vs}	5.12	5.1240	5.1020
P_{ap}	14.64	14.6329	14.6009
P_{vp}	4	3.9737	3.9643
$P_{\ell v}$	2.4	44.2803	44.1557
R_{sp}	0.9505	0.9570	0.9561
S_{rv}	5.4115	5.4115	5.4115
σ_{rv}	0	0	0

Table A.8: Initial and equilibrium mean values during exercise condition.

State	Initial Value	Mean Value	
		(1st run)	(2nd run)
P_{sa}	105.3509	133.2252	132.6022
P_{fa}	101.5397	128.4260	127.8309
P_{as}	86.8040	107.5376	106.9687
P_{vs}	5.1020	4.7917	4.7700
P_{ap}	14.6009	18.4806	18.4367
P_{vp}	3.9643	4.1128	4.1003
$P_{\ell v}$	2.4	53.2380	53.0073
R_{sp}	0.9561	0.8801	0.8771
S_{rv}	7.3442	7.3442	7.3442
σ_{rv}	0	0	0

Appendix B

Derivations of Some Equations

This appendix provides the derivations of some equations presented in Chapter 2. Included also is the brief derivation of the derivative of the left ventricular pressure which is given in system (4.3). Furthermore, the entries of the Jacobian discussed in Chapter 4, Section 4.5 will be given.

B.1 The Derivations

- Equation (2.11):

$$\boxed{V_{rv}(t) \;=\; V_{\text{rv,syst}} e^{-t(c_{rv}R_{rv})^{-1}} + c_{rv}P_{vs}\left(1 - e^{-t(c_{rv}R_{rv})^{-1}}\right)}$$

  We want to derive the solution of the differential equation given by

$$\frac{dV_{rv}(t)}{dt} + \frac{1}{c_{rv}R_{rv}}V_{rv}(t) - \frac{1}{R_{rv}}P_{vs} \;=\; 0\ , \qquad V_{rv}(0) = V_{\text{rv,syst}}\ .$$

  To integrate this easily, let's recall the *constant of variation formula*: Given an initial-valued differential equation

$$x'(t) \;=\; ax(t) + f(t), \qquad x(0) \;=\; x_0\ ,$$

  the solution is given by

$$x(t) \;=\; x_0 e^{at} + \int_0^t e^{(t-s)a} f(s)\, ds\ .$$

Thus,

$$\begin{aligned}
V_{rv}(t) &= V_{\text{rv,syst}}e^{-t(c_{rv}R_{rv})^{-1}} + \int_0^t e^{(t-s)(-(c_{rv}R_{rv})^{-1})}\frac{1}{c_{rv}R_{rv}}\left(c_{rv}P_{vs}\right)\,ds \\
&= V_{\text{rv,syst}}e^{-t(c_{rv}R_{rv})^{-1}} + \frac{1}{R_{rv}}P_{vs}\int_0^t e^{(t-s)(-(c_{rv}R_{rv})^{-1})}\,ds \\
&= V_{\text{rv,syst}}e^{-t(c_{rv}R_{rv})^{-1}} \\
&\quad + \frac{1}{R_{rv}}P_{vs}\left(e^{-(c_{rv}R_{rv})^{-1}t}\right)\int_0^t e^{((c_{rv}R_{rv})^{-1})s}\,ds \\
&= V_{\text{rv,syst}}e^{-t(c_{rv}R_{rv})^{-1}} \\
&\quad + \frac{1}{R_{rv}}P_{vs}\left(e^{-(c_{rv}R_{rv})^{-1}t}\right)\left(\frac{1}{(c_{rv}R_{rv})^{-1}}e^{((c_{rv}R_{rv})^{-1})s}\Big|_0^t\right) \\
&= V_{\text{rv,syst}}e^{-t(c_{rv}R_{rv})^{-1}} \\
&\quad + \frac{1}{R_{rv}}P_{vs}\left(e^{-(c_{rv}R_{rv})^{-1}t}\right)\left(\frac{1}{(c_{rv}R_{rv})^{-1}}\left[e^{((c_{rv}R_{rv})^{-1})t}-1\right]\right)
\end{aligned}$$

$$V_{rv}(t) = V_{\text{rv,syst}}e^{-t(c_{rv}R_{rv})^{-1}} + c_{rv}P_{vs}\left(1-e^{-t(c_{rv}R_{rv})^{-1}}\right)$$

■

- Equation (2.23)

$$\boxed{V_{\text{rv,str}} = \frac{c_{rv}P_{vs}a_r(H)f(S_{rv},P_{ap})}{a_r(H)P_{ap}+k_r(H)f(S_{rv},P_{ap})}}$$

Substituting equation (2.14) to equation (2.16) we obtain

$$\begin{aligned}
V_{\text{rv,str}} &= \left(k_r(H)V_{\text{rv,syst}} + c_{rv}P_{vs}a_r(H)\right) - V_{\text{rv,syst}} \\
&= \left(k_r(H)-1\right)V_{\text{rv,syst}} + c_{rv}P_{vs}a_r(H) \\
&= c_{rv}P_{vs}a_r(H) - V_{\text{rv,syst}}a_r(H) \qquad (a_r(H) = 1-k_r(H)) \\
V_{\text{rv,str}} &= \left(c_{rv}P_{vs} - V_{\text{rv,syst}}\right)a_r(H)
\end{aligned}$$

Solving $V_{\text{rv,syst}}$ in terms of $V_{\text{rv,str}}$ from the above equation gives

$$\begin{aligned}
\frac{V_{\text{rv,str}}}{a_r(H)} &= c_{rv}P_{vs} - V_{\text{rv,syst}} \\
\implies V_{\text{rv,syst}} &= c_{rv}P_{vs} - \frac{V_{\text{rv,str}}}{a_r(H)} \quad (\spadesuit)
\end{aligned}$$

From equation (2.17) we have $\frac{P_{ap}}{S_{rv}} V_{\mathrm{rv,str}} = V_{\mathrm{rv,diast}}$. Subtracting this from equation (2.16) yields

$$\begin{aligned}
V_{\mathrm{rv,str}} - \frac{P_{ap}}{S_{rv}} &= -V_{\mathrm{rv,syst}} \\
\left(1 - \frac{P_{ap}}{S_{rv}}\right) V_{\mathrm{rv,str}} &= -V_{\mathrm{rv,syst}} \\
(S_{rv} - P_{ap})\, V_{\mathrm{rv,str}} &= -S_{rv} V_{\mathrm{rv,syst}} \\
(S_{rv} - P_{ap})\, V_{\mathrm{rv,str}} &= -S_{rv}\left(c_{rv} P_{vs} - \frac{V_{\mathrm{rv,str}}}{a_r(H)}\right) \qquad \text{from } (\spadesuit) \\
(S_{rv} - P_{ap})\, V_{\mathrm{rv,str}} &= -c_{rv} P_{vs} S_{rv} + \frac{S_{rv}}{a_r(H)} V_{\mathrm{rv,str}} \\
\left(S_{rv} - P_{ap} - \frac{S_{rv}}{a_r(H)}\right) V_{\mathrm{rv,str}} &= -c_{rv} P_{vs} S_{rv} \\
(a_r(H) S_{rv} - a_r(H) P_{ap} - S_{rv})\, V_{\mathrm{rv,str}} &= -c_{rv} P_{vs} a_r(H) S_{rv} \\
((a_r(H) - 1)\, S_{rv} - a_r(H) P_{ap})\, V_{\mathrm{rv,str}} &= -c_{rv} P_{vs} a_r(H) S_{rv} \\
(-k_r(H) S_{rv} - a_r(H) P_{ap})\, V_{\mathrm{rv,str}} &= -c_{rv} P_{vs} a_r(H) S_{rv} \\
\\
V_{\mathrm{rv,str}} &= \frac{c_{rv} P_{vs} a_r(H) S_{rv}}{k_r(H) S_{rv} + a_r(H) P_{ap}}
\end{aligned}$$

■

- Equation (2.37):

$$\boxed{\frac{dR_{sp}}{dt} = \frac{1}{K}\left(A_{\mathrm{pesk}}\left(\left(\frac{P_{as} - P_{vs}}{R_{sp}}\right) C_{\mathrm{a,O_2}} - M_{\mathrm{T}}\right) - (P_{as} - P_{vs})\right)}$$

$$\begin{aligned}
\frac{dR_{sp}}{dt} &= A_{\mathrm{pesk}} \frac{d}{dt} C_{\mathrm{v,O_2}} \quad \text{(differentiating (2.35))} \\
&= -A_{\mathrm{pesk}} \frac{M_b}{K} \quad \text{(by (2.33))} \\
&= -\frac{A_{\mathrm{pesk}}}{K}\left(M_T - F^*_{sp}\left(C_{\mathrm{a,O_2}} - C_{\mathrm{v,O_2}}\right)\right) \quad \text{(by (2.32))} \\
&= -\frac{A_{\mathrm{pesk}}}{K}\left(M_T - \frac{1}{R_{sp}}\left(P_{as} - P_{vs}\right)\left(C_{\mathrm{a,O_2}} - C_{\mathrm{v,O_2}}\right)\right) \quad \text{(by (2.36))} \\
&= -\frac{A_{\mathrm{pesk}}}{K}\left(M_T - \frac{1}{R_{sp}}\left(P_{as} - P_{vs}\right)\left(C_{\mathrm{a,O_2}} - \frac{R_{sp}}{A_{\mathrm{pesk}}}\right)\right) \quad \text{(by (2.35))} \\
&= -\frac{A_{\mathrm{pesk}}}{K}\left(M_T - \frac{1}{R_{sp}}\left(P_{as} - P_{vs}\right) C_{\mathrm{a,O_2}} + \frac{1}{A_{\mathrm{pesk}}}\left(P_{as} - P_{vs}\right)\right)
\end{aligned}$$

Rearranging the terms we obtain

$$\frac{dR_{sp}}{dt} = \frac{1}{K}\left(A_{\text{pesk}}\left(\left(\frac{P_{as}-P_{vs}}{R_{sp}}\right)C_{\text{a,O}_2} - M_{\text{T}}\right) - (P_{as}-P_{vs})\right)$$

■

- Seventh equation in the full system (4.3):

$$\boxed{\frac{dP_{\ell v}(t)}{dt} = E_{\ell v}(t)\left(\frac{\frac{dE_{\ell v}(t)}{dt}P_{\ell v}(t)}{E_{\ell v}(t)^2} + \frac{P_{vp}(t)-P_{\ell v}(t)}{R_{mv}(t)} - \frac{P_{\ell v}(t)-P_{sa}(t)}{R_{av}(t)}\right)}$$

Differentiating equation (2.27) with respect to t gives us

$$\frac{dP_{\ell v}(t)}{dt} = \frac{dE_{\ell v}(t)}{dt}\left(V_{\ell v}(t)-V_d\right) + E_{\ell v}(t)\frac{dV_{\ell v}(t)}{dt}\ .$$

Using the relation (2.7) and substituting it from above and finally rearranging the terms yield

$$\frac{dP_{\ell v}(t)}{dt} = \frac{dE_{\ell v}(t)}{dt}\left(\frac{P_{\ell v}(t)}{E_{\ell v}(t)}\right) + E_{\ell v}(t)\left(\frac{P_{vp}(t)-P_{\ell v}(t)}{R_{mv}(t)} - \frac{P_{\ell v}(t)-P_{sa}(t)}{R_{av}(t)}\right)$$

$$\frac{dP_{\ell v}(t)}{dt} = E_{\ell v}(t)\left(\frac{\frac{dE_{\ell v}(t)}{dt}P_{\ell v}(t)}{E_{\ell v}(t)^2} + \frac{P_{vp}(t)-P_{\ell v}(t)}{R_{mv}(t)} - \frac{P_{\ell v}(t)-P_{sa}(t)}{R_{av}(t)}\right)$$

■

B.2 The Jacobian $\mathcal{F}(\hat{x},\hat{p},W,0)$ with respect to $\hat{x}$

For the modified simplified model with finger arterial compartment, we have

$$\hat{x} = (P_{sa}, P_{fa}, P_{as}, P_{vs}, P_{ap}, R_{sp}, S_{\ell v}, \sigma_{\ell v}, S_{rv}, \sigma_{rv}, H)^T \in \mathbb{R}^{11}\ , \tag{B.1}$$

and the coordinates of $\mathcal{F}(\hat{x},\hat{p},W,0)$ are given by (4.33) with $u(t)\equiv 0$. Setting

$$a_{i\,j} = \frac{\partial \mathcal{F}_i}{\partial \hat{x}_j}(\hat{x},\hat{p},W,0)\,, \qquad i,j=1,\ldots,11,$$

we obtain

$$
\begin{aligned}
a_{11} &= \frac{1}{c_{sa}}\left(\frac{\partial Q_{\ell v}}{\partial P_{sa}} - \frac{1}{R_{sc_2}} - \frac{1}{R_{sc_2}}\right), & a_{12} &= \frac{1}{c_{sa}}\left(\frac{\partial Q_{\ell v}}{\partial P_{fa}} + \frac{1}{R_{sc_1}}\right),\\
a_{13} &= \frac{1}{c_{sa}}\left(\frac{\partial Q_{\ell v}}{\partial P_{as}} + \frac{1}{R_{sc_2}}\right), & a_{14} &= \frac{1}{c_{sa}}\frac{\partial Q_{\ell v}}{\partial P_{vs}},\\
a_{15} &= \frac{1}{c_{sa}}\frac{\partial Q_{\ell v}}{\partial P_{ap}}, & a_{17} &= \frac{1}{c_{sa}}\frac{\partial Q_{\ell v}}{\partial S_{\ell v}},\\
a_{16} &= a_{18} = a_{19} = a_{110} = 0, & a_{111} &= \frac{1}{c_{sa}}\frac{\partial Q_{\ell v}}{\partial H},
\end{aligned}
$$

$$
\begin{aligned}
a_{21} &= \frac{1}{c_{fa}R_{sc_1}}, & a_{22} &= -\frac{1}{c_{fa}}\left(\frac{1}{R_{sc_1}} + \frac{1}{R_{sp_f}}\right),\\
a_{23} &= 0, & a_{24} &= \frac{1}{c_{fa}R_{sp_f}},\\
a_{25} &= a_{26} = a_{27} = a_{28} = 0, & a_{29} &= a_{210} = a_{211} = 0,
\end{aligned}
$$

$$
\begin{aligned}
a_{31} &= \frac{1}{c_{as}R_{sc_2}}, & a_{32} &= 0,\\
a_{33} &= -\frac{1}{c_{as}}\left(\frac{1}{R_{sc_2}} + \frac{1}{R_{sp}}\right), & a_{34} &= \frac{1}{c_{as}R_{sp}},\\
a_{35} &= 0, & a_{36} &= \frac{1}{c_{as}}\left(\frac{P_{as}-P_{vs}}{{R_{sp}}^2}\right),\\
a_{37} &= a_{38} = a_{39} = 0, & a_{310} &= a_{311} = 0,
\end{aligned}
$$

$$
\begin{aligned}
a_{41} &= 0, & a_{42} &= \frac{1}{c_{vs}R_{sp_f}},\\
a_{43} &= \frac{1}{c_{vs}R_{sp}}, & a_{44} &= -\frac{1}{c_{vs}}\left(\frac{1}{R_{sp}} + \frac{1}{R_{sp_f}} + \frac{\partial Q_{rv}}{\partial P_{vs}}\right),\\
a_{45} &= \frac{1}{c_{vs}}\frac{\partial Q_{rv}}{\partial P_{ap}}, & a_{46} &= \frac{1}{c_{vs}}\left(\frac{P_{vs}-P_{as}}{{R_{sp}}^2}\right),\\
a_{47} &= a_{48} = 0, & a_{49} &= -\frac{1}{c_{vs}}\frac{\partial Q_{rv}}{\partial S_{rv}},\\
a_{410} &= 0, & a_{411} &= -\frac{1}{c_{vs}}\frac{\partial Q_{rv}}{\partial H},
\end{aligned}
$$

$$
\begin{aligned}
a_{51} &= -\frac{c_{sa}}{c_{ap}c_{vp}R_{pp}}, & a_{52} &= -\frac{c_{fa}}{c_{ap}c_{vp}R_{pp}},\\
a_{53} &= -\frac{c_{as}}{c_{ap}c_{vp}R_{pp}}, & a_{54} &= \frac{1}{c_{ap}}\left(\frac{\partial Q_{rv}}{\partial P_{vs}} - \frac{c_{vs}}{c_{vp}R_{pp}}\right),\\
a_{55} &= \frac{1}{c_{ap}}\left(\frac{\partial Q_{rv}}{\partial P_{ap}} - \frac{1}{R_{pp}}\left(1+\frac{c_{ap}}{c_{vp}}\right)\right), & a_{56} &= a_{57} = a_{58} = a_{510} = 0,\\
a_{59} &= \frac{1}{c_{ap}}\frac{\partial Q_{rv}}{\partial S_{rv}}, & a_{511} &= \frac{1}{c_{ap}}\frac{\partial Q_{rv}}{\partial H},
\end{aligned}
$$

$$a_{61} = a_{62} = 0, \qquad a_{63} = \frac{1}{K}\left(\frac{A_{\text{pesk}} C_{\text{a,O}_2}}{R_{sp}} - 1\right),$$

$$a_{64} = \frac{1}{K}\left(1 - \frac{A_{\text{pesk}} C_{\text{a,O}_2}}{R_{sp}}\right), \qquad a_{66} = \frac{1}{K}\left(\frac{A_{\text{pesk}}(P_{vs} - P_{as}) C_{\text{a,O}_2}}{{R_{sp}}^2}\right),$$

$$a_{65} = a_{67} = a_{68} = 0, \qquad a_{69} = a_{610} = a_{611} = 0,$$

$$a_{71} = a_{72} = a_{73} = a_{74} = 0, \qquad a_{75} = a_{76} = a_{77} = 0,$$

$$a_{78} = 1, \qquad a_{79} = a_{710} = a_{711} = 0,$$

$$a_{81} = a_{82} = a_{83} = 0, \qquad a_{84} = a_{85} = a_{86} = 0,$$

$$a_{87} = -\alpha_{\ell v}, \qquad a_{88} = -\gamma_{\ell v},$$

$$a_{89} = a_{810} = 0, \qquad a_{811} = \beta_{\ell v},$$

$$a_{91} = a_{92} = a_{93} = a_{94} = 0, \qquad a_{95} = a_{96} = a_{97} = 0,$$

$$a_{98} = a_{99} = a_{911} = 0, \qquad a_{910} = 1,$$

$$a_{101} = a_{102} = a_{103} = a_{104} = 0, \qquad a_{105} = a_{106} = a_{107} = 0,$$

$$a_{108} = 0, \qquad a_{109} = -\alpha_{rv},$$

$$a_{1010} = -\gamma_{rv}, \qquad a_{1011} = \beta_{rv},$$

$$a_{111} = a_{112} = a_{113} = \cdots = a_{119} = a_{1110} = a_{1111} = 0.$$

The derivatives of $Q_{\ell v}$ and Q_{rv} are as follows:

$$\begin{aligned}
\frac{\partial Q_{\ell v}}{\partial P_{sa}} &= \frac{H c_{\ell v} a_\ell(H) S_{\ell v}}{c_{vp}} \\
&\quad \times \frac{a_\ell(H)\left(c_{fa}P_{fa} + c_{as}P_{as} + c_{vs}P_{vs} + c_{ap}P_{ap} - V_{\text{tot}}\right) - c_{sa}k_\ell(H)S_{\ell v}}{\left(a_\ell(H)P_{sa} + k_\ell(H)S_{\ell v}\right)^2}, \\
\frac{\partial Q_{\ell v}}{\partial P_{fa}} &= -\frac{c_{\ell v}c_{fa}}{c_{vp}} \cdot \frac{H a_\ell(H) S_{\ell v}}{a_\ell(H)P_{sa} + k_\ell(H)S_{\ell v}} \\
\frac{\partial Q_{\ell v}}{\partial P_{as}} &= -\frac{c_{\ell v}c_{as}}{c_{vp}} \cdot \frac{H a_\ell(H) S_{\ell v}}{a_\ell(H)P_{sa} + k_\ell(H)S_{\ell v}} \\
\frac{\partial Q_{\ell v}}{\partial P_{vs}} &= -\frac{c_{\ell v}c_{vs}}{c_{vp}} \cdot \frac{H a_\ell(H) S_{\ell v}}{a_\ell(H)P_{sa} + k_\ell(H)S_{\ell v}} \\
\frac{\partial Q_{\ell v}}{\partial P_{ap}} &= -\frac{c_{\ell v}c_{ap}}{c_{vp}} \cdot \frac{H a_\ell(H) S_{\ell v}}{a_\ell(H)P_{sa} + k_\ell(H)S_{\ell v}} \\
\frac{\partial Q_{\ell v}}{\partial S_{\ell v}} &= \frac{H c_{\ell v} a_\ell(H)^2 \left(V_{\text{tot}} - c_{sa}P_{sa} - c_{fa}P_{fa} - c_{as}P_{as} - c_{vs}P_{vs} - c_{ap}P_{ap}\right) P_{sa}}{c_{vp}\left(a_\ell(H)P_{sa} + k_\ell(H)S_{\ell v}\right)^2}, \\
\frac{\partial Q_{\ell v}}{\partial H} &= \frac{c_{\ell v}S_{\ell v}\left(V_{\text{tot}} - c_{sa}P_{sa} - c_{fa}P_{fa} - c_{as}P_{as} - c_{vs}P_{vs} - c_{ap}P_{ap}\right)}{c_{vp}\left(a_\ell(H)P_{sa} + k_\ell(H)S_{\ell v}\right)^2} \\
&\quad \times \left(a_\ell(H)^2\left(P_{sa} - S_{\ell v}\right) + S_{\ell v}\left(1 - k_\ell(H) - H k'_\ell(H)\right)\right), \\
\frac{\partial Q_{rv}}{\partial P_{vs}} &= \frac{H c_{rv} a_r(H) S_{rv}}{a_r(H)P_{ap} + k_r(H)S_{rv}}, \\
\frac{\partial Q_{rv}}{\partial P_{ap}} &= -\frac{H c_{rv} a_r(H)^2 S_{rv} P_{vs}}{\left(a_r(H)P_{ap} + k_r(H)S_{rv}\right)^2}, \\
\frac{\partial Q_{rv}}{\partial S_{rv}} &= \frac{H c_{rv} a_r(H)^2 P_{vs} P_{ap}}{\left(a_r(H)P_{ap} + k_r(H)S_{rv}\right)^2}, \\
\frac{\partial Q_{rv}}{\partial H} &= \frac{c_{rv}S_{rv}P_{vs}}{\left(a_r(H)P_{ap} + k_r(H)S_{rv}\right)^2} \\
&\quad \times \left(a_r(H)^2\left(P_{ap} - S_{rv}\right) + S_{rv}\left(1 - k_r(H) - H k'_r(H)\right)\right),
\end{aligned}$$

where we have used

$$k'_\ell(H) = -\frac{1}{c_{\ell v}R_{\ell v}}k_\ell(H)t'_d(H), \qquad k'_r(H) = -\frac{1}{c_{rv}R_{rv}}k_r(H)t'_d(H),$$

$$\text{and} \quad t'_d(H) = \frac{1}{H^2}\left(\frac{\kappa}{2}H^{1/2} - 1\right).$$

B.3 The Jacobian $\mathcal{B}(\check{x},\check{p},W,0)$ with respect to $\check{x}$

For the modified simplified model without the finger arterial compartment, we have

$$\check{x} = (P_{sa}, P_{as}, P_{vs}, P_{ap}, R_{sp}, S_{\ell v}, \sigma_{\ell v}, S_{rv}, \sigma_{rv}, H)^T \in \mathbb{R}^{10} \ , \tag{B.2}$$

and the coordinates of $\mathcal{B}(\check{x},\check{p},W,0)$ are given by (4.39) with $u(t) \equiv 0$. Setting

$$b_{i\,j} \ = \ \frac{\partial \mathcal{B}_i}{\partial \check{x}_j}\,(\check{x},\check{p},W,0)\,, \qquad i,j = 1,\ldots,10,$$

we obtain

$$\begin{aligned}
b_{1\,1} &= \frac{1}{c_{sa}}\left(\frac{\partial Q_{\ell v}}{\partial P_{sa}} - \frac{1}{R_{sc_2}}\right), & b_{1\,2} &= \frac{1}{c_{sa}}\left(\frac{\partial Q_{\ell v}}{\partial P_{as}} + \frac{1}{R_{sc_2}}\right),\\
b_{1\,3} &= \frac{1}{c_{sa}}\frac{\partial Q_{\ell v}}{\partial P_{vs}}, & b_{1\,4} &= \frac{1}{c_{sa}}\frac{\partial Q_{\ell v}}{\partial P_{ap}},\\
b_{1\,5} &= 0 & b_{1\,6} &= \frac{1}{c_{sa}}\frac{\partial Q_{\ell v}}{\partial S_{\ell v}},\\
b_{1\,7} &= b_{1\,8} = b_{1\,9} = 0, & b_{1\,10} &= \frac{1}{c_{sa}}\frac{\partial Q_{\ell v}}{\partial H},
\end{aligned}$$

$$\begin{aligned}
b_{2\,1} &= \frac{1}{c_{as}R_{sc_2}}, & b_{2\,2} &= -\frac{1}{c_{as}}\left(\frac{1}{R_{sc_2}} + \frac{1}{R_{sp}}\right)\\
b_{2\,3} &= \frac{1}{c_{as}R_{sp}}, & b_{2\,4} &= 0,\\
b_{2\,5} &= \frac{1}{c_{as}}\left(\frac{P_{as}-P_{vs}}{{R_{sp}}^2}\right), & b_{2\,6} &= 0,\\
b_{2\,7} &= b_{2\,8} = 0, & b_{2\,9} &= b_{2\,10} = 0,
\end{aligned}$$

$$\begin{aligned}
b_{3\,1} &= 0, & b_{3\,2} &= \frac{1}{c_{vs}R_{sp}},\\
b_{3\,3} &= -\frac{1}{c_{vs}}\left(\frac{1}{R_{sp}} + \frac{\partial Q_{rv}}{\partial P_{vs}}\right), & b_{3\,4} &= \frac{1}{c_{vs}}\frac{\partial Q_{rv}}{\partial P_{ap}},\\
b_{3\,5} &= \frac{1}{c_{vs}}\left(\frac{P_{vs}-P_{as}}{{R_{sp}}^2}\right), & b_{3\,6} &= 0,\\
b_{3\,7} &= 0, & b_{3\,8} &= -\frac{1}{c_{vs}}\frac{\partial Q_{rv}}{\partial S_{rv}},\\
b_{3\,9} &= 0, & b_{3\,10} &= -\frac{1}{c_{vs}}\frac{\partial Q_{rv}}{\partial H},
\end{aligned}$$

$$b_{41} = -\frac{c_{sa}}{c_{ap}c_{vp}R_{pp}}, \qquad b_{42} = -\frac{c_{as}}{c_{ap}c_{vp}R_{pp}},$$

$$b_{43} = \frac{1}{c_{ap}}\left(\frac{\partial Q_{rv}}{\partial P_{vs}} - \frac{c_{vs}}{c_{vp}R_{pp}}\right), \qquad b_{44} = \frac{1}{c_{ap}}\left(\frac{\partial Q_{rv}}{\partial P_{ap}} - \frac{1}{R_{pp}}\left(1+\frac{c_{ap}}{c_{vp}}\right)\right),$$

$$b_{45} = 0, \qquad b_{46} = 0,$$

$$b_{47} = 0, \qquad b_{48} = \frac{1}{c_{ap}}\frac{\partial Q_{rv}}{\partial S_{rv}},$$

$$b_{49} = 0, \qquad b_{410} = \frac{1}{c_{ap}}\frac{\partial Q_{rv}}{\partial H},$$

$$b_{51} = 0, \qquad b_{52} = \frac{1}{K}\left(\frac{A_{\text{pesk}}C_{\text{b,O}_2}}{R_{sp}} - 1\right),$$

$$b_{53} = \frac{1}{K}\left(1 - \frac{A_{\text{pesk}}C_{\text{a,O}_2}}{R_{sp}}\right), \qquad b_{54} = 0,$$

$$b_{55} = \frac{1}{K}\left(\frac{A_{\text{pesk}}(P_{vs}-P_{as})C_{\text{a,O}_2}}{{R_{sp}}^2}\right), \qquad b_{56} = 0,$$

$$b_{57} = b_{58} = 0, \qquad b_{59} = b_{510} = 0,$$

$$b_{61} = b_{62} = b_{63} = 0, \qquad b_{64} = b_{65} = b_{66} = 0,$$

$$b_{67} = 1, \qquad b_{68} = b_{69} = b_{610} = 0,$$

$$b_{71} = b_{72} = b_{73} = 0, \qquad b_{74} = b_{75} = 0,$$

$$b_{76} = -\alpha_{\ell v}, \qquad b_{77} = -\gamma_{\ell v},$$

$$b_{78} = b_{79} = 0, \qquad b_{710} = \beta_{\ell v},$$

$$b_{81} = b_{82} = b_{83} = b_{84} = 0, \qquad b_{85} = b_{86} = b_{87} = 0,$$

$$b_{88} = b_{810} = 0, \qquad b_{89} = 1,$$

$$b_{91} = b_{92} = b_{93} = 0, \qquad b_{94} = b_{95} = b_{96} = 0,$$

$$b_{97} = 0, \qquad b_{98} = -\alpha_{rv},$$

$$b_{99} = -\gamma_{rv}, \qquad b_{910} = \beta_{rv},$$

$$b_{10\,1} \;=\; b_{10\,2} \;=\; b_{10\,3} \;=\; \cdots = \; b_{10\,9} \;=\; b_{10\,10} \;=\; 0.$$

The derivatives of $Q_{\ell v}$ and Q_{rv} are as follows:

$$\begin{aligned}
\frac{\partial Q_{\ell v}}{\partial P_{sa}} &= \frac{H c_{\ell v} a_\ell(H) S_{\ell v}}{c_{vp}} \\
&\quad \times \frac{a_\ell(H)\left(c_{as}P_{as} + c_{vs}P_{vs} + c_{ap}P_{ap} - V_{\text{tot}}\right) - c_{sa}k_\ell(H)S_{\ell v}}{\left(a_\ell(H)P_{sa} + k_\ell(H)S_{\ell v}\right)^2}\,, \\
\frac{\partial Q_{\ell v}}{\partial S_{\ell v}} &= \frac{H c_{\ell v} a_\ell(H)^2 \left(V_{\text{tot}} - c_{sa}P_{sa} - c_{as}P_{as} - c_{vs}P_{vs} - c_{ap}P_{ap}\right) P_{sa}}{c_{vp}\left(a_\ell(H)P_{sa} + k_\ell(H)S_{\ell v}\right)^2}, \\
\frac{\partial Q_{\ell v}}{\partial H} &= \frac{c_{\ell v} S_{\ell v}\left(V_{\text{tot}} - c_{sa}P_{sa} - c_{as}P_{as} - c_{vs}P_{vs} - c_{ap}P_{ap}\right)}{c_{vp}\left(a_\ell(H)P_{sa} + k_\ell(H)S_{\ell v}\right)^2} \\
&\quad \times \left(a_\ell(H)^2\left(P_{sa} - S_{\ell v}\right) + S_{\ell v}\left(1 - k_\ell(H) - H k'_\ell(H)\right)\right), \\
\frac{\partial Q_{rv}}{\partial P_{vs}} &= \frac{H c_{rv} a_r(H) S_{rv}}{a_r(H)P_{ap} + k_r(H)S_{rv}},
\end{aligned}$$

where $\dfrac{\partial Q_{\ell v}}{\partial P_{as}}$, $\dfrac{\partial Q_{\ell v}}{\partial P_{vs}}$, $\dfrac{\partial Q_{\ell v}}{\partial P_{ap}}$, $\dfrac{\partial Q_{rv}}{\partial P_{vs}}$, $\dfrac{\partial Q_{rv}}{\partial P_{ap}}$, $\dfrac{\partial Q_{rv}}{\partial S_{rv}}$, $\dfrac{\partial Q_{rv}}{\partial H}$, $k'_\ell(H)$, $k'_r(H)$, and $t'_d(H)$ are the same as in Appendix B.2.

Bibliography

[1] M. Athans and P. L. Falb, *Optimal Control: An Introduction to the Theory and Its Applications*, McGraw-Hill, New York, 1966.

[2] J. Batzel, F. Kappel, D. Schneditz, and H. Tran, *Cardiovascular and Respiratory Systems: Modeling, Analysis and Control*, SIAM, Philadelphia, PA, 2007.

[3] H. Bazett, *An analysis of the time-relations of electrocardiograms*, Heart, **7** (1920), 353–370.

[4] W. E. Boyce and R. C. DiPrima, *Elementary Differential Equations and Boundary Value Problems*, John Wiley & Sons, 7th ed., 2001.

[5] R. Brockett, *Finite Dimensional Linear Systems*, John Wiley, New York, 1969.

[6] R. Bucy, *Global theory of the riccati equation*, Journal of Computer and System Sciences, **1** (1967), 349–361.

[7] ——, *Two-point boundary value problems of linear hamiltonian systems*, SIAM Journal of Applied Mathematics, **15** (1967), 1385–1389.

[8] L. Dai, *Singular Control Systems, Lecture Notes in Control and Information Sciences*, Springer Verlag, Berlin, 1989.

[9] H. Falls, ed., *Exercise Physiology*, Academic Press, New York, 1968.

[10] W. Fincham and F. Tehrani, *A mathematical model of the human respiratory system*, Journal of Biomedical Engineering, **5** (1983), 125–137.

[11] M. Franz, J. Schaefer, M. Schöttler, and W. S. amd M.I.M. Noble, *Electrical and mechanical restitution of the human heart at different rates of stimulation*, Circulation Research, **53** (1983), 815–822.

[12] F. Grodins, *Integrative cardiovascular physiology: a mathematical synthesis of cardiac and blood vessel hemodynamics*, The Quarterly Review of Biology, **34** (1959), 93–116.

[13] ——, *Control Theory and Biological Systems*, Columbia University Press, New York, 1963.

[14] F. Grodins, J. Buell, and A. Bart, *Mathematical analysis and digital simulation of the respiratory control system*, Journal of Applied Physiology, **22** (1967), 2260–276.

[15] A. Guyton and J. Hall, *Textbook of Medical Physiology*, Elsevier, 11th ed., 2006.

[16] M. Hautus, *Controllability and observability conditions for linear autonomous systems*, Nederl. Akad. Wet. Proc., **A72** (1969), 443–448.

[17] T. Heldt, E. Shim, R. Kamm, and R. Mark, *Computational modeling of cardiovascular response to orthostatic stress*, Journal of Applied Physiology, **92** (2002), 1239–1254.

[18] M. W. Hirsch, S. Smale, and R. L. Devaney, *Differential Equations, Dynamical Systems, and an Introduction to Chaos*, Elsevier Academic Press, 2nd ed., 2004.

[19] F. Hoppensteadt and C. Peskin, *Modeling and Simulation in Medicine and the Life Sciences*, Springer, 2nd ed., 2002.

[20] J. Howard T. Milhorn, R. Benton, R. Ross, and A. C. Guyton, *A mathematical model of the human respiratory control system*, Biophysical Journal, **5** (1965), 227–46.

[21] E. D. D. Jr, *Least energy regulation of the arterial system*, Bulletin of Mathematical Biology, **40** (1978), 79–93.

[22] R. E. Kalman, *Contributions to the theory of optimal control*, Boletin Sociedad Matemática Mexicana, **5** (1960), 102–119.

[23] F. Kappel, *Course 1 on control theory.* Ovide Arino, Summer School on Biomathematics, Schloss Seggau, July 25 - August 5, 2005.

[24] F. Kappel, M. Fink, and J. Batzel, *Aspects of control of the cardiovascular-respiratory sytem during orthostatic stress induced by lower body negative pressure*, Mathematical Biosciences, **206** (2007), 273–308.

[25] F. Kappel, S. Lafer, and R. Peer, *A model for the cardiovascular system under an ergometric workload*, Survey on Mathematics for Industry, **7** (1997), 239–250.

[26] F. Kappel and R. Peer, *A mathematical model for fundamental regulation processes in the cardiovascular system*, Journal of Mathematical Biology, **31** (1993), 611–631.

[27] T. Kenner, *Physical and mathematical modeling in cardiovascular systems*, in Clinical and Research Applications of Engineering Principles, N. Hwang, E. Gross, and D. Patel, eds., Baltimore, 1979, University Park Press, 41–109.

[28] T. Kenner and K. Pfeiffer, *Studies on the optimal matching between heart and arterial system*, in Cardiovascular Dynamics, J. Baan, A. Artnezenius, T. Yellin, and M. Nijhoff, eds., The Hague, 1980.

[29] R. E. Klabunde, *Cardiovascular Physiology Concepts*, Lippincott Williams & Wilkins, 2005.

[30] H. Kwakernaak and R. Sivan, *Linear Optimal Control Systems*, Wiley-Interscience, New York, 1972.

[31] S. Lafer, *Mathematical Modelling of the Baroreceptor Loop*, PhD thesis, University of Graz, Institute for Mathematics and Scientific Computing, 1996.

[32] J. Levick, *An Introduction to Cardiovascular Physiology*, Oxford University Press, New York, 4th ed., 2003.

[33] D. Luenberger, *Introduction to Dynamic Systems: Theory, Models and Applications*, John Wiley & Sons, New York, 1979.

[34] M.Fink, J. Batzel, and F. Kappel, *An optimal control approach to modeling the cardiovascular-respiratory system: An application to orthostatic stress*, Cardiovascular Engineering, **4** (2004), 27–38.

[35] J. B. Moore and B. D. O. Anderson, *Extensions of quadratic minimization theory i. finite time results 1*, International Journal of Control, **7**.

[36] E. Noldus, *Optimal control aspects of left ventricular ejection dynamics*, Journal of Theoretical Biology, **63** (1976), 275–309.

[37] A. Noordergraaf, *Hemodynamics*, in Biological Engineering, H. Schwan, ed., New York, 1969, McGraw-Hill, 391–545.

[38] A. Noordergraaf and J. Melbin, *Introducing the pump equation*, in Cardiovascular System Dynamics: Models and Measurements, T. Kenner, R. Busse, and H. Hinghofer-Szalkay, eds., New York, 1982, Plenum Press, 19–35.

[39] M. Olufsen, J. Ottesen, H. Tran, L. Ellwein, L. Lipsitz, and V. Novak, *Blood pressure and blood flow variation during postural change from sitting to standing: Model development and validation*, Journal of Applied Physiology, **99** (2005), 1523–1537.

[40] K. Ono, T. Uozumi, C. Yoshimoto, and T. Kenner, *The optimal cardiovascular regulation of the arterial blood pressure*, London New York, 1982, Plenum Press.

[41] J. Ottesen, M. Olufsen, and J. Larsen, *Applied Mathematical Models in Human Physiology*, SIAM, Philadelphia, PA, 2004.

[42] J. Palladino and A. Noordergraaf, *A paradigm for quantifying ventricular contraction*, Cellular and Molecular Biology Letters, **7** (2002), 331–335.

[43] S. Patterson, H. Piper, and E. Starling, *The regulation of the heart beat*, Journal of Physiology, **48** (1914), 465–513.

[44] C. Peskin, *Mathematical Aspects of Physiology (Lectures in Applied Mathematics)*, American Mathematical Society, 1981.

[45] K. Pfeiffer and T. Kenner, *On the optimal strategy of cardiac ejection*, in Cardiovascular System Dynamics: Models and Measurements, T. Kenner and R. B. and. H. Hinghofer-Szalkay, eds., London New York, 1981, Plenum Press, 133–136.

[46] S. Pope, L. Ellwein, C. Zapata, V. Novak, C. Kelley, and M. Olufsen, *Estimation and identification of parameters in a lumped cerebrovascular model*, Mathematical Biosciences and Engineering, **6** (2009), 93–115.

[47] V. Rideout, *Mathematical and Computer Modeling of Physiological Systems*, Prentice Hall, Englewood Cliffs, NJ, 1991.

[48] L. Rowell, *Human Cardiovascular Control*, Oxford University Press, Oxford, 1993.

[49] D. L. Russel, *Mathematics of Finite-Dimensional Control Systems*, Marcel Dekker, New York, 1979.

[50] A. Schumitzky, *On the equivalence between matrix riccati equations and fredholm resolvents*, Journal of Computer and System Sciences, **2** (1968), 76–87.

[51] W. Seed and J. Walker, *Relation between beat interval and force of the heartbeat and its clinical implications*, Cardiovascular Research, **22** (1988), 303–314.

[52] K. Sunagawa and K. Sagawa, *Models of ventricular contraction based on time-varying elastance*, Critical Reviews in Biomedical Engineering, **7** (1982), 193–228.

[53] G. Swan, *Applications of Optimal Control Theory in Biomedicine*, Marcel Dekker, Inc., New York, 1984.

[54] S. Timischl, *A global model of the cardiovascular and respiratory system*, PhD thesis, University of Graz, Institute for Mathematics and Scientific Computing, 1998.

[55] N. Westerhof, N. Stergiopulos, and M. Noble, *Snapshots of Hemodynamics*, Springer, 2005.

[56] B. Wohlfart, *Relationships between peak force, action potential duration and stimulus interval in rabbit myocardium*, Acta Physiologica Scandinavica, **106** (1979), 395–409.